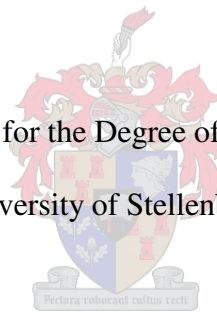


**CHARACTERISING AND MAPPING OF WIND TRANSPORTED
SEDIMENT ASSOCIATED WITH OPENCAST GYPSUM
MINING.**

Francis van Jaarsveld

Thesis presented for the Degree of Master of Science
University of Stellenbosch



Supervisor:

Mr. W. P. de Clercq

Co-supervisor:

Prof. A. Rozendaal

March 2008

Declaration

I, the undersigned, hereby declare that the work contained in this thesis is my own original work and that I have not previously in its entirety or in part submitted it at any other university for a degree

Signature:

Date:

Copyright © 2008 Stellenbosch University

All rights reserved

Abstract

This study aims to provide a practical tool for the prediction and management of dust generated by the activities of an opencast mining operation. The study was conducted on opencast gypsum mines in the semi-arid environment of the Bushmanland, 90 km north of Loeriesfontein in the Northern Cape Province from April 2000 to October 2007. The vertical and horizontal components of wind transported sediment were sampled and a dust settling model was designed to predict the settling pattern of dust generated by opencast mining operations. The model was applied to soil samples collected from an area surrounding a mine. The influence sphere of the mining operation was predicted by the application of the model and then mapped. Once the influence sphere is mapped, the dust influence can be managed with the aid of an onsite weather station. By further applying the predictions based on climatic data, the influence sphere can be modelled. The model is not only applicable to the planning phase of an opencast mine to plan the position of dust sensitive areas like the living quarters, office buildings and workshops etc., but also to indicate the historical impact that a mining operation had once a quarry on an active mine is worked out and rehabilitated or a mine is closed. The model application can also aid with the explanation and visual or graphic representation of the predicted impact of planned mining operations on communities or neighbouring activities to them and thus avoid later penalties.

Uittreksel

Die oogmerk van hierdie studie is 'n praktiese hulpmiddel vir die voorspelling en bestuur van stof wat deur die aktiwiteite van oopgroefmyne veroorsaak word. Die studie is gedoen op 'n oopgroef gipsmyn in die halfdroë omgewing van die Boesmanland, 90 km noord van Loeriesfontein in die Noordkaap Provinsie vanaf April 2000 tot Oktober 2007. Die vertikale en horisontale komponente van windvervoerde sedimente is gemonster en 'n stofafsettingsmodel is hiervolgens ontwerp om te voorspel wat die stof afsettingspatroon van oopgroefmynaktiwiteite sal

wees. Die model is toegepas op grondmonsters wat geneem is in die omgewing rondom 'n myn. Die stof geaffekteerde area rondom die myn is hierdeur voorspel. Indien die invloed sfeer voorspelbaar is, kan stof produksie bestuur word deur gebruik te maak van 'n weerstasie. Deur die toepassing van voorspellings geskoei op klimaatinligting kan die invloed sfeer gemodelleer word. Hierdie model is nie net van toepassing in die beplanningsfase van 'n oopgroefmyn om te bepaal waar stof sensitiewe fassette soos wooneenhede, kantoorgeboue en werksinkels opgerig word nie, maar kan ook 'n aanduiding gee van die historiese impak van 'n steengroef wat uitgemyn en gerehabiliteer is of ook van 'n myn wat reeds gesluit is. Die modeltoepassing kan voorts help met die verduideliking van die beplande invloed van 'n myn en verwante aktiwiteite op 'n gemeenskap. Dit kan gedoen word deur middel van 'n grafiese voorstelling aan die gemeenskap of naburige boerdery-aktiwiteit. Sodoende kan latere eise voorkom word.

Acknowledgements

I would like to give special thanks to the following people:

My wife Amanda for her tremendous support and patience throughout this study.

Mr. Willem de Clercq and Prof. Rozendaal for their interest in the study and their valuable guidance.

Anél Blignaut for the research that she made available and her ongoing interest and involvement in the continued monitoring at the mine.

The Directors of Saint-Gobain Construction Products for the financial support and the opportunity to conduct the research; especially Mr. Leon de Jager and Mr. Stephen du Toit for the high premium that they place on the research.

My colleagues, Stephen Salisbury and Burger Roux, mine manager of the Waterkuil and Dikpens mines and Lampies Lamprecht and the Research and Development team.

My family, family-in-law and friends for their support.

Contents

1	General Introduction and Thesis Structure	1
1.1	Introduction.....	1
1.2	The Study Area	3
1.3	Study Structure.....	6
1.4	Aims and objectives:.....	8
2	Dust, Man and the Environment	9
2.1	Introduction.....	9
2.2	General Discussion	9
2.2.1	Control of Dust in Frequently Used Areas.....	12
2.2.2	Climate and Dust Storms	13
2.2.3	Human Causes	15
2.2.4	Impact of Agriculture.....	15
2.2.5	Impact of Mining Related Origin.....	16
2.3	Effects on the Environment.....	20
2.3.1	Effects on the Fauna.....	20
2.3.2	Effects on the Flora.....	21
2.3.3	Effects on the Soil.....	26
2.4	Legislation Regarding Dust Deposition.....	28
2.5	Conclusion	29
3	Dust Settling Model, Climate of the Study Area and First Application of the Model.....	32
3.1	Introduction.....	32
3.2	Dust Settling Model	32
3.2.1	Method of Monitoring.....	32
3.2.2	Results and Discussion of the Dust Settling Monitoring.....	36
3.3	Climatic Investigation	40
3.3.1	Method of Monitoring.....	40
3.3.2	Results and Discussion of the Climatic Information	40
3.4	Expansion of the Dust Monitoring Process	44
3.4.1	Method of Monitoring.....	45
3.4.2	Results and Discussion of the Expanded Monitoring.....	45
3.5	Conclusion	49
4	Wind Transported Sediment Monitoring and Monitoring of its Impact.....	50
4.1	Introduction.....	50
4.2	Methodology	50
4.2.1	Climate.....	50
4.2.2	Dust Monitoring.....	51
4.2.3	Vegetation Monitoring.....	53
4.3	Results.....	58
4.3.1	Climate.....	58
4.3.2	Dust Monitoring.....	65
4.3.3	Vegetation Monitoring.....	68
4.4	Discussion of the Findings.....	72

4.5	Conclusion	76
5	Windblown Sediment and its Origin.....	78
5.1	Introduction.....	78
5.1.1	Gypsum	79
5.2	Method	81
5.3	Results and Discussion	81
5.4	Conclusion	92
6	Proposing and testing a Sediment Distribution Model	93
6.1	Introduction.....	93
6.2	Methodology	94
6.2.1	Chemical Investigation	97
6.3	Discussion	108
6.4	Conclusion	110
7	Conclusions.....	111
8	References.....	113
	Addendum.....	119

List of Figures

Figure 1.01	The study area located in the Northern Cape Province.....	3
Figure 1.02	Dust generation associated with a) the mining of gypsum in an open cast operation b) the transportation of the production across unpaved roads c) stockpiling and d) loading of the gypsum at the station at Loop 8.	5
Figure 1.03	Dust that forms on the dry pan surface that borders the gypsum mining operation.	7
Figure 2.01	A diagram to illustrate the penetrability of particulate matter in the human respiratory system. (TSP is the abbreviation of total suspended particulate) (Dämon, 2007).	11
Figure 2.02	A general wind erosion model for the calculation of PM ₁₀ dust emissions in open cast mining operations for the various operational sections (Dämon, 2007).	16
Figure 2.03	An example from the study area close to a transport road where sedimentation is very heavy.	22
Figure 2.04	Dust trapped in a gypsum outcrop on the mine at Waterkuil.....	27
Figure 2.05	The dust deposition is visible as the grey fine grained top layer in the soil profile at this particular location in the study area.	30
Figure 3.01	Dust traps containers on the eastern side of the road at the modelling site.	34
Figure 3.02	Map indicating the modelling site and the general geography of the investigated area.....	35
Figure 3.03	A graphic representation of the dust settling model for the two opposite monitoring directions.	37

Figure 3.04	The average fallout dust, integrating all measuring points, measured in relation to the amount of passing vehicles and the influence of the introduction of a speed limit and later on, the influence of regular maintenance in combination with the speed limit.	38
Figure 3.05	The average fallout dust measured in relation to the wind speed.	39
Figure 3.06	Wind rose diagrams indicating the wind direction frequency in average number of winds in blue and the wind speed in m/s in pink.....	43
Figure 3.07	Map indicating the test sites of the expanded monitoring system.	46
Figure 3.08	Comparison between the settling model and the averages of data collected with the expanded monitoring system.	48
Figure 3.09	The equation of the data trend of the empirical dust settling model....	48
Figure 3.10	A comparison between the trend of the expanded monitoring system and the equation of the dust settling model applied to the data of the expanded system.	49
Figure 4.01	The Automatic Weather Station (AWS) at Monitoring Site 4: Konnes. .	51
Figure 4.02	The POLCA sampler used for measuring windblown dust (Goossens et al., 2000).	52
Figure 4.03	Map indicating the position of the Monitoring Sites	54
Figure 4.04	Showing the Monitoring Sites 1 to 5	55
Figure 4.05	The line intercept method at A: Monitoring Site 2: Boegoefontein and B: Monitoring Site 3: Dikpens. Photo C of the Honnepisbos illustrates the canopy spread strike method and D bears as a reminder that small annuals like this <i>Heliophilla</i> should not be overlooked.	56
Figure 4.06	Average rainfall in mm for the monitored period from August 2003 to September 2007.	59
Figure 4.07	The potential for precipitation (calculated from >80% RH) to occur in the form of dew, mist or frost is represented for the monitored period from August 2003 to September 2007.....	62
Figure 4.08	Fog that occurs in the Bushmanland region (Photo was taken during June 2004).	62
Figure 4.09	The average day and night relative humidity for the monitored period from August 2003 to September 2007.	63
Figure 4.10	The average day and night temperatures for the monitored period from August 2003 to September 2007.....	63
Figure 4.11	The average wind direction frequency (average number of winds) in blue and average wind speed recorded in m/s in red for the monitored period from August 2003 to September 2007 at Monitoring Site 4: Konnes.	65
Figure 4.12	The relative production increase/decrease year by year experienced at the Dikpens mine since operation commenced in 2003.....	66
Figure 4.13	The average dust collected per year at each monitoring point A and B at each Monitoring Site 1 to 5.....	66
Figure 4.14	The average fallout of the two monitoring points A and B per year per Monitoring Site. The overall average is also indicated.....	67
Figure 4.15	Histogram indicating the percentage cover over time.....	70
Figure 4.16	Number of species recorded per Monitoring Site.	71
Figure 4.17	The wind pattern over the monitored period from August 2003 to September 2007. Figure A reflects the wind pattern for 2003, B for 2004, C 2005, D 2006 and E 2007.	73

Figure 4.18	A comparative graph of the climatic variation over the monitored period August 2006 and September 2007. Note that the Y-axis scale represents °C for the temperature, % for the relative humidity, mm for the rain and hours for the precipitation.	74
Figure 4.19	Negative correlation between the amount of fallout dust and the percentage cover at the Monitoring Sites for the period 2003 to 2007.....	75
Figure 4.20	A comparison of the settling model with the dust monitoring data.	76
Figure 5.01	Two separate areas where heavier dust fallout is obvious. A. At Monitoring Site 2: Boegoefontein, B. At the intersection of the Loeriesfontein – Brandvlei road and the turnoff to Pofadder at Bitterputs.	78
Figure 5.02	A typical ore body profile	80
Figure 5.03	Sediment collected at monitoring point 1: Station. A was collected in the container and B in the polca sampler at collection point 1A. C was collected in the container and D in the polca sampler at point 1B, 50 m further away from the dust source. The scale is the same for all the photos.	82
Figure 5.04	Particle size analyses of sediment particles collected at Monitoring point 1A.	83
Figure 5.05	Particle size analyses of sediment particles collected at Monitoring point 1B.	84
Figure 5.06	Sediment collected at monitoring point 5: Quarry. A was collected in the container and B in the polca sampler at collection point 5A. C was collected in the container and D in the polca sampler at collection point 5B, 50 m further away from the dust source. The scale is the same for all photos.	85
Figure 5.07	Particle size analyses of sediment particles collected at Monitoring point 5A.	86
Figure 5.08	Particle size analyses of sediment particles collected at Monitoring point 5B.	86
Figure 5.09	SEM images of the polca sampler sediments collected at Monitoring Site 1. A was collected at collection point A (Mag = 100K X, line scale = 20µm). B as collected at collection point B (Mag = 100K X, line scale = 20µm)	87
Figure 5.10	SEM images of the polca sampler sediments collected at Monitoring Site 5. A was collected at collection point A (Mag = 100K X, line scale = 20µm). B was collected at collection point B (Mag = 100K X, line scale = 30µm)	88
Figure 5.11	Position where sample 2W was taken from the ore body at Waterkuil at a depth of 60 cm below the surface.....	90
Figure 6.01	Map indicating the sampling area as the red, dash lines. It also shows a wind rose representing the average wind direction frequency and speed recorded by the onsite AWS.	95
Figure 6.02	A view of the quarry with the sampling area on the right.....	95
Figure 6.03	Waterkuil mine soil sampling positions.....	96
Figure 6.04	Sieved fractions of the selected samples to isolate the silt and clay fractions representing the dust generated by the mining operation.....	96
Figure 6.05	Indicating the poor relationship between the percentage particles smaller than 53µm and the distance from the quarry edge.	97
Figure 6.06	Images of sample 17 sieved fractions. A is the >250µm, B the >106 µm, C the >53 µm and D the <53 µm fraction. The scale is the same for all photos.	98
Figure 6.07	Images of sample 17 at A: Mag = 106 X, line scale = 200µm, B: Mag = 1.88K X, line scale = 10 µm and C: Mag = 6.76K X, line scale = 1 µm.....	99

Figure 6.08	Map of the Kriged EC surfer model. The sieve analyses sample positions and the position of sieve sample 17 are also indicated. Note the wind rose in the map legend.	102
Figure 6.09	Exponential semi-variogram and variogram model of the soil samples from Waterkuil mine.....	103
Figure 6.10	Graph A shows the strong correlation between calcium and EC and Graph B shows the equally strong correlation between sulfate and EC.	104
Figure 6.11	Water sources in the region are commonly high in soluble salt content. A: is a water trench on the mine at Dikpens. B: Evaporitic salt deposits are visible on the sides of the trench. C: NaCl is mined on the pan at Dikpens. The salt deposit is visible around the base of the fence pole. D: The Sout (Salt) river drains the region, some 40 km away from the mine.	106
Figure 6.12	The EC values of the “slice” samples and the trend equation.....	109
Figure 6.13	The linear prediction trend between dust accumulation and EC values.	109

List of Tables

Table 3.01	Data collected monthly over the monitoring period	36
Table 3.02	A. The mean monthly and annual rainfall (in mm) for the area and B. The number of days per month with measurable precipitation.....	41
Table 3.03	The maximum rainfall intensities per month, 24 hours and 50 year events	42
Table 3.04	The mean monthly A. maximum and B. minimum temperatures in °C calculated from three stations in vicinity the study area.	42
Table 3.05	A. Wind direction frequency (average number of winds) and B. wind speed (m/s) tables for Pofadder (1940 to 1990).....	43
Table 3.06	The mean monthly evaporation figures for Upington and Vredendal for the past 30 years.....	44
Table 3.07	Data collected over the period of monitoring.	47
Table 4.01	Rainfall in mm for the measured period from August 2003 to September 2007 at Monitoring Site 4: Konnes.....	59
Table 4.02	The maximum rainfall per 24 hour period and the year in which it occurred for the monitored period from August 2003 to September 2007 at Monitoring Site 4: Konnes.....	60
Table 4.03	Wind direction frequency (average number of winds) in table A and speed (m/s) in table B for the monitored period August 2003 to September 2007..	64
Table 4.04	Average fallout dust per transect (g/day) and the percentage increase or decrease that was measured over the 5 year monitoring period.....	68
Table 4.05	List of species identified at the Monitoring Sites. (Blignaut, 2007)	69
Table 4.06	Average percentage cover as well as the percentage change experienced by the Monitoring Sites over the 5 year monitoring period.....	70
Table 4.07	Summary of the dominant species change over time at the different Monitoring Sites.....	71

Table 4.08	Change in the relative frequency of the dominant species over time at the monitoring Sites.	72
Table 5.01	The SEM point chemical analyses of the polca sampler samples for monitoring point 1, collection point A and B.	87
Table 5.02	The SEM point chemical analyses of the polca sampler samples for Monitoring Site 5, collection point A and B.	88
Table 5.03	The results of the lanthanides analyses expressed in ppm.	91
Table 6.01	Point chemical analyses performed on various soil samples.	100
Table 6.02	The distribution parameters of the EC data (mS/m) from the Waterkuil soil samples.	103
Table 6.03	The correlation matrix between the EC, pH and the chemistry of the soil samples.	105
Table 6.04	A record of the region's water sources. Note that they are compared to Brakpan tap water and sea water.	107

1 GENERAL INTRODUCTION AND THESIS STRUCTURE

1.1 Introduction

Surface mining is unavoidable. Minerals are extracted and transported the world over. Transportation also generates dust and fumes, more so on unpaved roads. BPB Gypsum Pty Ltd (henceforth referred to as BPB Gypsum in this document) has been operating opencast gypsum mines in the Northern Cape Province for more than twenty years. With increased production and transportation pressures it became evident that the settling of wind transported sediment should be investigated to determine the influence and possible changes that might occur in the surface geology and vegetation surrounding the mining operation (Van Jaarsveld, 2002). The generation of dust is often a direct result of aridification (Reheis and Kihl, 1995). Not only does it appear to mirror the effects of climatic change, but also of human impacts on dust-prone areas. The study area, as later described, falls within an arid, dust-prone area. Each year 30 million tons of dust enter the atmosphere world wide. More than half of this, 17 million tons, is generated by agricultural related industries such as cotton ginning, alfalfa mills and lime kilns in combination with extracting industries, such as cement factory smelters and mines. According to Faith & Atkisson (1972) smoke is the most widespread air pollutant. Various types of particulate matter, sub classified as dusts, fumes and mists, account for the second most common air pollutants. They describe dusts as solid particles of natural or industrial origin, usually formed by disintegration processes (Faith and Atkisson, 1972). Billions of tons of mineral dust aerosols are released each year from arid and semi-arid regions to the atmosphere (Goossens and Offer, 1995; Tanaka and Howard, 2007).

Dust often accumulates on plants and impairs the growth or quality of crops (Mudd and Kozlowski, 1975). The influence or toxicity of dust depends mostly on three factors, namely chemical composition, particulate size and deposition rate. Very often concentrated particulates pervade the air in mining areas. Pollution is commonly caused by blasting which releases particulates and noxious fumes. In the BPB Gypsum situation, no blasting is done. The mining method is described at a later stage in this

thesis. Pollution is further commonly caused by wind blowing across open-cast mine quarries, waste heaps and stockpiles and across open dumps of toxic mined products like asbestos (Dämon, 2007). Again, the latter does not apply to BPB Gypsum's mining operation. Mining activities commonly degrade the landscape by laying bare the land and opening the huge chasms of opencast mining or by choking the landscape by a layer of dust that settles on the agricultural fields (Gupta, 1988). There is an increasing awareness that fine-grained aeolian sediments are important in many issues related to mineral exploration and environmental management. A more detailed understanding of aeolian sedimentation and its interactions with other regolith materials is required. The overall impact of fine particulate pollutants, as well as air contaminants in general, on the aggregate of living things in nature is not always very well understood. Much of this atmospheric pollution is smoke and dust of such a size that it falls out or is washed out of the atmosphere within a day or two (Sittig, 1977).

Driving over unpaved roads as well as other mechanical disturbances loosen soil structure and soil packing density. The soil cohesion and mechanical stability are reduced. This results in accelerated wind erosion and emission of dust particles into the air (Weinan et al., 1998). For every vehicle travelling 1 mile (1,6 km) of unpaved roadway once a day, every day of the year, 1 ton of dust is deposited along a 1000 foot (305m) corridor centred on the road (Jones, 1999). For coarser particles it appears that increased stickiness of the surface facilitates greater particulate capture, whilst for finer particles it is the roughness of the surface that has the greater influence on uptake (Beckett et al., 1998).

Dust is one of the most widespread air pollutants (Arslan and Boybay, 1990). A large variety of dust is found in the atmosphere, which originates from a variety of sources. Dust can have natural or anthropogenic origins and has significant impact on the quality of life of humans and the environment they live in. Determining the type, source and amounts of dust generated and putting in place the appropriate control measures is very important. Human activities such as the burning of fossil fuels also generate aerosols. Averaged over the globe, anthropogenic aerosols currently account for about 10 percent of the total amount of aerosols in our atmosphere.

1.2 The Study Area

The study area is located 90 km north of Loeriesfontein in the Northern Cape Province of South Africa, in an area known as the semi-arid transition between the Hantam Karoo and the Bushmanland (Cowling et al., 1986) (Figure 1.01). The vegetation in the study area is classified as Bushmanland Nama Karoo (Low and Rebelo, 1998). An indication of this transition is the large number of *Rhigozum trichotomum* (Driedoring) present in the area (Blignaut, 2007). The Waterkuil mining area was prospected from 1977 to 1979 when a gypsum bearing area of 500 ha was identified. The lease area extended over 600 ha. Mining commenced in 1984 and ceased during December 2003, when the Waterkuil Gypsum mine was closed. BPB Gypsum relocated mining operations to a new location called the BPB Gypsum Dikpens mine. It was prospected from 1980 to 1981 when an area of 430 ha was identified as gypsum-bearing. An area of 400 Ha is under lease and mining commenced in June 2003.



Figure 1.01 The study area located in the Northern Cape Province.

Common complaints from people in dust prone regions range from the additional cleaning of homes and cars to fugitive dust that causes low visibility on unpaved roads (Beckett et al., 1998; Jones, 1999). Low visibility is a cause of danger to motorists, cyclists, pedestrians and live-stock. Furthermore it is also abrasive to mechanical equipment and damaging to electronic equipment such as computers. Dust can also cause health problems, alone or in combination with other air pollutants. Infants and elderly people, or people with respiratory problems are more likely to be affected (Ferguson et al., 1999). Materials high in soluble salts could cause problems in salinity of ground waters and over-cultivation the production of respirable dust, 4 μm in size, believed to be detrimental to human health (Green et al., 2001). Farmers around the mining operation and the transport route of the gypsum to the rail loading station echoed some of these complaints like dust on the grazing, poor visibility, but mostly poor road maintenance.

The erosion, transportation and deposition of atmospheric dust are largely determined by the nature and state of the earth's surface and the characteristics of the atmosphere (Goossens and Offer, 1995). The source, transportation and deposition of aeolian dust are topics of increasing interest in the scientific community and increasing importance to the global community. Some topics that have recently been addressed are:

- 1) Dust generation is a direct result of aridification and therefore it mirrors the effects of climatic change and of human impact on dust-prone areas. An increased frequency and magnitude of dust storms will have a strong negative impact on human infrastructure.
- 2) Dust has been shown to be a major component of soils in both arid and semi-arid areas. Dust is important to soil fertility and can control the chemistry of precipitation.
- 3) In arid and semi-arid areas aeolian dust plays a significant role in soil formation and the geomorphic process (e.g. the formation of desert pavements) (Green et al., 2001).
- 4) Detailed studies of dust influx can permit better estimations of paleoclimate from soil properties such as the amount and depth of pedogenic carbonate. The climatic factors that affect dust flux interact with each other and with the factors of source type, source lithology, geographic area and human disturbance. Surface mining and transportation of ore is unavoidably an environmental destructive process (Schmidt, 2002). Three main areas of dust generation were identified namely the mining of the

gypsum, road transportation over unpaved or dirt roads and thirdly loading of the gypsum at the station (Paige-Green and Jones, 2000) (Figure 1.01).

Gypsum mining in this instance is done with Wirtgen continuous surface milling miners. The gypsum is cut in strips 1, 9 m wide with a cutting depth of 120 mm. The strips are 200 to 600 m long. The Wirtgen miners are set and operated to cut and crush the gypsum to a size of 20 mm or less, ready for shipment. Quality control is done visually and by sampling analyses, continuously with the mining process. The Wirtgen miners cut, crush and dump the gypsum behind it in windrows. It is then picked up with self elevating scrapers and stockpiled. From the stockpile the gypsum is loaded onto trucks and transported to the rail siding at Loop 8 on the Sishen-Saldanha line.



Figure 1.02 Dust generation associated with a) the mining of gypsum in an open cast operation b) the transportation of the production across unpaved roads c) stockpiling and d) loading of the gypsum at the station at Loop 8.

1.3 Study Structure

Khalaf (1989) conducted a study in the Kuwait Desert and concluded that semi-arid environments are characterised by scarce rainfall, high rate of evaporation and sparse vegetation. This description related very closely to the present study area. He further described the integrated harmony in sensitive ecosystems that exists between the natural processes of sediments and the fauna and flora. He found that the most significant influences are that of aeolian processes as a result of wind action, namely erosion, transportation and deposition.

Wind action is controlled by wind velocity, sediment grain size (clay, silt, sand) and surface protection in the form of vegetation. Terrain morphology and topography also play an important role. A proper description of the natural environment of the study area is very important to put the influences and findings into perspective.

Climate plays a major role in sediment movement in these semi-arid regions with their warm, dry climate. Monitoring temperature, the relative humidity, rainfall and other precipitation, wind speed and direction is essential to understand the integrated sediment movement within these areas. Khalaf (1989) concluded that when subjected to the right wind action, the mud fraction (silt and clay fractions) is transported as dust storms while the sand fraction is transported in bed load mode as a sandstorm. He concluded that in dust storms, the visibility is less than 1 km and that wind speed is less than 18 knots. The sediments consist of sandy silt with a median of 0.02 to 0.12 mm diameter. The average was found to be around 0.05 mm. In his study he found that 66% of the sediment consisted of quartz, calcite and feldspar. In sand storms he found that sand will mobilize to a height of 1.8 m at speeds greater than 20 km/h. The most common forms of sediment movement he found to be deflation of pans or Playa mud. Figure 1.02 illustrates this phenomenon in the study area.



Figure 1.03 Dust that forms on the dry pan surface that borders the gypsum mining operation.

The photo in Figure 1.02 was taken on 9 September 2004 between 11h00 and 13h00. The wind speed was recorded between 22.5 and 27 km/h, wind direction was east to east northeast. The temp during that time was between 17 and 22 °C and the relative humidity dropped from 36 % to 27% during the recorded period. The final aspect that he addressed was overgrazing. This phenomenon should not be underestimated in semi-arid regions.

With the strong similarities between the Khalaf research and this study in mind, the following chapter of this thesis will focus on a literature review of the classifications of wind-transported sediments and dust; in particular those associated with open cast mining operations. The next chapter will address the deriving of a road dust settling model, the historical climatic data and the expansion of the monitoring system. With the findings of the model in mind, it will also test the predictions of the model against the findings of the expanded monitoring system. Chapter 4 will focus on the onsite weather monitoring and findings that were made as well as fallout dust quantification and the possible influence of both these factors individually and combined, on the vegetation of the area. Chapter 5 will concentrate on the physical examination and analysis of the wind transported sediments, while the penultimate chapter will aim to

provide a model to illustrate the sediment settling correlation between road dust and quarry dust or dust generated by the mining operation. This model will be based on the geostatistical analyses of the sediments accumulated around the quarries. The final chapter will provide a conclusion to the study and thesis.

This study evolved over the past seven years and two hypotheses are set for the study:

- 1) The successful monitoring of climatic indicators and the application thereof will increase the manageability of dust generated by opencast mines.
- 2) The influence sphere of the mine can be predicted from historical weather data and the information can be used in the planning phase of new mines, or assist in the management of current operations.

1.4 Aims and objectives:

The aims and objectives of this study are to investigate the application of onsite weather information to predict and control dust originating from opencast mining operations. The monitoring and control of dust is necessary for the minimising of environmental impacts of the different operation elements of an open cast mining operation. The establishing of a successful dust settling model could aid with keeping dust pollution below acceptable levels.

2 DUST, MAN AND THE ENVIRONMENT

2.1 Introduction

This review will aim to discuss some of the classifications of dust, the origin and amounts, the effects on the environment and the monitoring and control thereof. There will not be a detailed discussion of all the types of dusts and their specific effects, but rather a more general discussion with examples of the more common or problematic types of dust. It will aim to place the study into the global scale of dust generation and investigates the influence of weather indicators, particle size, human influences and natural occurrences. Possible model applications will be investigated in order to try and answer questions such as: Is dust fallout measurable? What are the impacts on the different aspects of the environment? What is the impact of climate on the fallout?

2.2 General Discussion

Dust is particulate matter (PM) consisting of very small liquid and solid particles. Under the USA Environmental Protection Agency (EPA) classification dust is defined as particulate matter and is classified as one of six principal air pollutants. Particulate matter includes carbon monoxide, lead, nitrogen dioxide, ozone and sulphur dioxide (Ferguson et al., 1999). The EPA standard for ambient airborne particulate matter is based on the mass concentration of particles in two size classes, those under 2.5 μm diameter ($\text{PM}_{2.5}$) and those under 10 μm diameter (PM_{10}) (Prospero, 1999). The size of the particulate matter greatly influences the transport distance of dust. While large sand particles quickly fall to the ground, smaller particles, less than 10 μm , stay suspended in the air as dust aerosol (Tanaka and Howard, 2007). The particle size of dust transported over long distances normally corresponds to the medium to small silt fraction on the Wentworth scale. It is composed mostly of grain sizes below 20 μm (Dässler and Börtitz, 1988; Ramsperger et al., 1998). Dust transported over long distances is usually somewhat finer than loess (1 to 20 μm) that travelled for short distances (Yaalon and Ganor, 1973). Often soil particles, process dust, industrial

combustion products and marine salt particles fall typically in this size range, between 1 and 10 μm in diameter (Smith, 1974).

Fugitive dust is particulate matter suspended in the air by the wind and originates from human activities. It originates primarily from the soil and is not emitted from vents, chimneys, stacks, gravel quarries or grain mills (Beckett et al., 1998; Ferguson et al., 1999). It is typically a result of construction site work, or material handling where outdoor storage piles are used (Tanaka and Howard, 2007). Other important sources are unpaved roads, agricultural cropland and construction sites. It originates in small quantities over large areas. Most people living next to unpaved roads are familiar with the nuisance of fugitive dust, as well as the associated health problems.

Exposure to ambient fine particulate matter (particulate matter with an aerodynamic diameter $\leq 2.5 \mu\text{m}$ ($\text{PM}_{2.5}$)) has been associated with a wide range of PM-related human health effects in general populations, including the aggravation of heart and lung disease and premature mortality (Brook et al., 2004; Holgate et al., 1999; Samet et al., 2000). When breathing in, the hairs in our nose and air passages remove particles larger than PM_{10} . Particles smaller than PM_{10} can penetrate into the lungs. $\text{PM}_{2.5}$ will penetrate the alveoli where they cause problems and affect the health of people (Figure 2.01). Some of the most common health effects include irritation of eyes, throat and lungs. People with existing respiratory conditions, such as asthma or bronchitis, often find that breathing in particles can make the conditions worse. Particles can also reduce the capacity to resist infection. A significant rise in the incidence of nasorespiratory and eye infections during dust storms has also been reported and also a high correlation between dust fallout and allergic manifestations (Beckett et al., 1998; Khalaf, 1989).

The sources of dust can be classified as industrial, natural (including agriculture) and domestic. Under each class there will be tremendous variations in amount, chemical composition, particle size and density. Dust generation is predominantly related to the silt content, plasticity characteristics, hardness and relative density of the aggregate and to the threshold shear velocity of the wind generating the dust (Jones, 1999). Natural and man-made processes have been known to result in metal contamination of air-borne particles (Behairy et al., 1985). The origin of dust particles can only be

determined by detailed examination of the mineralogy of dusts carried by winds away from a source area (Whalley and Smith, 1981).

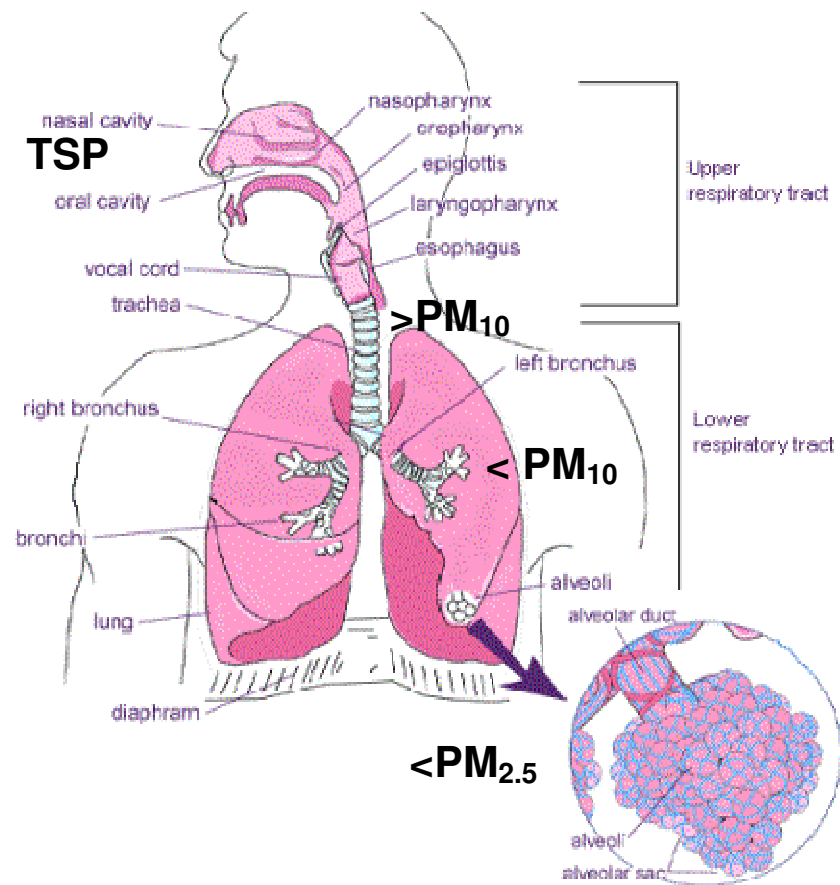


Figure 2.01 A diagram to illustrate the penetrability of particulate matter in the human respiratory system. (TSP is the abbreviation of total suspended particulate) (Dämon, 2007).

Dust emission is associated with many environmental parameters. Generally, dust storms are caused by strong, gusty winds associated with synoptic-scale disturbances or meso- or micro-scale thermal convective activities. Dust emission is inhibited by surface-covering elements such as vegetation, snow cover, and giant rocks, and soil-binding elements including high soil moisture and salt content. With these conditions, active dust-producing areas are confined to bare ground or sparsely vegetated ground with annual rainfall under 200 to 250 mm, and to regions with strong winds. (Tanaka and Howard, 2007)

Weather often contributes to fugitive dust generation. For example, Idaho, USA experiences a distinctive wet season and a dry season. Long, hot summers allow the soil to dry out thoroughly and, if the surface is disturbed repeatedly, the soil may have months to blow away before normal rainfall can again saturate and hold it in place. Some areas are also prone to high winds, making matters worse. A combination of human activity and unfavourable weather conditions can dramatically increase fugitive dust levels. During the 1930's in the United States, heavy tillage of marginally productive land combined with the extended drought created a huge fugitive dust problem. Construction projects often leave large areas of disturbed earth unprotected for long periods. These sites are often a source of fugitive dust as well as water erosion. Since these sites are often near cities they contribute to the overall air quality problems for metropolitan areas (Ferguson et al., 1999).

2.2.1 Control of Dust in Frequently Used Areas

In general, the most obvious way of controlling dust generation is to:

- 1) Pave haul roads and storage areas. Heavy vehicles pulverise the surface material and create a constant source of dust. If wholesale paving is too costly, only the entrance and exit can be paved to minimise carryout. The remainder can be gravelled to reduce surface silt.
- 2) Enclose storage and handling areas. If dusty materials are frequently loaded and unloaded in storage and handling areas, enclose the areas to reduce fugitive dust emissions. Use storage silos, three-sided bunkers, or open-ended buildings. If handling is less frequent, try wind fencing. Conveyor loading may require enclosure or the use of water or foam spray bars both above and below the belt surface to reduce emissions.
- 3) Keep storage piles covered. When storage piles are not in use, apply a physical cover or a dust suppressant spray to help reduce fugitive dust emissions. Limit the working face of the pile to the downwind side. Most emissions come from loading the pile, load out from the pile, and truck and loader traffic in the immediate area if the pile is batch loaded. Keep the drop height low to reduce dust and the ground at the base of the pile clear of spills.

4) Water and/or sweep often. To ensure that vehicle traffic is not picking up dust for wind action and carryout, water and sweep roadways often. Fewer treatments are necessary in cool, wet weather.

5) Reduce speed limits. Reduce speed limits on unpaved surfaces to 15 to 25 km/h for well-travelled areas and heavy vehicles. Never exceed 40 km/h for any vehicle on any unpaved surface. Prevent transport of dusty material offsite. The transport of dusty material offsite can be minimized by rinsing vehicles before they leave the property and tightly covering loaded trucks.

2.2.2 Climate and Dust Storms

Dust storms (SYNOP WW Code 09 – dust or sandstorm within sight at the time of observation, or at the station during the preceding hour) are the result of turbulent winds raising large quantities of dust into the air and reducing visibility to less than 1000m (McTainsh et al., 1989). Dust storms are common phenomena in many parts of the world, especially in arid and semi-arid regions (Khalaf and Al-Hashash, 1983; Middleton, 1986), which are characterised by bare soils and are a major source of small particulates that produce dust (Péwé, 1981). Wind-blown dust occasionally travels from arid to temperate areas and causes a sudden increase in particulate loading in the air (Monteith, 1975). In general fine dust is lifted by strong upward motion ahead of a vigorous dry front. Heated air pockets carry the dust to a height of 1.5 to 5 km and can distribute it over large areas. The residence time of the fine dust is generally several days. The removal mechanism is often by washout in rainfall (Khalaf and Al-Hashash, 1983).

Dust storms are controlled by three groups of factors, which include soil or sediment erodibility, vegetation cover and climatic factors. The first two groups operate at a local scale while the third operates on a much broader scale and can influence the first two (Bücher, 1993). The meteorological processes that generate dust storms in the Middle East can be classified as:

- 1) Convective weather systems.
- 2) Passage of frontal systems.
- 3) Winds associated with permanent pressure systems.

4) Low-level winds associated with upper-level jet streams (Middleton, 1986).

There seems to be a relationship between the progress of desertification and the number of dust winds. This non-linear relationship of increasing dust storms with aridity peaks at rainfalls of 200 mm per annum and decreases for lower rainfalls. Both the spatial and temporal occurrences of dust storms are strongly influenced by drought (Goudie, 1978; McTainsh et al., 1989). The central Nevada region is a good example where the lack of precipitation on the playas in summer permits drying of soils and encourages wind erosion (Young and Evans, 1986). It has been shown in the northern Negev, Israel, that air-dust relationship and wind speed show no clear correlation and that dust in the air originates from long distance deflation. Natural dust in the atmosphere may be influenced by the local synoptic situation as well as by the circulation in the upper atmosphere (Offer and Goossens, 1990). Nearly all dust erosion takes place during storms that occur only once or a few times a year (Goossens and Offer, 1997). Dust accumulation during the day is significantly higher than dust accumulation during the night (Goossens and Offer, 1995).

The Arabian Peninsula is one of the five major regions where global dust originates. In this area, dust storms are usually caused by the action of strong persistent winds on dry, fine-grained and loose soil (Middleton, 1986). The annual dust fallout over Kuwait, for example, is 1mm. Much of the fallout gets re-suspended here and is transported to the Arabian Gulf where it is deposited. Dust-storms in Kuwait are created by usually calm, hot weather when thermal instability of the near-ground air masses is responsible for tiny particles rising into the atmosphere. This process is initiated by vehicle traffic on unpaved roads (Khalaf, 1989), smokestacks and vehicle exhaust fumes, but the largest single source is unpaved roads (Ferguson et al., 1999). Wind erosion occurs continuously, especially in arid open areas with a low vegetation cover.

The Environmental and Earth Sciences Division of the Kuwait Institute for Scientific Research began their research on dust storms in 1979, due to the adverse effects it had on quality of life and development activities. Their research was aimed at assessing the nature of these aeolian processes and the resulting weather phenomena. Sand and dust storms are recognized as one of the most unpleasant features of desert life. Reduced visibility due to dust storms affects safety, frequency of take-off and landing

at airports, movement of shipping, and land transport are affected severely during dust storms. Infiltration of dust creates problems of sanitation and house-keeping. The presence of desert dust in the atmosphere has many environmental implications. It has effects on climatic change, marine sedimentation, air pollution, soil formation and crop growth (Middleton, 1986). Some dusts are enriched with trace metals from anthropogenic sources for example the dust in Kuwait which is enriched with Ag, Cd, Pb and Zn. Operations of oil-well pumps and drilling operations are usually hampered during dust storms (Khalaf and Al-Hashash, 1983). Wind storms have a large impact on the dust balance in rocky deserts.

2.2.3 Human Causes

While dust storms are natural events, human activities such as inappropriate agricultural practices, overgrazing and deforestation cause soil degradation and desertification, thus strongly influencing the availability of dust by surface disturbances. It has been pointed out that the atmospheric dust loading has been increased as a result of such activities. The contribution of anthropogenically disturbed soils to global dust emissions has been estimated to be as high as 30% to 50%. However, recent research suggests that agricultural areas contribute less than 10% to the dust load. Thus, natural causes are currently considered to be the primary source of dust emission on a global scale. (Tanaka and Howard, 2007)

2.2.4 Impact of Agriculture

Cultivated areas generally yield about 20 percent more dust than uncultivated areas and recently large quantities of dust may come from tilled soils in semi-arid regions (Cooke et al., 1993). The dust flux in an arid urbanizing area may be as much as twice that as before disturbance, but decreases when construction stops (Reheis, 1997). Appreciable quantities of particulate pollutants are also contributed by field burning of agricultural brush, debris and refuse (Treshow, 1970). The destruction of vegetation due to over-grazing or for fuel use is usually followed by the loss of topsoil by wind deflation.

2.2.5 Impact of Mining Related Origin

A major cause of dust in the atmosphere in Kuwait is sand and gravel quarrying. Great quantities of aggregate materials for production of concrete, road pavement and coastal area reclamation are needed in Kuwait due to the rapid development in urbanization (Khalaf, 1989). This gravel exploitation in Kuwait has led to the destruction of vegetation and associated faunal communities on the production site, but also in surrounding areas. It also led to the removal of gravel lag that used to cover the underlying finer material from wind action and huge amounts of sandy and silty tailings were accumulated in the quarries, which presents an important source for suspended dust. It finally led to the excavation releasing large amounts of fine particles that can easily be airborne, which is aggravated by sieving and crushing of gravels. Heavy dust clouds that reduce visibility to a few meters are often observed in crushing sites (Khalaf, 1989).

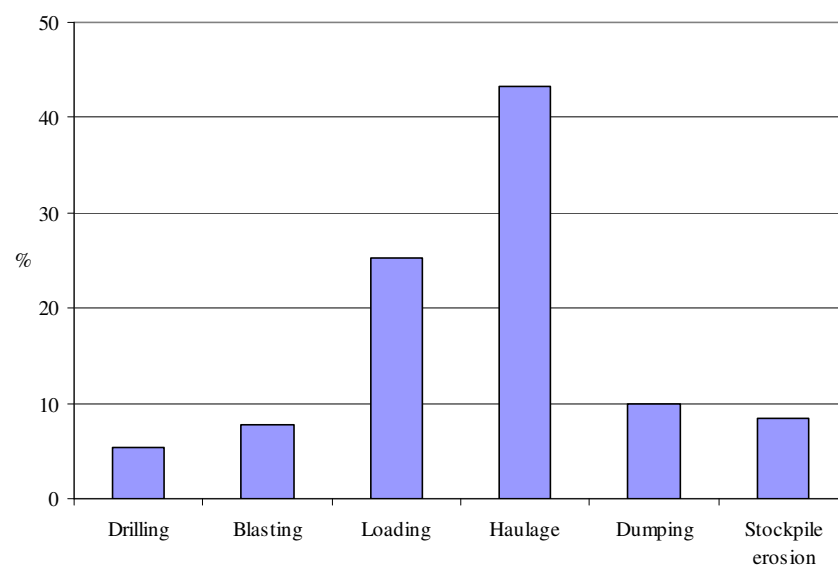


Figure 2.02 A general wind erosion model for the calculation of PM_{10} dust emissions in open cast mining operations for the various operational sections (Dämon, 2007).

Given the deferent operational elements, including drilling and blasting, Dämon (2007) measured average dust emissions of 12 kg PM₁₀ per hour in an open cast mining quarry at a production rate of 1200 t per 8 hour working day. He measured average emission of 80 g PM₁₀/t of ore mined, ranging from 50 g PM₁₀/t to 120 g PM₁₀/t. Figure 2.02 represent the percentage contribution per activity.

According to Khalaf (1989), dust created by off-road traffic significantly contributes to a chronic dusty atmosphere. The main consequences of unpaved road dust include visual restraints for vehicles thus creating a safety risk for motorists, cyclists, pedestrians and live-stock as well as economic impacts pertaining to loss of road construction material, increased building maintenance, higher vehicle operating costs, reduced agricultural yields and also health hazards (Jones, 1999).

Unacceptable levels of dust are experienced on many unpaved roads. Previously, dust was only considered as a nuisance factor. Recent studies have indicated that dust resulting from traffic on unpaved roads, could have significant environmental and social impacts like health and safety issues and visual pollution (Jones, 1999). Furthermore it also has some economic impacts in terms of loss of road construction material, increased building maintenance and higher vehicle operating costs. The moisture content of the material and the period since the road was last bladed also influence the level of dust. Other negative aspects are discomfort for pedestrians, vehicle occupants and residents of properties adjacent to the road, reduced agricultural yields and pollution (Jones, 1999). In a series of tests conducted, a strong linear trend was detected between vehicle speed, weight and PM₁₀ fugitive dust emission. The size of the wake created by a vehicle was observed to be dependent on the size of the vehicle, increasing roughly linearly with vehicle height (Gillies et al., 2004). Off-road traffic plays an important role in damaging soil cover. Uncontrolled traffic by any type of vehicle ranging from heavy duty machinery to small cars and motorcycles is responsible for massive destruction of vegetative cover and wild fauna as well as the deflation of the topsoil and compaction of the sub-soil which results in a sterilization effect of the ground. Several tons of fine particles get concentrated in the air due to the vehicle-induced aerodynamic forces (Khalaf, 1989). Plant growth is inversely related to traffic density (Colwill et al., 1982). Various particles are deposited on roadside plants, such as abrasion from tyres, brake linings and clutch plates and the

road surface. Leaves of roadside plants are covered with black deposits, when the traffic density is high (Thompson et al., 1984).

Dispersion of dust is mainly determined by meteorological factors. Wind direction and intensity (speed) plays a very important role. The distance at which dust particles could still have biological effects is determined by their properties, e.g. size of the particles and their transformation rate during transport. Precipitation results in cleaning of the air. Dust particles are incorporated into the drops of water and fall to the ground. Vegetation and buildings increase the irregularity of the ground surface and thus the turbulence. They therefore promote the sedimentation of airborne dusts (Dässler and Börtitz, 1988).

It has been assumed that the active surface layer charges on dust particles come from inter-grain collisions (Whalley and Smith, 1981). Many dust particles become electrically charged during their transport (Offer and Goossens, 1990). Laboratory experiments conducted on the electrification of dust clouds created by blowing different types of dusts into a dust chamber indicated that the polarity and magnitude of the space charge in such dust clouds have been found to be sensitive to the mineral constituents of the dust. Even a single dust cloud, if allowed to settle under gravity in a field-free space with no charge added to it, can have opposite polarities of space charge at different times of its sedimentation. The space charge produced increases with an increase in the length of the surface over which the dust is blown. It also increases with an increase in the temperature and velocity and a decrease in the relative humidity of the blowing air. External electric fields of up to a few hundred Volt/cm, applied to the surface from which the dust is blown, have little effect on the generated space charge. Size distributions of positively and negatively charged particles show a greater abundance of smaller ($< 3 \mu\text{m}$) particles compared to those of small neutral particles (Kamra, 1973). Whilst in transit, coarse dust travels near the ground, and fine dust moves higher up, concentrations and grain sizes following power-law patterns of decline with height (Bauer et al., 2002; Cooke et al., 1993; Nickling, 1989). Dust is sorted as it travels, and particle size decreases down-wind from a source (Pye, 1987). Dust settles to the ground by gravity in places where wind speed declines, as around topographic obstacles or where the surface roughness is increased by vegetation. Particles $<15\mu\text{m}$ are deposited only if they are washed out by

rain, if they are aggregated by electrostatic charges, or if they are brought down by adhering to coarser grains (Cooke et al., 1993).

Dust is difficult to quantify as wind blown sediments and deposition rates are highly variable. It differs from site to site and month to month and does not show a distinct seasonal pattern. Local components seem to play an important role in dust-related processes (Ramsperger et al., 1998). The dustiest areas are areas with lower rainfall of 100 to 200 mm per annum. This is possibly due to factors such as:

- 1) The fact that most of the dust has been removed from very dry areas
- 2) Little dust is generated in very dry areas by weathering or fluvial action and
- 3) The fact that there is less wind disturbance in deserts (Cooke et al., 1993).

The pattern of particle deposition or sedimentation in urban areas is quite complex due to factors that do not exist in other areas. More than just a small number of spot measurements are necessary to monitor the sedimentation process (Beckett et al., 1998). Very small changes in the grain size of particulate matter, or small changes in the stability of the atmosphere, can have drastic effects on the sedimentation of dust (Goossens and Offer, 1995). Fugitive dust measurements in the United States decreased drastically from 55 million tons in 1988, during a drought year, to 25 million tons in 1990. This decrease is mostly due to the paving of roads and improved agricultural practices (Ferguson et al., 1999). Dust deposition was found to be very variable in the Argentinean Pampa, both from site to site and from month to month. The deposition does not show a distinct seasonal pattern. It ranged from 6 to 110 kg/ha/month (Ramsperger et al., 1998). Rain wash-out deposition is the main reason for the imbedding of desert dust into Israel's soils, and probably is the main reason for the even thickness of fine dust accretion in many areas, including deep-sea sediments. The mechanism of dry fallout deposition results in a decrease in thickness of the aeolian deposit from the source (Yaalon and Ganor, 1973). The great abundance of silt in the sediments of the north-western Arabian Gulf can also be attributed to the deposition of considerable amounts of dust fallout (Khalaf and Al-Hashash, 1983).

There appears to be quite a strong correlation between average dust flux and mean annual temperature. A weak relation exists between average dust flux and an increase in mean annual precipitation. This phenomenon may be attributed to the fact that

prevailing winds bring dust to relatively wet areas (Reheis and Kihl, 1995). The retention of deposited particles could be increased by moistness, roughness, stickiness and electrical charge. At sufficiently high wind speeds, however, the particles could bounce off a surface to avoid deposition, but once lodged, it requires strong forces to dislodge the majority of particles again (Beckett et al., 1998).

2.3 Effects on the Environment

The investigation of environmental pollution in Saudi Arabia revealed that dust deposition might be a major contributor. The correlation is so strong that wind speed and atmospheric pressure could be used to predict the concentration of Al, As, Cu, Fe and Pb particulates. Dust storms may enhance many environmental problems, since they have potential effects on crop growth, soil formation and the spread of disease. They also cause a great degree of erosion in arid regions. It is suggested that the largest source of these heavy metal concentration in dust, could be motor vehicles emissions (Modaihsh, 1997). However, atmospheric effect related to proximity to the road will decline with distance from the road (Spencer et al., 1988). At cement works at Kymore, India, a penalisation index of the biotic environment was developed. It indicated that of all the constituents, particulate matter pollution most severely affected humans, followed by agricultural crops and then the animal population (Mishra and Sai, 1988).

Dust has various effects on plants and animals, some direct and others indirect. Direct influence on plants would include necrosis of leaves. Indirect influences will include contamination of soil that influences root growth. In animals, the influence is usually indirect. The amount of food available might decrease, the quality of the food might decrease and diseases might increase as a result of pollution.

2.3.1 Effects on the Fauna

Dust pollution may not always result in clinical signs in animals, but rather more sub-clinical like performance reductions and changed behaviour. As little as 25 g/m²/day deposition of dust on pasture fodder may lead to negative effects like reduction in milk production and increased fodder residues (Dässler and Börtitz, 1988). Dust

emissions can have an effect on some performance parameters of animal production, particularly breeding. Particulate matter pollution from cement works showed a high incidence of gastro intestinal tract diseases in cattle, ranging from 60% to 80% up to 6 km from the cement works (Mishra and Sai, 1988). Dust particles mainly stick to pasture grass and field fodder, which might result in the reduction of feed-intake or bad silage quality. Reduced milk, fat and fattening performances are often the result of dust pollution. A study done in the U.S.A. showed that gypsum dust does not hold any health hazard for humans or animals (Drinker and Hatch, 1954).

The increase in nitrogen content in plants closer to roads may be a major contributing factor causing outbreaks of insect herbivores on roadside plants. Dusty grape and sassafras leaves had greatly increased numbers of bacteria and fungi when compared to clean leaves (Spencer et al., 1988). *Streptomyces* were isolated almost exclusively from dusty leaves (Smith, 1974). Because of their high susceptibility, bees usually indicate the emissions of fluorine and arsenic dusts earlier than recognizable visible damage in plants and might even be used as possible bio-indicators (Dässler and Börtitz, 1988). In the southern deserts of Iraq, in spring time, small living creatures such as fish and frogs are carried upwards with sand and dust in the convective currents, only to descend later as a “mud rain”(Middleton, 1986).

2.3.2 Effects on the Flora

The quantity or amount of fallout dust is not nearly as important to the plant's welfare as the dust's composition. Unfortunately, early reports of smoke and dust damage were concerned more with the tons of dust settling than the composition thereof (Treshow, 1970). PM₁₀ is often predominant on plant surfaces and shrubs bordering unpaved roads or down wind of a barren source area, such as a dry lake or mining quarries. In the case of desert shrubs growing next to unpaved roads, heavy dust on leaves often appears to reduce the vigour of impacted shrubs. In the Mojave Desert of Nevada, dust deposition has been shown to cause plant defoliation and shoot death (Sharifi et al., 1997). In steep contrast some plants, for example *Osteospermum sinuatum*, had twice the size and four times as much flower than the ones growing in areas away from the unpaved roads (Batanouny, 1979; Milton and Dean, 1987). In the

latter case, the plants might find the positive effect of increased runoff from the road, overriding the negative impacts of dust accumulation.

Critical loads can be regarded as the accumulated amount of a pollutant which will result in physical damage. Figure 2.03 indicates an area within the study area where very heavy sedimentation is visible. Some tree species have developed mechanisms to avoid damage specifically from dust particles. These include the timing of bud break or leaf fall and the ability to produce new shoots when injured. The susceptibility to damage due to fallout dust varies greatly between species, as can the efficiency of pollutant uptake (Beckett et al., 1998). Water-repellent leaf surfaces exhibit almost perfect self-cleaning properties (Lotus effect). Dust is removed by water droplets rolling off the leaves, which is an important function of epicuticular wax crystals (Neinhuis and Barthlott, 1988).



Figure 2.03 **An example from the study area close to a transport road where sedimentation is very heavy.**

It was found that the radiation intake of plants polluted by cement dust increased, causing an increase in plant temperature and evapotranspiration (Dässler and Börtitz,

1988). The higher radiation values had a negative effect on dry matter production. Plant height, phytomass, net primary productivity, chlorophyll content, metabolites and yield were all reduced in response to cement dust in polluted areas. The percentages of dead branches on three halophytic species studied, increased with the amount of dust deposited. This in turn resulted in a reduction in plant yield. The water content, however, improved in the living parts of these plants in response to the more dusty conditions. Generally the chlorophyll concentration was reduced and the pH of the cell sap was disturbed (Magihid and El-Darier, 1995). Further effects of cement dust were necrosis of the leaf tissue (Neinhuis and Barthlott, 1988) and an 8.3% increase in water usage due to increased plant temperature and evapotranspiration. This is very important in areas with irregular or little precipitation (Anda, 1986). Sunflowers exhibit the influence of cement kiln dust as not only a reduction in the plants' vegetative parts but also a reduction in the formation of reproductive organs and in fertilisation. Some principal metabolic processes are also disturbed. These effects resulted in the reduced yield of seeds by 2-7% (Borka, 1980). Cement dust pollution is particularly unfavourable for fruit setting (Anda, 1986). Solid particles affect plant growth by reducing the light energy available for photosynthesis (Barfield and Gerber, 1979; Sai et al., 1987). The crop characteristics for Arhar and wheat crops were found increasing steadily with increasing distance from the cement works factory. The decreased crop yield could be attributed to the low chlorophyll content and low fertilization of pollen on the ovaries of crop plants on account of heavy dust fall (Sai et al., 1987). At an Asian coal mine the dust resulted in alteration of the leaf sizes, leaf masses and leaf physiology of certain nearby garden plants. In a further study done at a coal-fired power plant, it was found that annuals germinated and grew earlier in the season in the warmer soil. The dark colour of dust caused the soil temperature to rise, giving these plants a competitive advantage over typically aggressive species. Growth of annual species in particular is accelerated on coal dust. Although there was a marked increase in the accumulation of coal in this area over the past 15 years, there were no marked differences in the vegetation that were exposed to the dust compared to those that were not exposed (Spencer and Tinnin, 1997).

The alkaline and acid dust effects on epiphytic lichen vegetation in the Mediterranean were investigated around limestone and sandstone quarries. Results showed that the

amount of dust, thus the distance from the quarry, rather than the chemistry thereof had an effect on the vegetation. All but a few resistant species of lichen die when subjected to high dust concentrations. This suggests that they could be used for monitoring dust fallout and the effects of dust contamination (Loppi and Pirintsos, 2000). The biologic soil crust (BSC) acts as a natural dust trap that records a change in aeolian dust source over several decades (Reynolds et al., 2000).

In a study done it was found that the average diameter of pores on leaves is 5 to 10 μm in diameter. Therefore, only particles of 5 μm will be able to block the stomata appreciably. The blocking of stomata will prevent closure of the stomata during hot and dry periods or at night (Flückiger et al., 1979). That could cause a decrease in water use efficiency and expose interiors of organs to increased oxidant air pollutants. This in turn has a direct or indirect effect on plant performance. This could happen to desert plants, but particles wedged into stomatal pores are unlikely to have a significant effect on plant water loss during the night (Ricks and Williams, 1974; Sharifi et al., 1997). As a consequence, air pollution only occasionally lead to drought injury of plants.

The effects of dust on the gas exchange of three species of Mojave Desert shrubs were investigated. Physiological influences of dust accumulation on photosynthetic surfaces of these desert shrubs parallel results obtained in previous research of dust impacts on European roadside plants (Eller, 1977; Thompson et al., 1984). It was found that the maximum rates of net photosynthesis of dust covered organs were reduced. The maximum leaf conductance, transpiration and instantaneous water-use efficiency were all reduced. Dust covers the stomatal pores of photosynthetic stems and leaves and results in temperature increases of 2 to 3°C higher than those of control plants. This was found to be mainly due to greater absorptance of infra-red radiation (Eller, 1977; Neinhuis and Barthlott, 1988; Sharifi et al., 1997; Tyson et al., 1988). The increased temperatures also cause plants to use more water and influence the productivity of the plants. Absorbed energy in the wavelengths over 700 nm is more than doubled for dusty leaves and is the major factor causing overheating (Eller, 1977). Leaf temperatures approaching or exceeding 45 °C have the potential to cause significant heat stress and permanent tissue damage (Sharifi et al., 1997).

Increased rate of dust per unit leaf surface was found to be inversely related to absorptance of photosynthetically active radiation (PAR) and thus suggesting that increased density of dust would further reduce the rate of photosynthesis under conditions of high ambient air temperatures in summer conditions. It could thus be argued that an increase in the density of dust would be beneficial to a desert plant, if the leaf operates above light saturation. Dust also significantly increased PAR reflectance. Smaller leaf areas and greater leaf-specific masses were found in heavily dusted shrubs. This suggests that the short-term effects of reduced photosynthesis and decreased water-use efficiency may cause lowered primary production in desert plants exposed to dust during seasons when photosynthesis is occurring (Sharifi et al., 1997).

The accumulation of soot and dark coloured particles on leaf surfaces may seriously alter their adsorption and reflectance characteristics to incident radiation so that the energy balance of the leaves could be significantly altered, affecting the sensible and latent heat exchange and photosynthesis. The lowest dust load which reduces photosynthesis (by 23%) was found to be 5 g/m^2 and a dust load of 10 g/m^2 reduced photosynthesis by 18%, 30% and 24% in different experiments (Thompson et al., 1984).

It was found that increased permeability of the cuticle was caused by the action of particles on the leaf surface, possibly mechanical or sorptive action (Eveling and Bataillé, 1984). Dust on photosynthetic surfaces could increase roughness of boundary layer conditions. A thicker coating of dust particles on a leaf surface theoretically would cause a small decrease in the boundary layer conductance across the leaf/air transition that would lower transpiration rate. This would lead to lower evaporative cooling and increased leaf temperature and reduced growth. Irregular accumulations of dust would produce changes in turbulence of air flow over the plant organ.

Under turbulent dust deposition conditions, trees exhibited increased callus tissue formation on leaf surfaces. The resultant crust of particles that can form on leaf and bark surfaces, disrupts other physiological processes such as bud break, pollination and light absorption and reflectance. Some authors also reported indirect effects such as predisposition of plants to infection by pathogens (Beckett et al., 1998; Manning and Feder, 1980; Neinhuis and Barthlott, 1988; Ricks and Williams, 1974) and the

long-term alteration of genetic structure (Beckett et al., 1998; Manning and Feder, 1980).

2.3.3 Effects on the Soil

Dust fallout has an important influence on pedogenic processes in desert and arid area margins and even elsewhere. The chemical and grain size characteristics of the dust play a major role (Goudie, 1978). Some types of dust have effects on the soil in the change of pH and trace element content of soil, causing growth retardation in roots and plants and uptake of toxic substances. Above all, dust accumulates in the soil (Dässler and Börtitz, 1988). The rarity of typical desert loess found in several continental regions, demonstrates the formation to be restricted to specific geomorphic situations. In Namibia, loess-like sediments occur as river silt deposits and as adjacent basin fills, especially in the north-western regions.

It is rather astonishing when considering that arid and semi-arid environments have persisted (with hygric fluctuations) since the Upper Tertiary, when the Benguela Current contributed to the establishment of the Namib Desert (Dickinson and Preece, 1976). The dust is documented in soils and hidden in calcretes and can now be identified in the silt of the river terraces as a prominent part of loessic alluvial sediments. These can be used as sedimentary and morphodynamic indicators of climatic (hygric) fluctuations or changes in western Namibia. Figure 2.04 illustrates how dust is trapped by a gypsum outcrop on the mine at Waterkuil.

Dust's nutrient input and replenishment may be an important factor for the maintenance of soil fertility. The high nutrient status of some dust could be expressed by the enrichment ratio (ER) between dust and topsoil. The surface (0 - 1 cm) is the layer that is directly influenced by dust deposition. Inputs of nutrients into the system are determined by the quantity of dust and the quality of rain (Ramsperger et al., 1998). Alkaline dust could, by raising pH levels of the soil, have a secondary effect of causing eutrophication (Gilber, 1976). In steep contrast, problems occur in areas from which this nutrient rich upper layer of soil is removed (Zaady et al., 2001). Cement

dust was found to change soil characteristics by increasing the alkalinity slightly because the total soluble salts increased relatively (Magihid and El-Darier, 1995).



Figure 2.04 Dust trapped in a gypsum outcrop on the mine at Waterkuil.

In a study done on a coal-fired power generation plant in Portland, U.S.A. soil temperatures were significantly higher where coal dust was present. Temperatures on different aspects of mounded soil with coal dust differed by as much as 9 °C. Coal dust could increase the soil temperatures as much as 2.5 °C and the pH and metal ion concentration of water leaching from coal pits was found to be higher than normal. Organic matter was found to be more abundant in the presence of coal dust and generally the nutrients were more readily available (Spencer and Tinnin, 1997).

The deposition of fine aeolian dust has an effect on the mineralogy and chemistry of surface soil. Deposition of dust on sandy soils might have an ameliorating effect on its productivity on a long-term basis (Modaihsh, 1997). Gypsum dust may be produced by the interaction of carbonate dust and anthropogenic sulphates (Reheis and Kihl, 1995) and could improve water infiltration and plant growth, especially for acid, sodic and erosion-prone-soils (Becker, 1997). Resistibility of surface soils against erosion depends on soil texture, water content and soil structure (Zaady et al., 2001).

Structural state and structural stability of surface soil are important factors relating to soil erodibility by wind. Anthropogenic agents affect soil structures, and as a result

influence soil resistance to wind erosion. These degraded soils lead to desertification. The eroded soil sediments provide a source of particulate pollutants to the atmosphere. In the northern Loess Plateau of China, owing to the dry climate, loose structure of the soil and the history of unreasonable land use, dust emissions are severe environmental problems.

Mechanical disturbances loosen soil structure and soil packing density and reduce soil cohesion and mechanical stability. This process dislodges particles from soil clods or aggregates and makes them readily available for wind erosion and transport. The fine topsoil which is the most fertile portion may be removed, leaving the coarse soil fraction which contains lower nutrient levels and has lower water-holding capacity (Modaihsh, 1997). Roadside soil is enriched by NO_2 from exhaust emissions (Spencer et al., 1988). Dust deposition also plays an important role in the formation of duricrusts (Goudie, 1978).

2.4 Legislation Regarding Dust Deposition

Apart from the mining industry, there is no legislation, either directly or indirectly which relates to negative environmental impacts due to road transportation and the generation of dust on unpaved roads. Dust control is therefore generally considered in terms of economic benefits rather than in terms of environmental benefits. Dust is often identified by interested and affected parties during environmental impact assessments as a potential problem, requiring assessment and possible mitigation in new development projects. Probable dust levels can be predicted with prediction models. The amount of dust fallout that is allowed by the Department of Environment and Tourism is specified as:

- a) Slight: $<0.25 \text{ g/m}^2/\text{day}$,
- b) Moderate: $0.25 \text{ to } 0.5 \text{ g/m}^2/\text{day}$,
- c) Heavy: $0.5 \text{ to } 1.2 \text{ g/m}^2/\text{day}$ and
- d) Very heavy: $>1.2 \text{ g/m}^2/\text{day}$ (Jones, 1999).

Particulate matter is specified by the EPA (Environmental Protection Agency) in the USA in two sizes, namely particles smaller than 2.5 microns are referred to as $\text{PM}_{2.5}$,

whilst larger particles up to 10 microns in diameter are designated PM₁₀. The PM₁₀ classification includes most types of fugitive dust. The current EPA standard for PM₁₀ is an annual average of no more than 50 micrograms per cubic meter air volume. There is also an additional standard of 150 micrograms per cubic meter in any 24-hour period. This is the maximum acceptable acute level; communities are allowed to exceed this level only once a year over a three-year period to stay in compliance with clean air standards (Ferguson et al., 1999).

In many communities in arid areas, there has been a demand for regulations towards the controlling of blowing dust from construction sites, stockpiles, unpaved parking lots and school yards, mining sites and similar operations. Sometimes regulations are put in place that forces the operator to take reasonable precautions to prevent particulate matter from becoming airborne (Faith and Atkisson, 1972).

2.5 Conclusion

The presence of natural dust in the atmosphere depends on a variety of factors at different size scales. It could be at local, regional and continental scales. Factors such as geography, topography, meteorology, human elements and agricultural elements play an important role. It would therefore be necessary to investigate the atmospheric dust problem in an integrated way (Offer and Goossens, 1990). Changing dust composition could affect ecosystem processes, including perhaps the invasion of exotic species (Reynolds et al., 2000). More extensive physical field and laboratory studies are required to elucidate how dust affects physiological performance of vegetation in the semi arid environment. Investigation of dust effects at multiple sites is also necessary (Sharifi et al., 1997).

There is a need for accepted definitions for dust and especially clay aggregates. Diagnostic criteria are also needed for the identification of aeolian dust. Criteria should be tested at sites accepted as dust deposits. Perhaps dust should be identified not by its characteristics, but by its source. Whole landscape studies are necessary in the identification of dust deposits and to improve our understanding of their distribution and thickness, these should include the mapping of deposits. Process modelling is required that tests the generally accepted theoretical models, for instance

the general decrease in particle size with distance travelled from the source region. Process modelling should also include the effects of changes in wind speed on the nature of the traction and suspension load. A greater understanding of the distribution of dust deposits is required. Questions whether deposits can be mapped in a predictive way through remote sensing techniques such as radiometrics, need answering. Knowledge of the physical properties of dust mantles in particular their permeability and bulk density is important for environmental management and mineral exploration.

Permeability influences the upward and downward movement of soil water which has implications for processes such as geochemical dispersion, soil moisture storage and plant growth, soil erosion and soil salinisation (Green et al., 2001). Better models are needed for the different dispersal mechanisms taking place in aeolian mantles. Methods for the estimation of the amount of aeolian material present in a soil profile need to be developed. The deposition of dust is visible in Figure 2.05.



Figure 2.05 The dust deposition is visible as the grey fine grained top layer in the soil profile at this particular location in the study area.

This will improve the identification of an aeolian material signature and the significance of particle size on geochemical signatures. The thickness of aeolian

deposits over mineralised areas and the impact of masking mineralisation and geochemical anomalies have to be investigated.

Better time relation to the processes of aeolian deposits can be calculated in order to determine the period within which geochemical signatures and dispersion signals develop. Identification of areas where aeolian accession is likely to be a problem for mineral exploration.

As mentioned above, there are a variety of aspects of particulate pollution that need to be looked at and quantified. In developing countries like South Africa there is a need to establish exactly what amounts of dust are being generated from unpaved roads for different size class vehicles, the deposition pattern and distance of the suspended dust and the effect on roadside plants.

3 DUST SETTLING MODEL, CLIMATE OF THE STUDY AREA AND FIRST APPLICATION OF THE MODEL

3.1 Introduction

As briefly described in Chapter 1, the farmers in the vicinity of the mine raised concerns regarding the amount of sedimentation that happens with regards to the road transport and the impact that it might have on the vegetation. BPB Gypsum embarked on a study to determine the settling patterns of windblown sediment (mainly dust) created by road transport (Van Jaarsveld, 2002). No previous research has been done on the influence of dust on the plants of the region. Climatic data is scarce and unreliable and no research has been done on dust settling models in the greater region. A desk study of the historical climatic conditions was done and applied to the settling model. Once the settling model was derived, the monitoring system was expanded to cover a wider area along the transport route from the mine to the loading station. The data obtained was tested against the settling model.

3.2 Dust Settling Model

As no previous work existed regarding a model for the area, BPB Gypsum initiated a monitoring programme. The placement and findings were often discussed at public meetings with the local farmers and other interested and affected parties.

3.2.1 Method of Monitoring

A dust monitoring program was implemented on 26 April 2000 to measure the amount and fallout rate of dust along the public road DR 2972. The CSIR - XT1123 monitoring method was adapted for the conditions (Jones, 1999; Van Jaarsveld, 2002). The monitoring method evolved through a number of in-house experiments and comparison of results. 5-litre containers were used as dust traps, henceforth referred to as “containers”. Early morning moisture in the air and regular dew precipitation assisted with retaining the dust. The most suitable method was found to

be containers covered with fly screen to keep out any large organic particles. The fly screen cover did not affect the results. The containers were secured to two dropper poles, one meter above ground surface and the sample points were surveyed (Figure 3.01).

In order to establish a dust settling model, an area was identified at the turnoff of a privately owned haul road from DR 2972 (Loeriesfontein - Brandvlei road) to the gypsum loading station at Loop 8, referred to in Figure 3.02. The test site is bordered by the two roads, increasing the amount of dust generated on the eastern side, making the site ideal for establishing a settling model. The containers at the collection points were surveyed and placed at 20 m intervals over the first 100m from the side of the road, followed by a 200m section with container intervals of 50m, from the 100m mark to the 300m mark. The final container was placed 100m from the 300m mark at 400m from the side of the road. Collection points 1 to 11 were placed on the eastern side of the road and collection points 12 to 20 on the western side of the road.

The containers were placed at a 45° angle between the roads on the eastern side, reducing the true distance to any of the two roads (Figure 3.02). The angle factor was taken into consideration during the modelling process. The ambient dust level was calculated using the average of 8 containers, placed both east and west of the road, at 4 sites along the length of the road for the duration of the trial period. These containers were not affected by dust created by vehicle. The containers were collected, treated and replaced at the same time and in the same way as the test containers. The following CSIR fallout classification of slight $<0.25 \text{ g/m}^2/\text{day}$; moderate $0.25 \text{ to } 0.5 \text{ g/m}^2/\text{day}$; heavy $0.5 \text{ to } 1.2 \text{ g/m}^2/\text{day}$ and very heavy $>1.2 \text{ g/m}^2/\text{day}$ was used to quantify the fallout rate (Jones, 1999). The data collected over the monitoring period are presented in Table 3.01



Figure 3.01 Dust traps containers on the eastern side of the road at the modelling site.

The settling model was derived over a period of 9 months from 26 April 2000 to 24 January 2001. The containers were positioned for certain periods of time, as described in Table 3.01. Once collected and replaced with another set of containers of the same dimensions, the collected dust was weighed and the fallout recorded. In order to apply the CSIR fallout classification, the dimensions of the 5 litre containers (19 cm by 19 cm) were converted to 0.0361 m^2 and the total amount of dust collected was divided by the dimensions of the container and the number of days resulting in $\text{g/m}^2/\text{day}$. The containers were sealed in individual plastic bags to avoid contamination or losses during transportation. As previously described, the ambient dust level was calculated using the average of 8 containers, placed both east and west of the road, at 4 sites. The containers were placed at distances of 400 m from the side of the road. These sites coincided with the expanded monitoring system sites (Chapter 3.4).

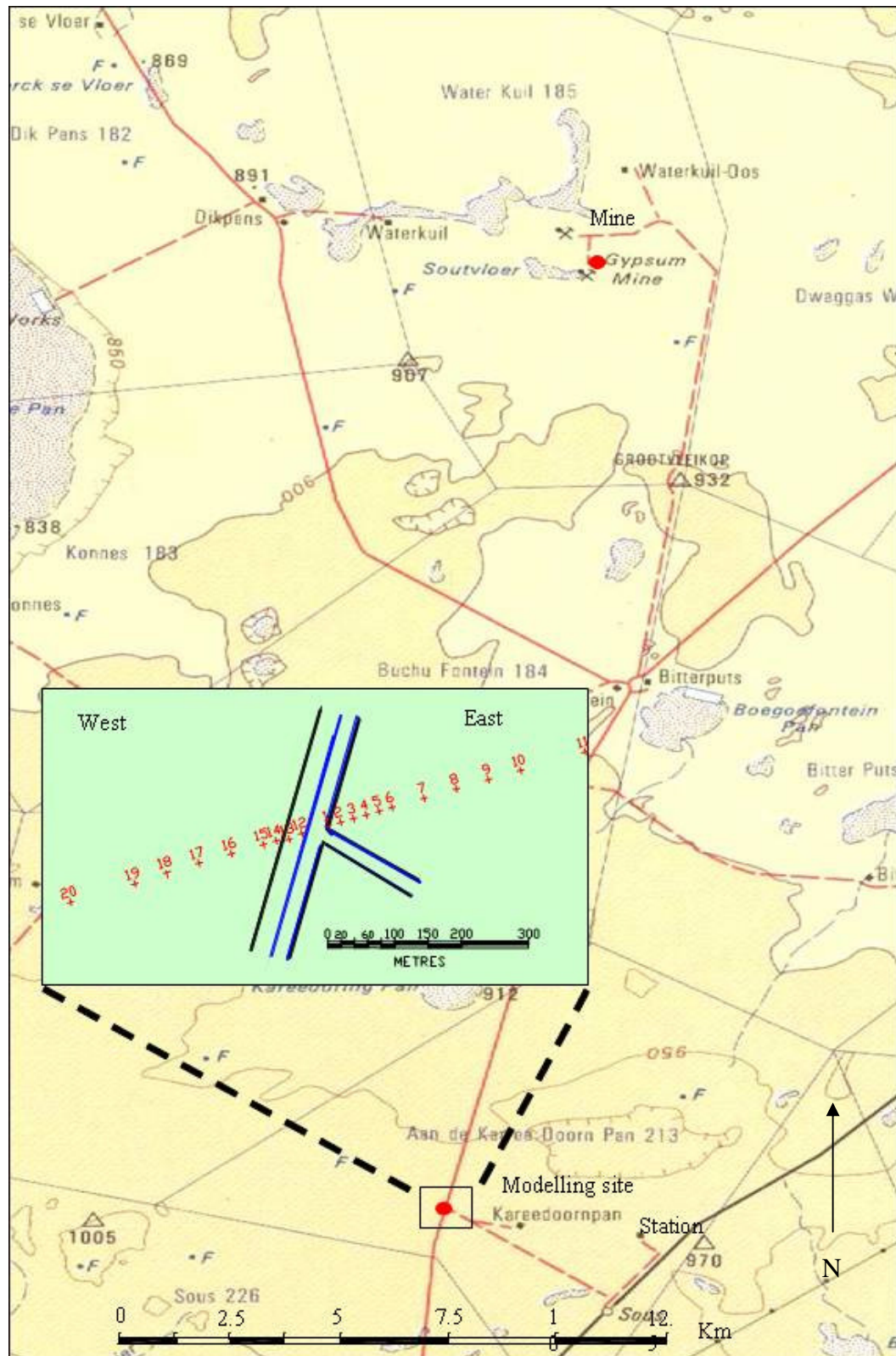


Figure 3.02 Map indicating the modelling site and the general geography of the investigated area.

3.2.2 Results and Discussion of the Dust Settling Monitoring

The average fallout for the period is proposed as a basis for the development of a model to predict dust fallout along the route. Data was collected for the months of May 2000 to January 2001.

Table 3.01 Data collected monthly over the monitoring period

Monitor no. East	Distance from Rd (m)	Corrected distance (m)	May-00 Fallout g/m ² /day	Jun-00 Fallout g/m ² /day	Jul-00 Fallout g/m ² /day	Aug-00 Fallout g/m ² /day	Oct-00 Fallout g/m ² /day	Jan-01 Fallout g/m ² /day	Average Fallout g/m ² /day	Classification
1	1	0.8	1.878	0.647	1.269	1.882	1.846	2.331	1.595	Very Heavy
2a	20	16.3	0.978	0.218	0.359	0.564	0.293	0.413	0.369	Moderate
3	40	32.6	0.834	0.105	0.211	0.368	0.111	0.114	0.182	Slight
4	60	48.9	0.859	0.130	0.169	0.374	0.132	0.202	0.201	Slight
5	80	65.1	0.803	0.053	0.164	0.358	0.142	0.109	0.165	Slight
6	100	81.4	0.822	0.063	0.132	0.382	0.093	0.081	0.150	Slight
7	150	122.1	0.790	0.017	0.138	0.160	0.127	0.129	0.114	Slight
8	200	162.8	0.794	0.011	0.070	0.126	0.069	0.091	0.073	Slight
9	250	203.5	0.802	0.023	0.091	0.254	0.059	0.038	0.093	Slight
10	300	244.3	0.769	0.010	0.117	0.331	0.061	0.040	0.112	Slight
11	400	325.7	0.797	0.005	0.098	0.335	0.156	0.079	0.135	Slight
Monitor no. West										
12	25.24	20.6	0.973	0.193	0.185	0.000	0.109	0.180	0.133	Slight
13	45.24	36.8	0.863	0.086	0.121	0.350	0.091	0.098	0.149	Slight
14	65.24	53.1	0.832	0.090	0.152	0.248	0.142	0.123	0.151	Slight
15	85.24	69.4	0.830	0.083	0.084	0.376	0.095	0.039	0.135	Slight
16	135.24	110.1	0.825	0.064	0.098	0.292	0.077	0.037	0.114	Slight
17	185.24	150.8	0.795	0.017	0.074	0.171	0.049	0.023	0.067	Slight
18	235.24	191.5	0.783	0.001	0.058	0.125	0.092	0.062	0.067	Slight
19	285.24	232.2	0.820	0.005	0.051	0.297	0.062	0.080	0.099	Slight
20	385.24	313.7	0.771	0.003	0.083	0.275	0.039	0.007	0.081	Slight

The containers were sabotaged during September and November 2000 and the data were discarded. The data for May were recorded, but because the containers were at ground level, the data were disregarded for modelling purposes.

From the results obtained over this period, it is apparent that the dust fallout is high over the first 16 m from the side of the road. It is moderate over the following 15 m and slight from there on. Thirty-eight percent of the dust settled within the first meter from the side of the road; 58% settled within a distance of 32 to 36 m. The remainder of the dust settled in a wave pattern, with slight variations in the frequency of the

wave. Settling peaks were apparent at 50 m and at 240 to 250 m from the side of the road. The reason for this settling pattern is not clear (Figure 3.03).

In total, 66% of the collected dust settled within 50 m from the side of the road. Within 100 m from the side of the road, 80% of the total collected dust settled.

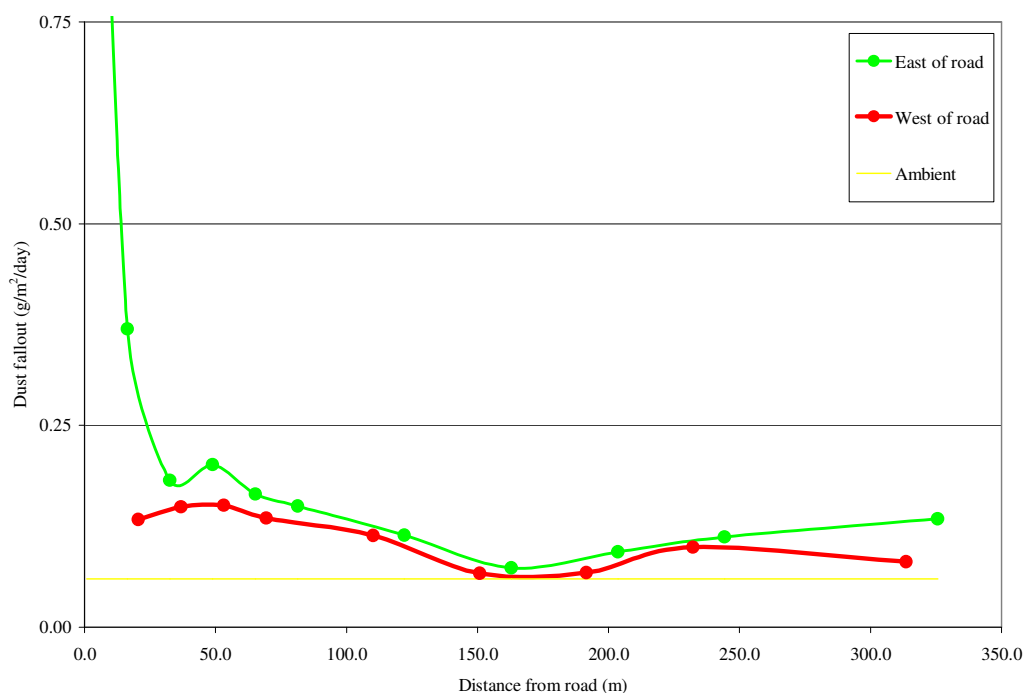


Figure 3.03 A graphic representation of the dust settling model for the two opposite monitoring directions.

The eastern side recorded marginally higher values, but both sides reflected the same settling pattern. After 350 m from the side of the road, the fallout was marginally higher than the ambient fallout. At worst the fallout is double the ambient fallout of 0.066 g/m²/day and at best 20% more than the ambient fallout. The fallout data showed a steady increase from June 2000, with August 2000 being the highest, and then decreasing for October 2000 and remaining more or less the same for December 2000 and January 2001. Various factors might influence the findings. Climatic conditions (mainly rain and wind), fluctuations in transport and road maintenance (condition of the road surface) were investigated for their influence on the results.

As previously indicated, the fallout results for May 2000 were disregarded as the containers were placed on the ground. September and November 2000 fallout rate

were also disregarded as the containers were sabotaged. A comparison between transport and fallout rate shows some correlation for June, July and August. During June, BPB introduced a speed limit of 70 km/h for its transport, reflected by the green line on the graph (Figure 3.04). No apparent affect of the introduction of the speed limit, transport frequency and fallout rate for June, July and August. In October and November, the transport frequency increased with a decrease in fallout rate.

During September, BPB started to sponsor increased road maintenance in the form of wet grading of the road surface. A hardened surface gradually formed over the period September to January. The positive result of the maintenance is visible as a sharp decrease in the fallout rate between August and October. However, fallout for the period December to January increased, while transport levels for this period decreased, and maintenance remained the same.

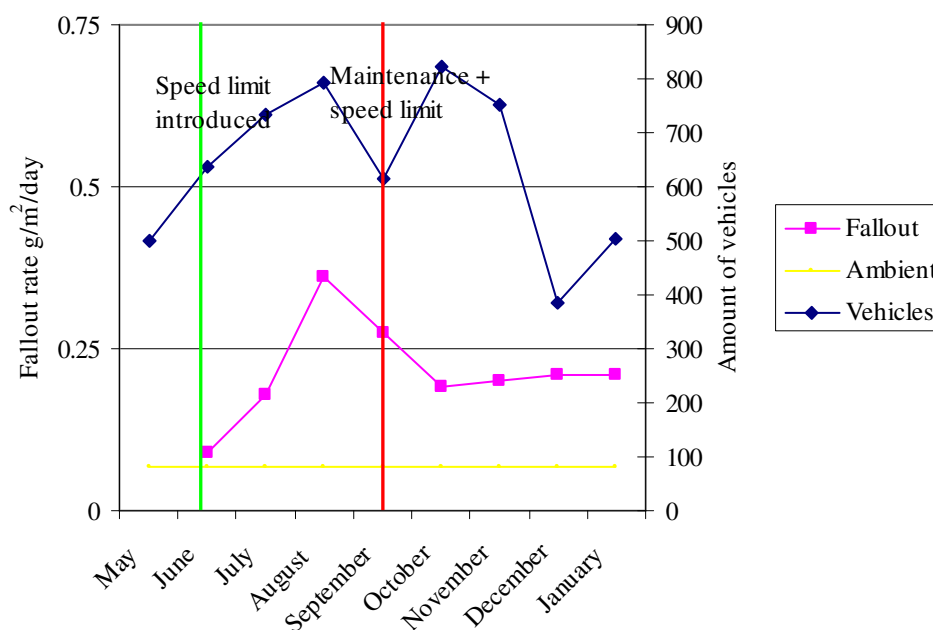


Figure 3.04 The average fallout dust, integrating all measuring points, measured in relation to the amount of passing vehicles and the influence of the introduction of a speed limit and later on, the influence of regular maintenance in combination with the speed limit.

Analysis of weather data (wind and precipitation) for this region has provided no definite correlation with the fallout rate (Figure 3.05). Rainfall data was obtained from a local farmer for the farm Kareedoorpan, while wind speed data was obtained from the Department of Environment Affairs recorded at the Brandvlei weather station.

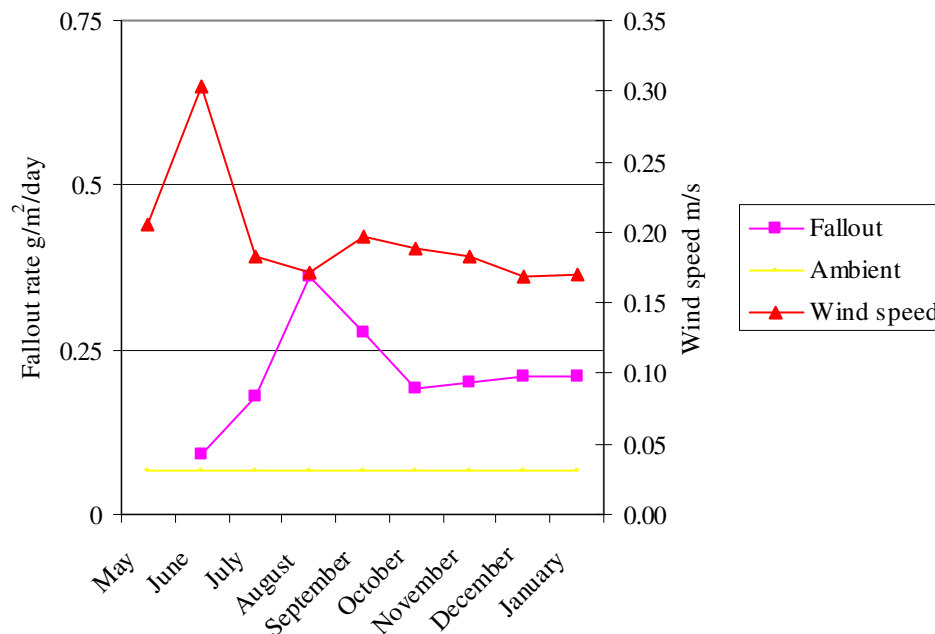


Figure 3.05 The average fallout dust measured in relation to the wind speed.

Precipitation in the form of rain for the period May 2000 to January 2001 was negligible apart from early morning dew. The possibility of dew formation for this area is more widely discussed in Chapter 5. The wind speed reflected a peak during June, while the fallout was low. The fallout increased sharply in August, while the wind speed decreased and remained mostly constant for the duration of the trial period. Large amounts of dust may have an important impact on the local weather or the atmospheric circulation in the desert boundary layer. They affect the amount of solar radiation reaching the ground, influence the shear and connectivity within the boundary layer and determine the visibility near the ground and at high altitudes (Offer & Goossens, 1990).

Wind speed and rainfall information did not explain the previously described incident where transport decreased, maintenance remained constant, but fallout increased

during December and January. Alternative explanations for this phenomenon are either: (i) an increase in ambient dust, or (ii) other road users contributing more to the fallout, than what was originally expected. The general tendency was that maintenance improved dust suppression, but more data are needed to confirm this.

3.3 Climatic Investigation

During this dust model monitoring period, it became evident that the climatic conditions might have a stronger long term influence. They played a minor role during the monitoring, hence the small difference in fallout east and west of the road.

3.3.1 Method of Monitoring

In order to investigate the possible long-term climatic influence, a desk study was conducted on the weather and climate conditions of the area. The historical information was collected from various sources. During this phase of the study, it became obvious that it would be beneficial to have an onsite weather station. The detail of the benefits will be discussed in the next chapter.

3.3.2 Results and Discussion of the Climatic Information

The study area is situated in the central Boesmanland. The greater region is described as desert and poor steppe, which is typified by cool, dry winters and hot summers. Rainfall is variable from 50 to 150 mm per annum (Table 3.02). This occurs mainly as summer and autumn showers, generally during 2 days per month. Single, very rare showers can account for as much as the normal annual precipitation. Extreme droughts occur in cycles of approximately 11 to 15 year intervals. Temperature varies greatly, both seasonally and diurnally. The average maximum daily temperature in January is about 35° C and 18° C in July. Extremes can reach up to 46° C in January and 32° C in July. The average daily minimum temperatures for January and July are 17° C and 3° C respectively, with extremes reaching 5° C in January and -10° C in July (Table 3.04). Frost is common in winter with rare occurrences of snow. An anticyclone dominates the weather pattern during the winter season. Hail is not very common in the area and occurs on less than 0.66 days per year. Table 3.03 indicates

the maximum rainfall intensities per month, over 24 hours and in 50 year events. The prevailing winds in spring and summer vary from south-east to south-west at average speeds of 4, 4 to 4, 5 m/s. Stronger winds of up to 17 m/s occur for approximately four days during the late winter and spring months of July to November. The autumn and winter months are dominated by south-easterly to north-easterly winds with speeds of 4 to 4, 1 m/s (Table 3.05 and Figure 3.06).

Table 3.02 A. The mean monthly and annual rainfall (in mm) for the area and B. The number of days per month with measurable precipitation.

A	BRANDVLEI	POFADDER	KENHARDT	
	1918-1990	1933-1990	1960-1978	MONTHLY
	72 YEARS	57 YEARS	18 YEARS	MEAN
Jan	12	9	15	12
Feb	17	16	29	21
Mar	27	21	31	26
Apr	16	13	17	15
May	10	7	11	9
Jun	6	3	6	5
Jul	6	5	5	5
Aug	4	3	4	4
Sep	5	5	5	5
Oct	9	4	8	7
Nov	11	11	9	10
Dec	9	8	11	9
Mean annual				129

B	BRANDVLEI	POFADDER	KENHARDT	
	1918-1990	1933-1990	1960-1978	MONTHLY
	72 YEARS	57 YEARS	18 YEARS	MEAN
Jan	0.4	0.2	0.5	0.37
Feb	0.3	0.5	1	0.6
Mar	1.1	0.8	1	0.97
Apr	0.6	0.4	0.4	0.47
May	0.4	0.1	0.3	0.27
Jun	0.2	0.1	0.1	0.13
Jul	0.1	0.1	0.2	0.13
Aug	0	0	0.2	0.07
Sep	0.2	0.2	0.1	0.17
Oct	0.3	0.1	0.1	0.17
Nov	0.4	0.2	0.5	0.37
Dec	0.3	0.2	0.3	0.27
Mean annual				0.33

Table 3.03 The maximum rainfall intensities per month, 24 hours and 50 year events

	max/month		max/24 hrs		max/24 hrs/50 years	
	mm		mm		mm	
Jan	164	Kenhardt	82	Kenhardt	56	Brandvlei
Feb	162	Kenhardt	78	Brandvlei	78	Brandvlei
Mar	130	Kenhardt	51	Brandvlei	51	Brandvlei
Apr	137	Brandvlei	98	Brandvlei	98	Brandvlei
May	70	Pofadder	38	Pofadder	38	Pofadder
Jun	52	Brandvlei	42	Brandvlei	42	Brandvlei
Jul	80	Kenhardt	51	Brandvlei	51	Brandvlei
Aug	75	Brandvlei	27	Brandvlei	27	Brandvlei
Sep	53	Kenhardt	43	Brandvlei	43	Brandvlei
Oct	85	Brandvlei	71	Brandvlei	71	Brandvlei
Nov	83	Brandvlei	61	Pofadder	61	Pofadder
Dec	68	Pofadder	68	Pofadder	68	Pofadder

Table 3.04 The mean monthly A. maximum and B. minimum temperatures in °C calculated from three stations in vicinity the study area.

A		BRANDVLEI	POFADDER	KENHARDT	Mean
		1940-1984	1939-1984	1930-1960	Max
	Jan	33.9	33	35.7	34.2
	Feb	33.3	32.2	34.4	33.3
	Mar	30.6	29.8	31.9	30.8
	Apr	25.9	25.6	27.7	26.4
	May	21.5	20.8	23.1	21.8
	Jun	18.5	17.8	20.2	18.8
	Jul	18.4	17.7	19.7	18.6
	Aug	20.3	19.3	22.2	20.6
	Sep	24	23.4	25.7	24.4
	Oct	27.1	26.6	29.3	27.7
	Nov	30.2	29.9	31.8	30.6
	Dec	32.2	31.9	34.6	32.9

B		BRANDVLEI	POFADDER	KENHARDT	Mean
		1940-1990	1939-1990	1930-1960	Min
	Jan	15.8	16.8	19.1	17.2
	Feb	15.7	17	18.5	17.1
	Mar	14.1	15.8	16.4	15.4
	Apr	9.7	12	11.8	11.2
	May	5.1	8	6.6	6.6
	Jun	1.9	5.5	3.3	3.6
	Jul	1.2	4.7	2.5	2.8
	Aug	2.6	5.8	4.3	4.2
	Sep	5.7	8.4	7.5	7.2
	Oct	9	10.6	11.3	10.3
	Nov	12.1	13.5	14.6	13.4
	Dec	14.3	15.4	17.7	15.8

Table 3.05 A. Wind direction frequency (average number of winds) and B. wind speed (m/s) tables for Pofadder (1940 to 1990)

A		N	NE	E	SE	S	SW	W	NW
	Jan	31	48	31	151	190	244	104	71
	Feb	38	60	42	152	160	191	93	96
	Mar	69	85	41	152	112	125	71	96
	Apr	71	96	59	137	77	91	62	89
	May	60	113	61	115	68	81	60	85
	Jun	68	156	73	104	60	67	58	78
	Jul	69	159	58	119	61	66	56	71
	Aug	61	124	45	137	89	109	82	66
	Sep	49	77	50	155	118	152	78	69
	Oct	32	65	45	155	137	188	97	77
	Nov	30	49	42	148	170	216	101	83
	Dec	24	38	41	146	184	227	110	79
	Ave	50	89	49	139	119	146	81	80

B		N	NE	E	SE	S	SW	W	NW
	Jan	3.4	4.3	4.4	4.7	5.3	4.7	3.8	3.9
	Feb	3.7	3.9	3.6	4.4	4.8	4.4	3.5	4
	Mar	4	3.8	3.6	4.1	4.2	4	3.7	4
	Apr	4.2	4.3	3.7	3.6	3.7	4	3.9	4.1
	May	4.1	4.4	3.2	3.4	3.5	4.5	4.7	4.2
	Jun	4.3	4.5	3.3	3.1	3.9	4.5	4.2	4.4
	Jul	4.4	4.3	3.3	3.3	3.7	4.2	4.3	4.4
	Aug	4.8	4.9	3.4	3.8	4	4.2	4.7	4.4
	Sep	4.3	4.6	4.2	4.3	4	4.5	4.2	4.4
	Oct	4.3	4.7	4.2	4.7	5	5.2	4.3	4.3
	Nov	4.5	4.5	5	5.1	5.5	4.9	4.2	4.1
	Dec	3.9	4	4.4	5.2	5.6	4.9	4.3	4
	Ave	4.16	4.35	3.86	4.14	4.43	4.50	4.15	4.18

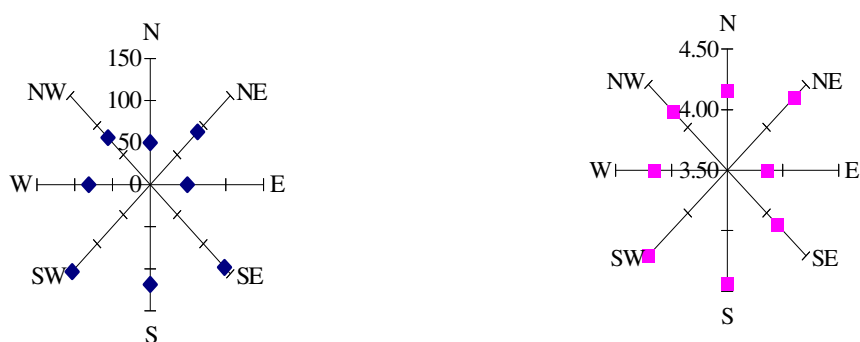


Figure 3.06 Wind rose diagrams indicating the wind direction frequency in average number of winds in blue and the wind speed in m/s in pink.

As Pofadder is the nearest weather station with wind information, this station was used to determine the historical wind speed and direction information. The information represents a 50 year time period between 1940 and 1990.

The information recorded in Table 3.06 was obtained from the Department of Water Affairs and Forestry: The mean evaporation figure for the greater region is 2200 – 2600 mm per annum (S-type pan). The nearest available mean monthly evaporation figures are these of Upington and Vredendal, recorded for the past 30 years.

Table 3.06 The mean monthly evaporation figures for Upington and Vredendal for the past 30 years

	mm / month	% Total Evaporation
Jan	260	12.10%
Feb	185	8.60%
Mar	175	8.20%
Apr	115	5.40%
May	85	4.00%
Jun	75	3.50%
Jul	95	4.40%
Aug	145	6.80%
Sep	195	9.10%
Oct	255	11.90%
Nov	260	12.10%
Dec	295	13.80%

3.4 Expansion of the Dust Monitoring Process

With reference to the settling model and the aforementioned climate information, the dust monitoring system was expanded to four monitoring positions along the route (Figure 3.06). Monitoring Sites were set up at locations described and are referred to as:

- 1) Gypsum road,
- 2) Boegoefontein
- 3) Kareedoring Pan
- 4) Station.

3.4.1 Method of Monitoring

The Monitoring Sites at Gypsum road, Boegoefontein and Kareedoonpan were chosen with intervals of approximately 6 to 8 km apart. The testing site at Station (at Loop 8) was chosen to monitor the influence of the dust created by the loading process (Figure 3.07). At each site, dust containers were surveyed and placed on both sides (east and west) of the road. The first container was sited next to the road servitude and then at 200m and 400m from the road. The containers placed next to the road and at 200m, were placed to roughly reflect the settling peaks around 0 to 20m and 200 to 250m as described in the model. The last containers placed at 400m, were placed to monitor the extreme limits of dust settling. The containers were placed perpendicular to the road (Van Jaarsveld, 2003).

Data were collected on a monthly basis for February, March, April and May 2001. June to August 2001 and September to November 2001 were replaced after three months to test the accuracy of the monitoring over a three month monitoring period. The results proved indicated that the monitoring period could be extended to 3 months without compromising the accuracy of the data. The dust settling model indicated 38% settling within the first meter, 58% within 32m and 80% within the first 100m.

3.4.2 Results and Discussion of the Expanded Monitoring

The data collected over the monitoring period is recorded in Table 3.07. Some of the data had to be discarded for various reasons, including sabotage and sheep bending the dropper poles and the collectors away from the dust source.

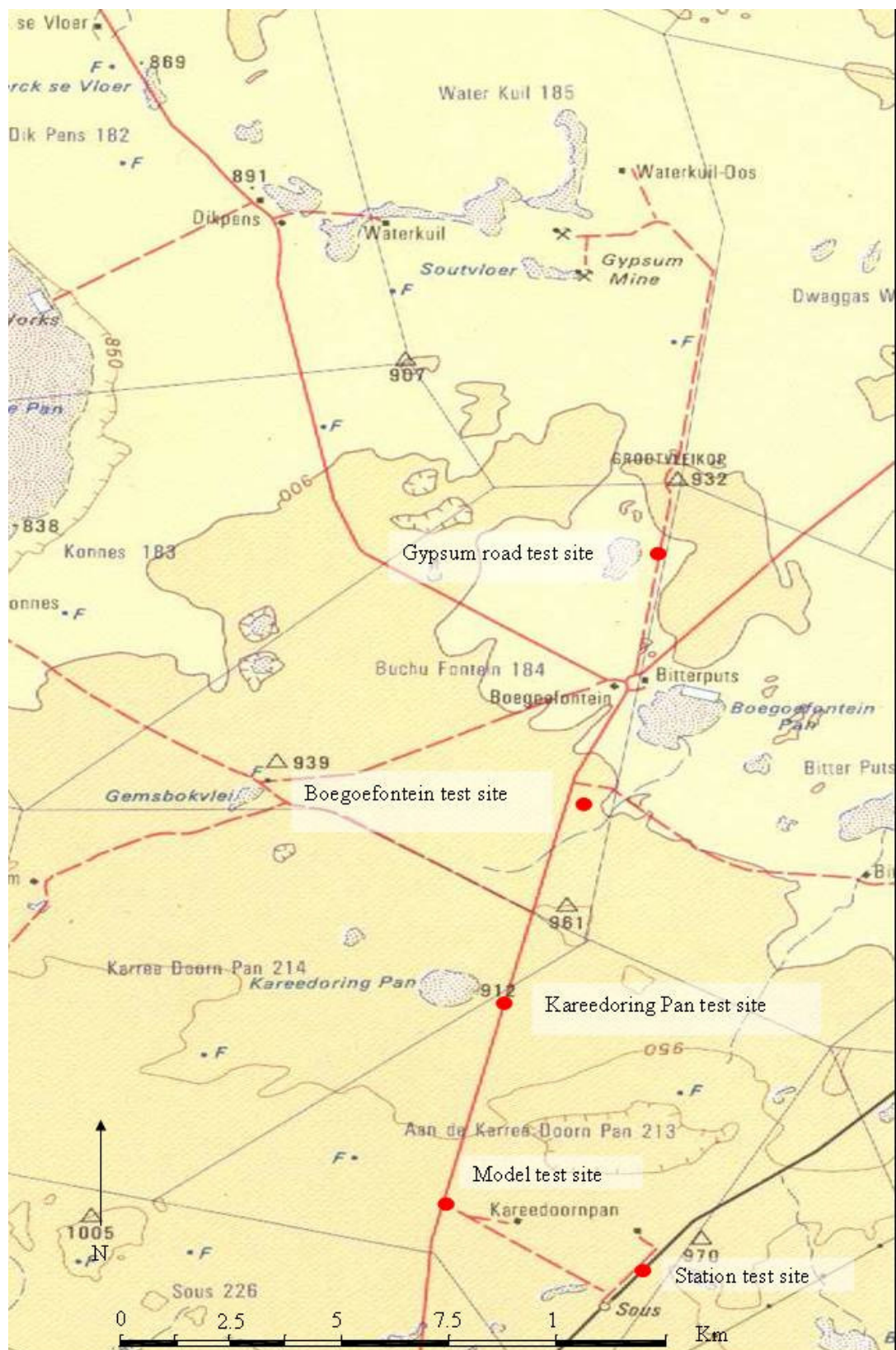


Figure 3.07 Map indicating the test sites of the expanded monitoring system.

Table 3.07 Data collected over the period of monitoring.

Monitor number	Distance from Rd (m)	Feb-01 Fallout g/m ² /day	Mar-01 Fallout g/m ² /day	Apr-01 Fallout g/m ² /day	May-01 Fallout g/m ² /day	Sep-01 Fallout g/m ² /day	Dec-01 Fallout g/m ² /day	Average g/m ² /day	Classification
Site: 1 - Gypsum road									
1 (east)	15	0.054	*	0.147	0.104	0.102	0.111	0.103	Slight
2 (east)	200	0.068	*	0.056	*	0.029	0.026	0.045	Slight
3 (east)	400	0.012	0.139	*	0.048	0.020	0.020	0.048	Slight
4 (west)	-10	0.032	0.449	0.087	0.091	0.062	0.140	0.143	Slight
5 (west)	-200	0.025	*	0.004	0.021	0.020	0.023	0.019	Slight
6 (west)	-400	0.060	0.068	*	0.032	0.022	0.011	0.039	Slight
Site: 2 - Boegoefontein									
7 (east)	12	0.172	0.072	0.168	0.104	0.190	*	0.141	Slight
8 (east)	200	0.033	0.074	0.083	0.067	0.016	0.030	0.051	Slight
9 (east)	400	0.068	*	0.031	0.047	0.014	0.024	0.037	Slight
10 (west)	-5	0.631	0.240	0.370	0.269	*	0.196	0.341	Moderate
11 (west)	-200	*	0.009	0.075	0.025	0.022	0.014	0.029	Slight
12 (west)	-400	*	0.041	0.059	0.053	0.025	0.025	0.041	Slight
Site: 3 - Kareedoringpan									
13 (east)	2	0.732	0.200	1.189	0.983	*	*	0.776	Heavy
14 (east)	200	0.122	0.053	0.063	0.043	*	0.022	0.061	Slight
15 (east)	400	0.067	0.034	0.061	0.066	0.047	0.013	0.048	Slight
16 (west)	-15	0.033	0.040	0.129	0.173	*	*	0.094	Slight
17 (west)	-200	0.016	0.061	0.015	0.080	*	0.047	0.044	Slight
18 (west)	-400	0.035	0.020	0.029	0.080	0.025	0.029	0.036	Slight
Site: 4 - Station									
19 (west)	-18	0.323	0.274	0.431	0.112	0.199	0.225	0.261	Moderate
20 (west)	-200	0.013	0.018	0.057	0.065	0.045	0.035	0.039	Slight
21 (west)	-400	0.020	0.088	0.041	0.056	0.030	0.015	0.042	Slight
22 (east)	30	0.241	0.025	0.158	0.296	0.100	0.236	0.176	Slight
23 (east)	200	*	0.072	0.068	0.035	0.041	0.029	0.049	Slight
24 (east)	400	*	0.068	0.178	0.147	0.045	0.113	0.110	Slight

* Data discarded

The average of the data collected over the monitoring period was directly compared to that of the dust settling model. Note that the distances from the centre of the road to the western side of the road are presented by negative x-axis values on Figure 3.08. The results indicated that the comparison was visually favourable (Figure 3.09). This confirmed that the settling model was able to predict the settling patterns along the transport route and that the model is acceptable as an empirical model. Further statistical analysis of the empirical dust settling model data indicated that the trend of the data can be described by the equation $y = 1.0244x^{-0.4599}$ in Figure 3.09 (Clark, 2001). The data of the expanded dust monitoring system was compared to the results after the settling model equation was applied to the data. The results are remarkably similar and the assumption is made that the equation of the dust settling model can be applied to further monitoring systems. The result of the application is presented in Figure 3.10.

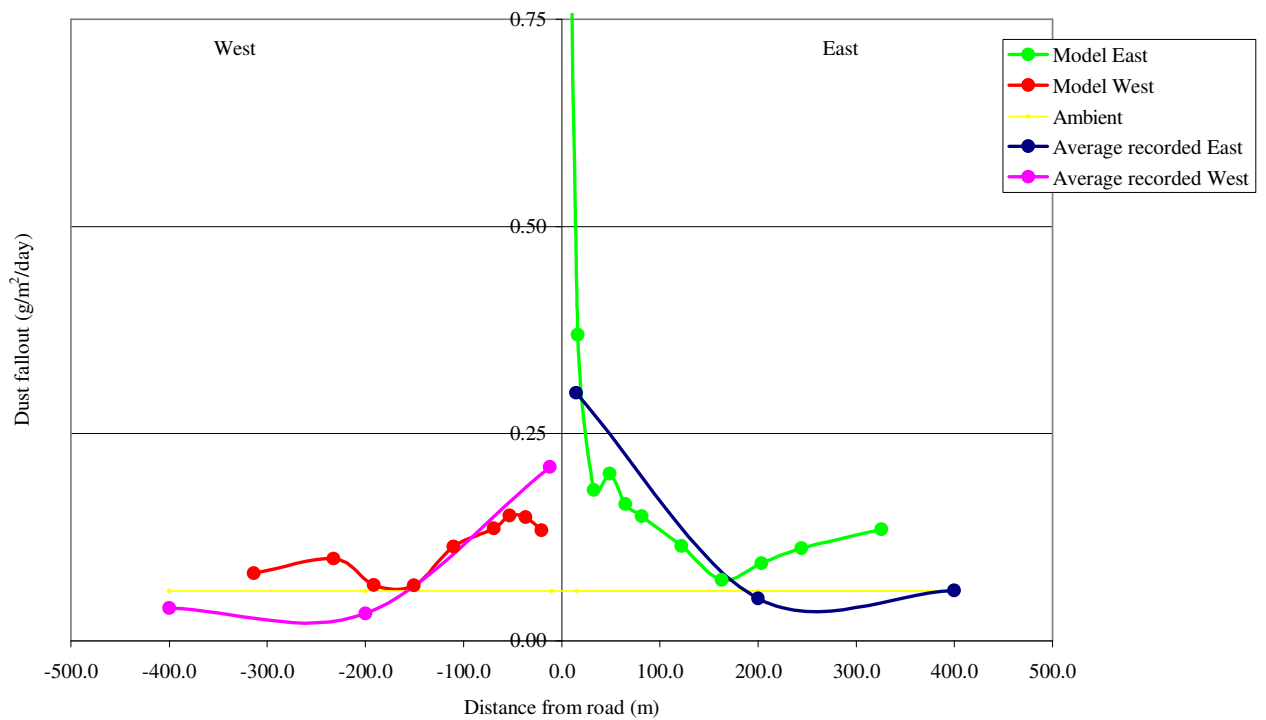


Figure 3.08 Comparison between the settling model and the averages of data collected with the expanded monitoring system.

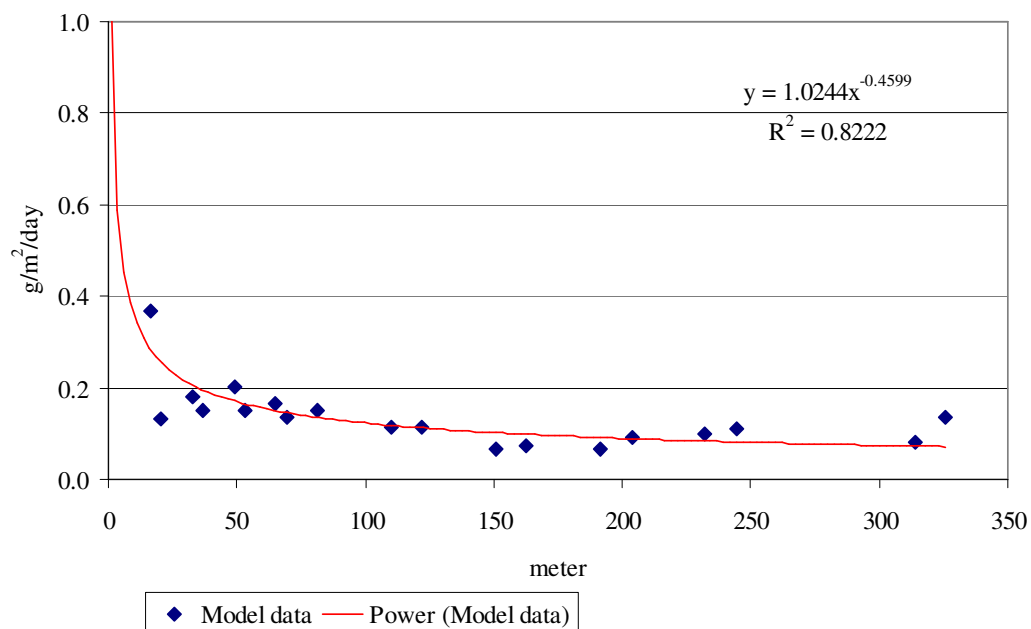


Figure 3.09 The equation of the data trend of the empirical dust settling model.

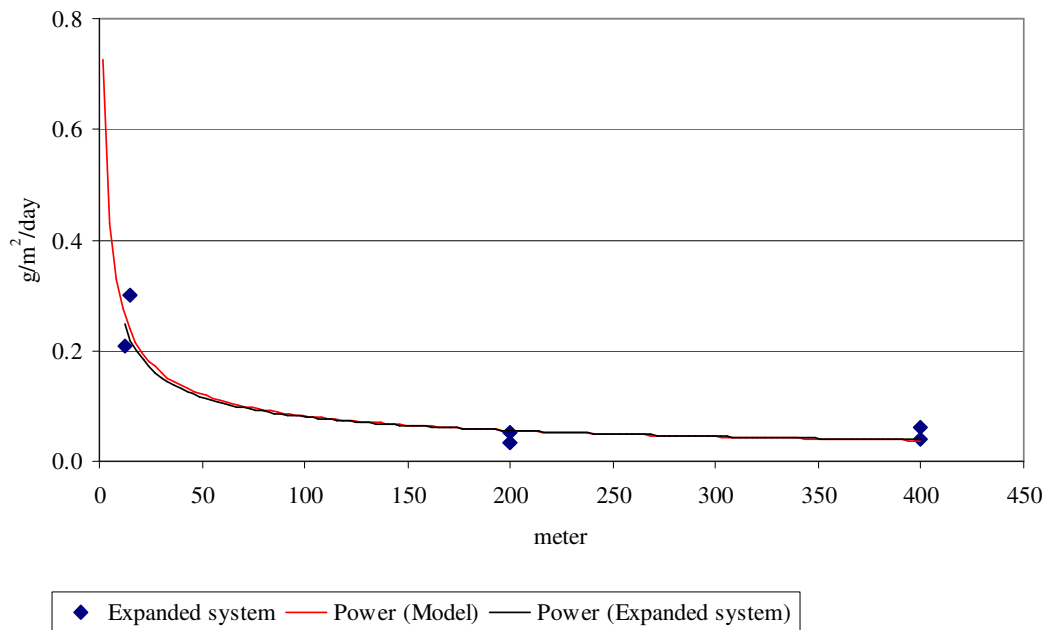


Figure 3.10 A comparison between the trend of the expanded monitoring system and the equation of the dust settling model applied to the data of the expanded system.

3.5 Conclusion

During the investigation of the model, various dust reducing practices were tested of which the introduction of speed limits in conjunction with regular maintenance proved to be quite effective. After the model was derived, the historical weather information was researched to aid with the placement of the expanded dust monitoring system.

The success of the investigation became evident when the settling model was applied to the data of the expanded monitoring. It became apparent that the model prediction was very similar to the actual recorded fallout. During the prolonged monitoring, it became obvious that climatic conditions played a more pronounced role in the longer term and that onsite weather monitoring might shed better light on dust management aspects. The application of climatic conditions could also aid in understanding the impact of the dust on the environment.

4 WIND TRANSPORTED SEDIMENT MONITORING AND MONITORING OF ITS IMPACT

4.1 Introduction

In order to monitor the impact of the wind transported sediment, it is necessary to have a better understanding of the climatic conditions. It is further necessary to monitor the impact on the vegetation of the area. In order to be able to draw three way correlations between the climatic indicators and the impact on vegetation, dust deposition and the impact on the vegetation and the climatic parameters and the impact on dust generation, the monitoring sites were combined and relocated to the same positions. BPB Gypsum moved their mining operations at the start of this investigation from the old Waterkuil mine to the mine at Dikpens (Figures 3.06 and 4.03). This provided an ideal situation to apply knowledge gained up to this point, as described in the previous chapter, to aid with the mine layout and quarry planning.

4.2 Methodology

This investigation combines three important monitored aspects. It includes climatic monitoring with an onsite automatic weather station, the dust fallout in the general region and the change in vegetation over time. It is important to note that the monitoring of these parameters is ongoing and data collection is still continuing. In order to avoid confusion, the data collection points were moved to five collection points named Monitoring Sites, followed by a number and name (Figure 4.03.).

4.2.1 Climate

As described in the previous chapters, it became apparent that more detailed climatic information was needed. BPB Gypsum placed an Automatic Weather Station (AWS) at the new Dikpens mine, Monitoring Site 4: Konnes. The AWS is located at 30°

12.969' S, 19° 28.921' E and the Monitoring Site is described in more detail elsewhere in this chapter (Figure 4.01). Data has been continually collected, averaged and recorded hourly since 27 July 2003. Parameters being measured are temperature, relative humidity, rainfall, wind speed and wind direction. This site was chosen next to Konnes pan, as it is free from mining and transport sedimentation and other influences.



Figure 4.01 The Automatic Weather Station (AWS) at Monitoring Site 4: Konnes.

4.2.2 Dust Monitoring

After the settling model was favourably compared to the expanded monitoring system, it was changed to monitor the new mining operation, as the mining operation relocated from the site at Waterkuil to the site next to the large pan, called Konnes Pan (Figure 4.03). The new mine is called Dikpens mine. The CSIR - XT1123 monitoring method was once again adapted with five-litre containers that measure fallout dust, covered with fly screen to keep out any particles larger than dust. The containers were secured to two dropper poles, one meter above ground level. The containers are effective in collecting the vertical or fallout dust component but it was found that in stronger wind conditions the windblown sediment or horizontal component was not

collected effectively (Goossens et al., 2000). An applied method of monitoring volumes of windblown dust, called a POLCA sampler, was adapted (Goossens et al., 2000). The Soil science Department of the University of Stellenbosch adapted the design. It consists of a glass bottle, lined with a sealable plastic bag (Figure 4.02). The bottle is sealed with a polystyrene lid with two glass pipes feeding windblown dust into the bottle. The effect created by the pipe system forms a low pressure inside the bottle, causing a weak suction effect and dust settles inside the plastic bag (Bueche, 1988). The bottle is orientated towards the main wind direction, facing the source of dust. The bottles are secured to the same poles as the fallout containers. These are referred to as “polca samplers” in this thesis. Polca samplers give a point source indication of windblown dust.

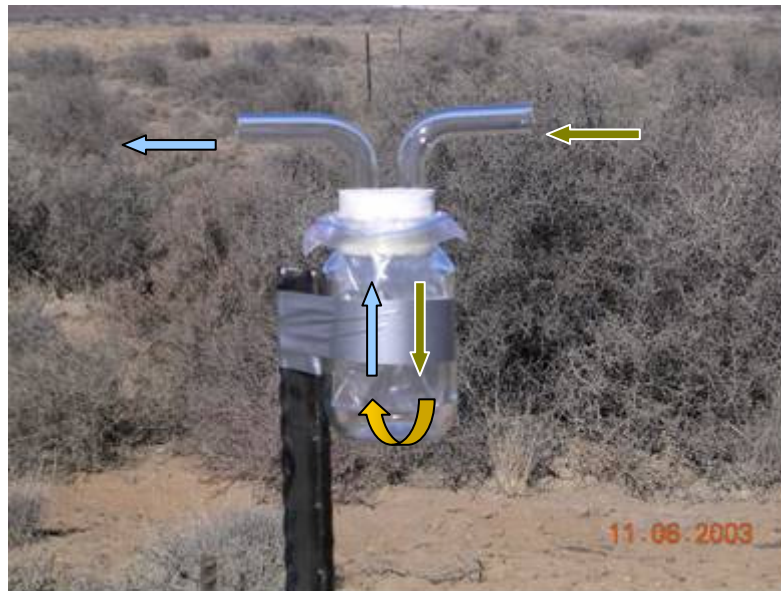


Figure 4.02 The POLCA sampler used for measuring windblown dust (Goossens et al., 2000).

Five Monitoring Sites were identified for dust monitoring. Their positions are indicated on Figure 4.03. Each Monitoring Site consisted of two data collection points numbered A and B (Figure 4.04). Both these data collection points had a container and a polca sampler. Collection points A and B were 50 m apart, making the A collection point thus 50 m closer to the source of dust than the B point. The distance from the

source varied from Monitoring Site to Monitoring Site. The container collected any fallout dust that passed over the collection point, thus presenting a line source. The polca sampler is orientated into the main direction of the wind, thus in effect, changing the line source into a point source (Van Jaarsveld, 2004).

The placement of the dust containers and polca samplers coincided with vegetation monitoring transects, described in more detail in the vegetation monitoring description. All the Monitoring Sites were clearly marked. The dust collectors were replaced three monthly. The same CSIR fallout classification was used to quantify the fallout rate.

4.2.3 Vegetation Monitoring

As with the climate and the dust monitoring, the vegetation monitoring is a continuing study. It aimed to describe the vegetation in the minerals area of the mine, along a section of the road and at the loading station of the gypsum in terms of: a) Percentage cover, b) dominance of individual species and c) the relative frequency at which individual species occur (Schmidt 2000; Blignaut, 2007). It monitored, recorded and described the general condition of the vegetation in terms of the influence that sedimentation and sediment movement might have had on the vegetation.

The vegetation in the study area was classified as Bushmanland Nama Karoo (Low and Rebelo, 1998). The area surrounding the proposed mine tended to be overgrazed in many places. An indication of this was the high numbers of *Rhigozum trichototum* (Driedoring) that was present (Blignaut, 2007; Shearing, 1994). The line intercept method was used to determine the relative density of individual species, the dominance and percentage cover and the frequency at which certain individual species occurred (Le Roux and Schelpe, 1981; Le Roux and Schelpe, 1997). This method was chosen since it was rapid, objective and accurate and well adapted for measuring changes in vegetation and therefore very well suited for monitoring vegetation in the surroundings of the mine (Blignaut, 2007).

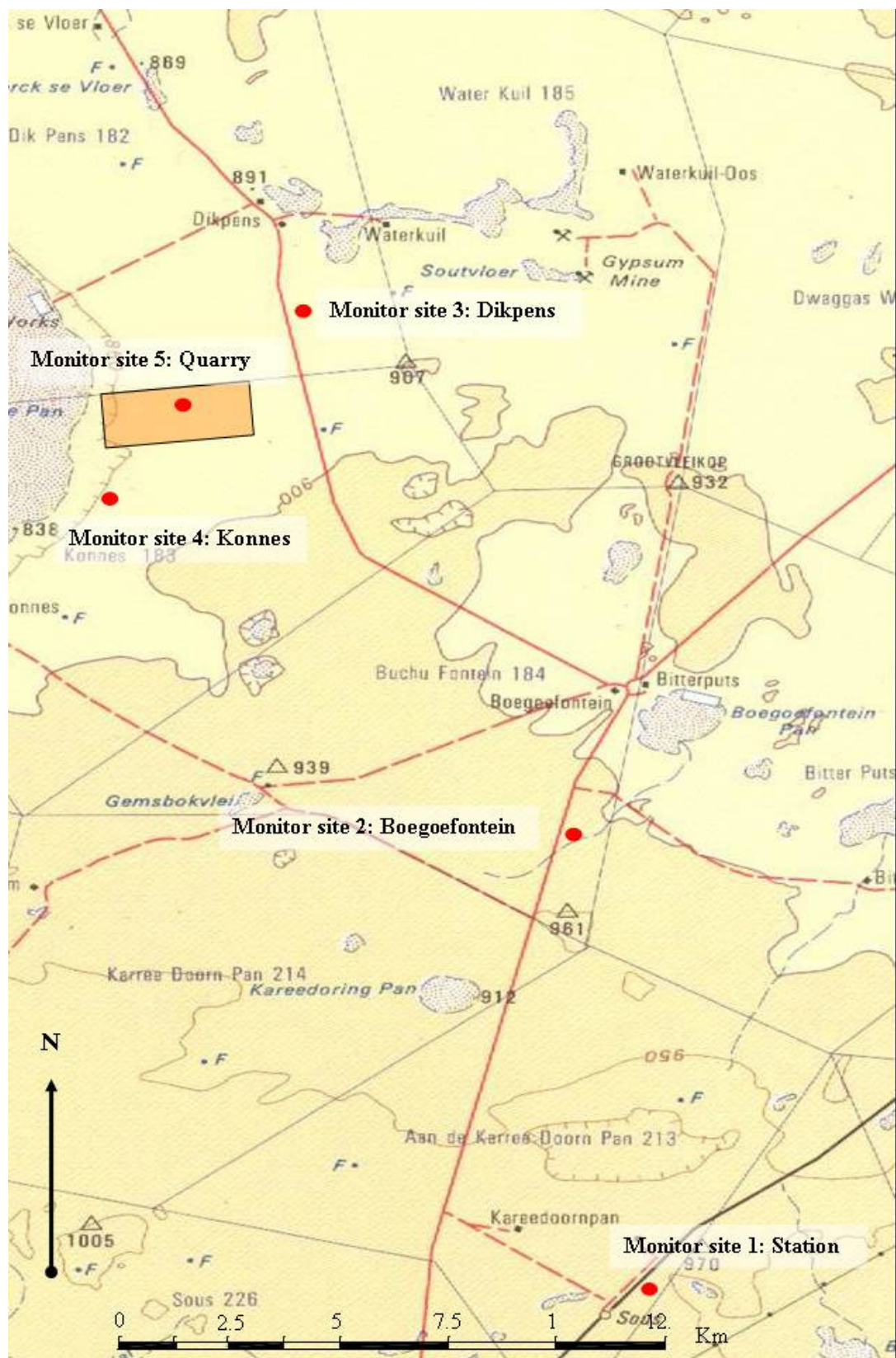


Figure 4.03 Map indicating the position of the Monitoring Sites

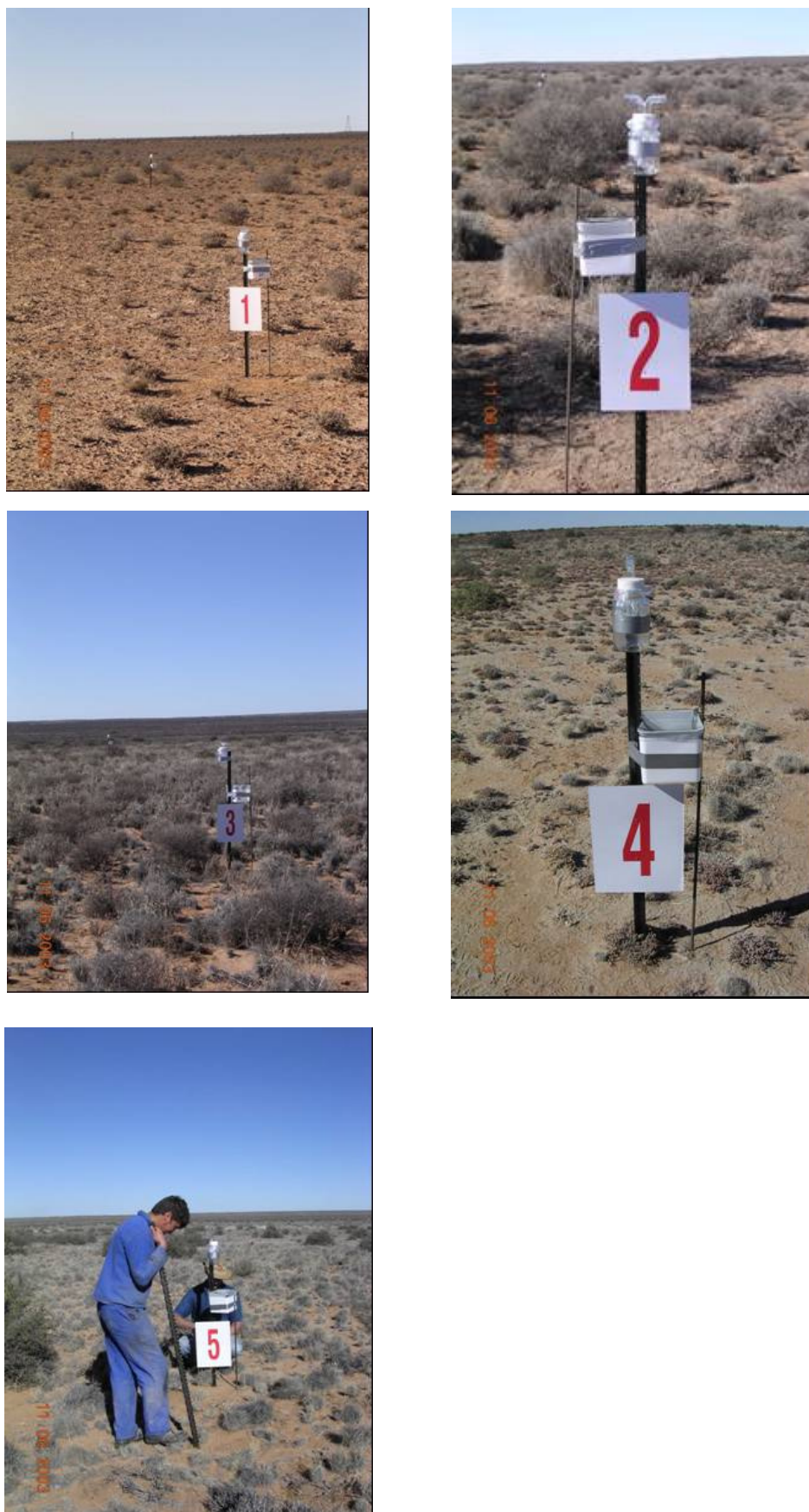


Figure 4.04 Showing the Monitoring Sites 1 to 5

The line intercept method is generally more accurate than quadrant sampling in mixed plant communities and is especially well suited for measuring low, shrubby vegetation. It consists of taking observations on a line or lines laid out randomly or systematically over the study area. The lines laid out were subdivided into 1m intervals and for each interval the plant species found were recorded as well as the distance they cover along that portion of the line intercept (Figure 4.04). Only plants touching the line or lying directly under or over it were considered. Only canopy spread strike were used. Photographic record keeping was of the utmost importance.

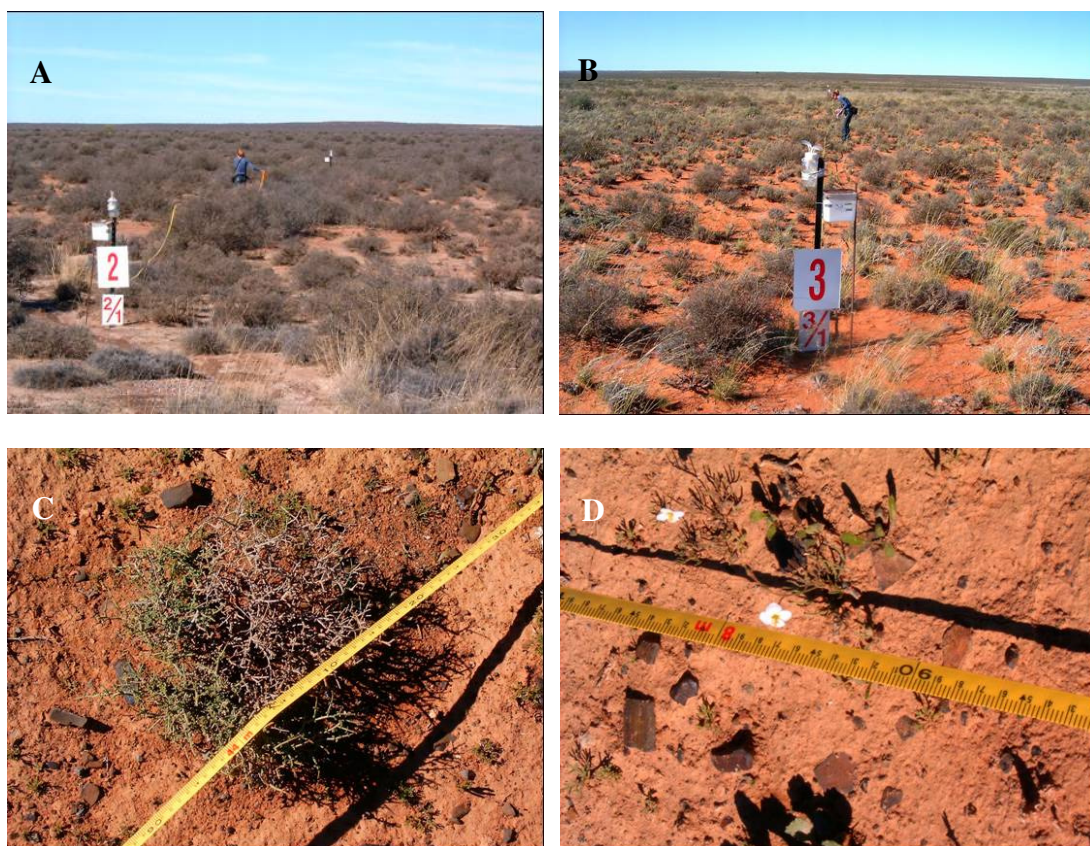


Figure 4.05 The line intercept method at A: Monitoring Site 2: Boegoefontein and B: Monitoring Site 3: Dikpens. Photo C of the Honnepisbos illustrates the canopy spread strike method and D bears as a reminder that small annuals like this *Heliophilla* should not be overlooked.

A pilot study was done on 8 May 2003 and the initial surveys were done on 11 June 2003. The vegetation monitoring sites were placed to coincide with the dust monitoring sites in order to correlate directly between vegetation conditions and sedimentation.

Monitor Site 1: Station: 30° 26.245'S; 19° 36.325'E: This site was chosen to monitor dust created by the loading of gypsum onto rail trucks. The monitoring site was placed on the eastern side of the rail line, downward from the main wind direction. The monitors were marked 1A, about 20m from the source of dust and 1B, 70m from the source of dust. Vegetation is naturally very poor with large bare areas present. The conditions are reminiscent of a pan surface area with sparse vegetation. Five 50m transects were delineated and marked out at this site. This site is subjected to sheep grazing.

Monitor Site 2: Boegoefontein: 30°19.527'S; 19°35.261'E This site was chosen as a continuation of the 2000 – 2001 monitoring system. The monitoring site remained at the same location. The aim was to continue to monitor road dust created by both BPB Gypsum and other transport using the road. The monitors, marked 2A, 15m from the source of dust and 2B, 50m further, were placed on the eastern side of the road, downward from the main wind direction. Three 50m transects were laid out and this site is also subjected to sheep grazing.

Monitor Site 3: Dikpens: 30° 11.657'S; 19° 31.565'E was chosen to monitor dust created by vehicles other than BPB Gypsum's. The monitors marked 3A, 20m from the source of dust and 3B, 70m from the source of dust, were placed on the eastern side of the road, down from the main wind direction. Again three 50m transects were laid out at this monitoring site. It is also subject to sheep grazing (Van Jaarsveld, 2007).

Monitor Site 4: Konnes: 30° 12.969' S; 19° 28.921' E: This site with monitors marked 4A and 4B was placed to monitor ambient dust and is 1.5 km away from the mine quarry and dust generated by the mining activities and 4.2 km away from any road dust. 4A is 400m and 4B 450m from the only source of dust, namely the pan surface. The long distance from the pan is also the reasons for placing the AWS at this site. Three 50m vegetation monitoring transects were laid out. As with all the other sites, this one is also subject to sheep grazing.

Monitor Site 5: Quarry: 30° 12.456' S; 19° 30.762' E: This site was placed on the mine. It monitored dust created by the mining operation as well as dust created by transport on the mine. Monitors 5A and 5B were placed at this site, where A is 15m and B 65m from the source of dust. They were placed between the main transport haulage and the quarry service road. As the mine site was fenced off, this monitoring site was the only one that is not subject to sheep grazing. Three 50m vegetation monitoring transects were laid out at this site.

At each monitoring site, except the station site, a total of 150 interval points were taken. At the station site a total of 250 interval points were taken due to the naturally poor condition of the vegetation. Each individual transect was 50 m, as it was obvious from the dust settling model, that the biggest influence is over the first 50 m. Relative species density or dominance provided an indication of the dominance or density of one species in relation to the other species (Blignaut, 2007; Schmidt, 2000; Schmidt, 2002; Schmidt, 2003). It is intended in the future to do the monitoring at the same time every year and preferably after the rainy season, since it is easier to correctly identify the species. Most of the geophytes and annuals are also present then. It is recommended not to protect the vegetation at the monitoring sites from grazing by either game or domestic animals. This will allow for measuring of the effect of mining activities on the vegetation whilst it is grazed. Should the area be fenced off, it would create an unrealistic situation, since this is part of farmland that will always be grazed (Schmidt, 2003).

4.3 Results

The results of the climate monitoring, dust monitoring and vegetation monitoring are presented under separate headings. Comparisons are drawn in the discussions of the findings.

4.3.1 Climate

The rainfall registered by the AWS during the monitoring period, appeared to be in line with the historical information in Chapter 3 (Figure 4.06). It has to be noted that 2004 was a very dry year for the region. The data recorded for 2003 and 2007 did not

represent full 12 month periods (Table 4.01). Data recording for this study commenced in July 2003 and ceased in October 2007.

Table 4.01 Rainfall in mm for the measured period from August 2003 to September 2007 at Monitoring Site 4: Kones.

	2003	2004	2005	2006	2007	Average
Jan		4.8	21	30.6	0	14.1
Feb		15.2	5	10.4	0	7.7
Mar		8.6	49.8	0.6	1.4	15.1
Apr		7.8	7	24	4	10.7
May		0	12.2	20.6	2.2	8.8
Jun		3.6	1.8	4.2	9.2	4.7
Jul		3.6	1	4.2	4.2	3.3
Aug	13.8	0.6	1.4	17.8	5	7.7
Sep	8.6	1.8	2	0.6	1	2.8
Oct	5.8	13.2	27.6	0		11.7
Nov	9	2.8	3.2	1.4		4.1
Dec	0.2	0.4	2.6	0		0.8
Total	37.4	62.4	134.6	114.4	27	

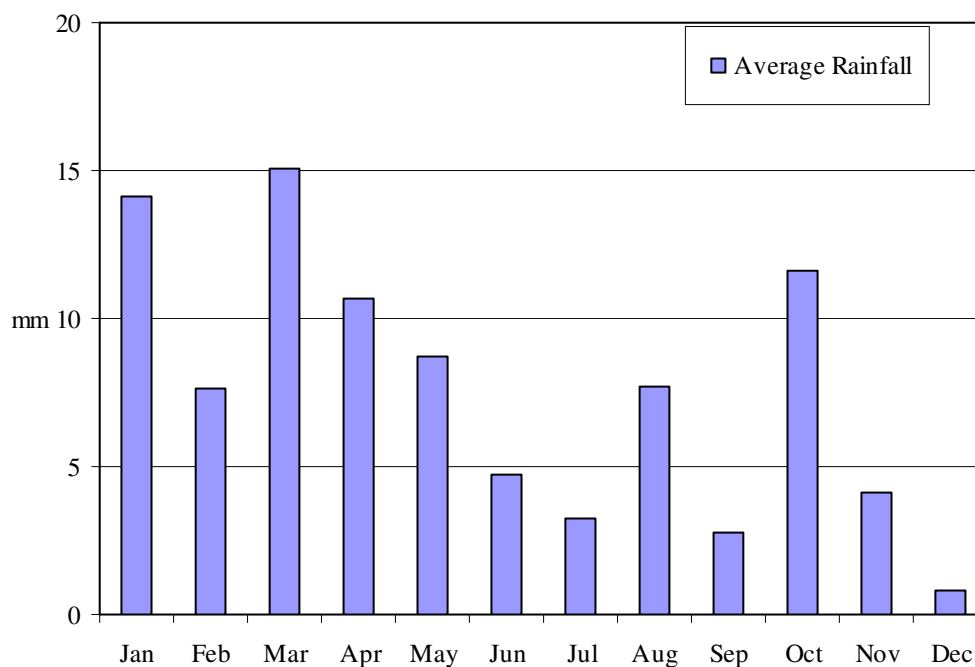


Figure 4.06 Average rainfall in mm for the monitored period from August 2003 to September 2007.

Recording is, however, still ongoing as longer term information might provide a better indication of the climate conditions and changes that might occur. Note that the 3 month dry spell from September 2006 to March 2007 was the worst since onsite monitoring commenced (Table 4.01).

No record 24 hour rain occurrence was recorded during the monitoring period (Table 4.02). Historical data indicate that as high as 90 mm have been recorded at Brandvlei in 24 hours in April 1984. Again, long-term information will provide a better idea of the rainfall pattern.

Table 4.02 The maximum rainfall per 24 hour period and the year in which it occurred for the monitored period from August 2003 to September 2007 at Monitoring Site 4: Konnes.

	2003	2004	2005	2006	2007	Max/24hrs
Jan		3.4	19.6	21.4	0	21.4
Feb		5.8	3.8	3.2	0	5.8
Mar		4.6	48.2	0.6	0.6	48.2
Apr		4.8	3.8	9.6	1.6	9.6
May		0	4.6	7.8	0.4	7.8
Jun		3	0.4	3	2	3
Jul		2.2	0.2	1.6	1	2.2
Aug	5.4	0.2	0.6	12	0.6	12
Sep	8.4	1.4	1.6	0.2	0.4	8.4
Oct	4.8	11.8	20.2	0		20.2
Nov	6.4	2.4	1.8	1.4		6.4
Dec	0.2	0.4	2.6	0		2.6

The onsite monitoring provided an opportunity to investigate a much more common form of precipitation, namely precipitation in the form of dew, mist and frost. This type of precipitation often exceeds that of rainfall in semi-arid and arid regions (Agam and Berliner, 2005). These forms of precipitation are often overlooked and disregarded as having an insignificant influence. In this region, it is of the utmost importance for various aspects of this investigation (Figure 4.08). Some will only be discussed in later chapters of this thesis.

The three most important parameters that were used to calculate the number of hours with the potential to form these types of precipitation were 1) relative humidity of higher than 80% combined with 2) wind speed smaller than 2.7 m/s and 3) maximum

air temperatures lower than 15°C. The AWS registered the climatic measurements at 1m above the surface. Relative humidity that is recorded as 80% at 1m above the surface is 100% on the surface. The opposite is true for wind speed. The speed drastically reduces at heights lower than 1m. This form of precipitation is often encountered first hand during early morning field work. For the measured period from August 2003 to October 2007, the colder months of May to August had the most hours in which dew or frost was likely to precipitate. As expected, the warmer months had less potential hours (Zangvil, 1996). During this period, 2006 had the highest occurrence of precipitation potential, while 2004 had the lowest average potential. The precipitation potential ranged from the lowest potential of 39 hours in January to the highest potential of 193 hours in August (Figure 4.07). This precipitation is crucial for the maintenance and re-establishment of vegetation in the general area.

This moisture does not just precipitate on the leaves of plants and the surface of the soil. Due to the heating of the air between sand grains and the subsequent cooling thereof, this form of moisture could penetrate into the soil profile to provide crucial moisture to vegetation (Agam and Berliner, 2005; Kawamoto et al., 2004). The relative humidity was not recorded in the historical climatic desk study in Chapter 3. For the monitored period from August 2006 to October 2007, the highest average relative humidity was recorded in June and the lowest average in December. The highest average monthly temperature was recorded in February, while the lowest average relative humidity was recorded in January. The lowest average temperature was recorded in June to coincide with the highest relative humidity (Van Jaarsveld, 2007) (Figures 4.09 and 4.10).

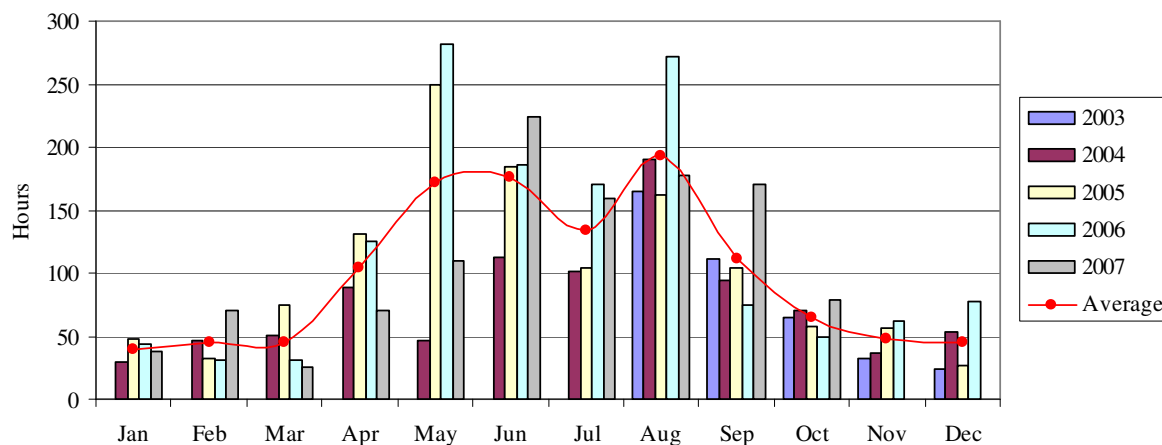


Figure 4.07 The potential for precipitation (calculated from $>80\%$ RH) to occur in the form of dew, mist or frost is represented for the monitored period from August 2003 to September 2007.



Figure 4.08 Fog that occurs in the Bushmanland region (Photo was taken during June 2004).

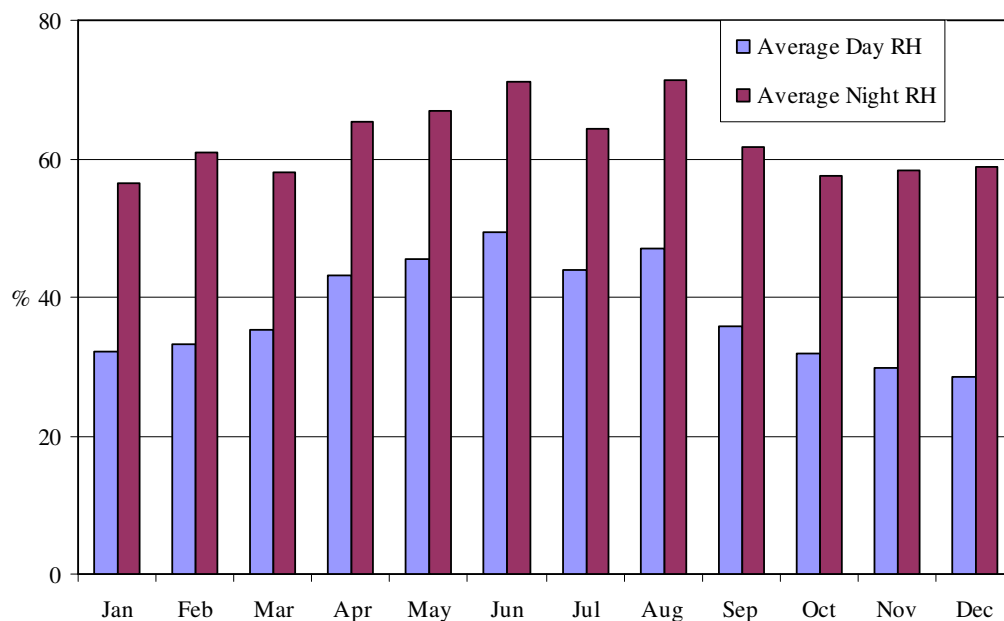


Figure 4.09 The average day and night relative humidity for the monitored period from August 2003 to September 2007.

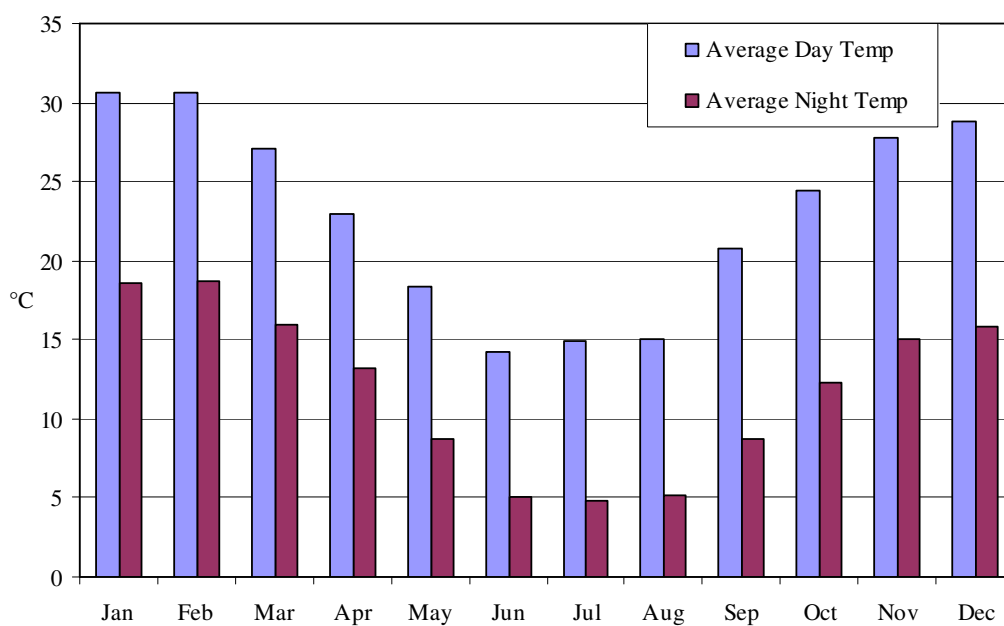


Figure 4.10 The average day and night temperatures for the monitored period from August 2003 to September 2007.

It is of interest to note that the average maximum temperature at 22.4 °C recorded by the AWS for the monitored period was 3.7°C lower than the 26.7 °C of the historical information. The average minimum temperature of 11.5 °C recorded for the period was 1.6 °C higher than the 9.9 °C of the historical information. Long term recording will confirm the trend or provide a better indication of the possible cause of the difference in the temperatures. Two possibilities to consider are that the monitoring period was too short for extreme conditions to occur or the difference in instrumentation accuracy.

As indicated in Chapter 3, historical wind information was only available for Pofadder, about 120 km away from the AWS site. When comparing the historical data with the AWS data, it was found that the wind direction is less dominant south and southeast at the AWS site and more often east than at Pofadder. The average wind speed recorded at the AWS is lower than the historical speed recorded at Pofadder (Table 4.03 and Figure 4.11).

Table 4.03 Wind direction frequency (average number of winds) in table A and speed (m/s) in table B for the monitored period August 2003 to September 2007.

A

	N	NNE	NE	ENE	E	ESE	SE	SSE	S	SSW	SW	WSW	W	WNW	NW	NNW
Jan	19	17	20	26	32	29	23	22	29	224	153	42	28	28	28	21
Feb	17	17	18	26	28	27	20	19	29	206	129	43	30	27	30	13
Mar	25	33	37	48	69	62	30	23	39	164	88	29	24	27	29	19
Apr	45	41	54	55	82	52	31	17	28	85	65	29	22	33	39	44
May	57	46	50	66	90	70	33	18	32	58	46	21	26	39	43	51
Jun	58	63	59	72	83	72	38	24	21	40	30	19	23	40	42	38
Jul	52	52	68	71	102	70	35	16	22	49	52	23	19	37	34	43
Aug	43	41	43	57	83	55	27	21	32	80	90	30	35	36	42	29
Sep	26	31	40	51	68	58	24	20	38	139	89	28	27	29	31	23
Oct	28	22	33	44	58	44	33	24	49	156	101	33	34	36	31	21
Nov	15	13	20	31	42	29	19	20	30	214	155	41	31	31	21	10
Dec	11	10	16	19	20	22	21	23	32	239	202	52	30	25	16	10
Average	33	32	38	47	63	49	28	21	32	138	100	32	27	32	32	27

B

	N	NNE	NE	ENE	E	ESE	SE	SSE	S	SSW	SW	WSW	W	WNW	NW	NNW
Jan	3.0	2.1	1.8	2.1	2.1	1.6	1.6	1.7	1.7	3.8	3.1	2.3	2.2	2.6	3.2	2.9
Feb	2.3	2.1	1.3	1.6	1.6	1.4	1.7	1.5	1.8	3.6	2.9	2.3	2.6	2.8	2.9	3.2
Mar	3.2	2.5	1.6	2.2	1.9	1.6	1.6	1.6	2.0	3.1	3.0	2.3	2.4	2.9	3.2	2.9
Apr	2.7	2.1	1.4	1.3	1.4	1.1	1.1	0.9	1.2	1.7	1.9	2.3	1.8	2.7	3.0	2.8
May	2.7	1.9	1.3	1.3	1.2	1.2	0.9	1.0	1.2	1.7	1.6	1.3	1.4	1.8	2.4	2.6
Jun	3.0	2.3	1.8	1.7	1.5	1.4	1.5	1.4	1.5	2.0	2.2	2.2	1.9	2.5	2.6	2.7
Jul	3.8	2.5	1.7	1.8	1.5	1.2	1.1	1.1	1.2	1.5	1.5	1.5	1.8	2.0	2.7	3.2
Aug	3.1	2.8	1.8	1.6	1.4	1.2	1.0	0.8	1.1	1.9	2.3	2.3	2.4	2.8	3.6	3.4
Sep	3.6	2.6	1.7	1.8	1.6	1.4	1.1	1.2	1.5	2.3	2.3	2.5	3.2	2.9	3.3	2.8
Oct	3.4	2.6	2.2	2.4	1.9	1.7	1.9	1.8	1.8	3.2	3.0	2.5	3.1	3.0	3.2	3.1
Nov	3.0	2.8	2.0	2.8	2.1	1.8	1.4	1.5	1.8	3.8	3.4	2.5	2.9	2.9	2.7	3.1
Dec	1.8	1.6	1.8	2.7	2.1	2.1	2.0	2.1	1.9	3.9	3.6	2.7	2.9	2.8	2.7	2.8
Average	3.0	2.3	1.7	1.9	1.7	1.5	1.4	1.4	1.5	2.7	2.6	2.2	2.4	2.6	3.0	2.9

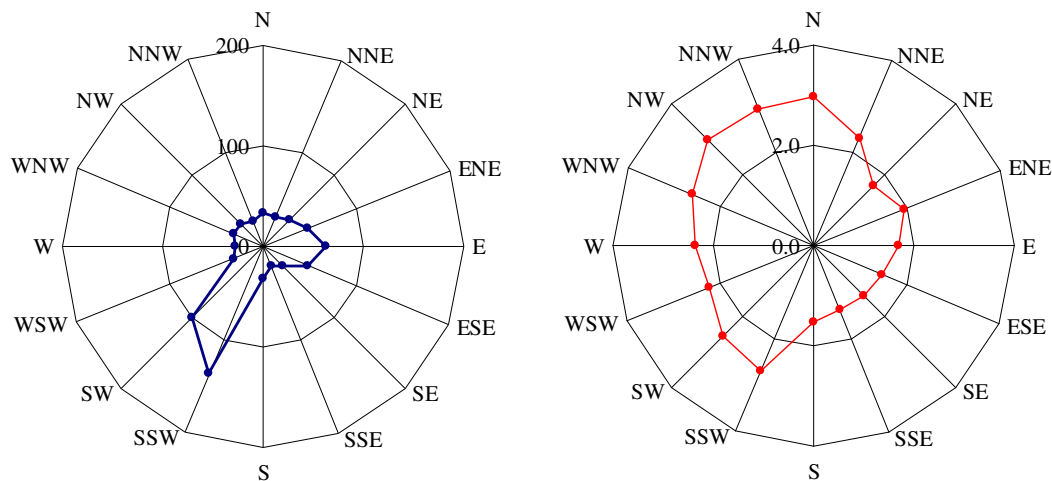


Figure 4.11 The average wind direction frequency (average number of winds) in blue and average wind speed recorded in m/s in red for the monitored period from August 2003 to September 2007 at Monitoring Site 4: Konnes.

The graphs in Figure 4.11 represent wind roses of the total winds that were measured over the 5 year period. The first rose indicates the frequency. Two distinct directions are seen, namely the winter months' easterly and the summer months' south westerly winds. Very little variation was observed on an annual basis. The wind patterns appeared to be very constant. (Figure 4.17)

4.3.2 Dust Monitoring

The first set of monitors was collected on 11 June 2003. The University of Stellenbosch measured the dust collected in the containers and the polca samplers. When considering the amount of dust generated, it is important to bear in mind what the production rate at the mine was during the monitoring period. Rather than absolute values, a relative increase/decrease table is presented in Figure 4.12. The Dikpens mine experienced a very large average increase of 34% on the 2004 production in 2005. 2006 saw a slight decline of -3% on the 2005 production and 2007 an increase in the 2006 production rate of 11%.

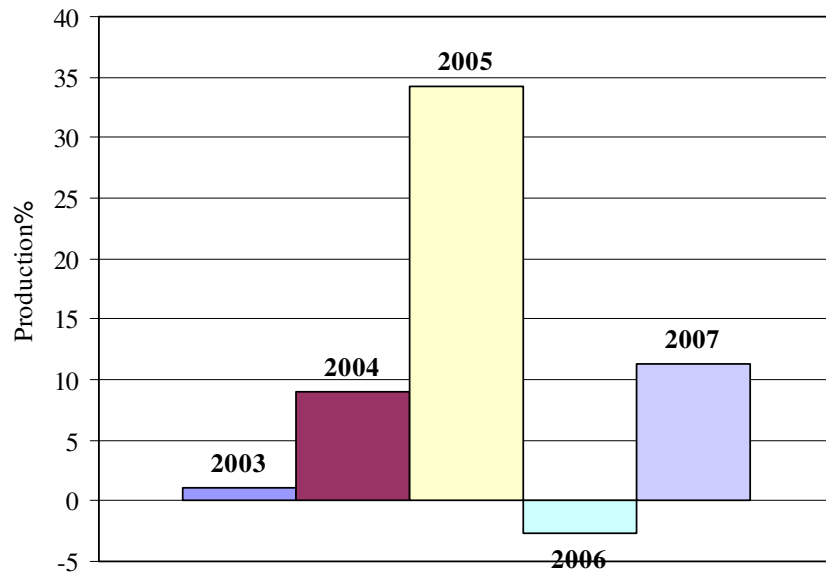


Figure 4.12 The relative production increase/decrease year by year experienced at the Dikpens mine since operation commenced in 2003.

Figure 4.13 represents the average amount of dust collected in grams per day by the collection points per site over the period 2003 to 2007. The data of the polca samplers and the containers were added together.

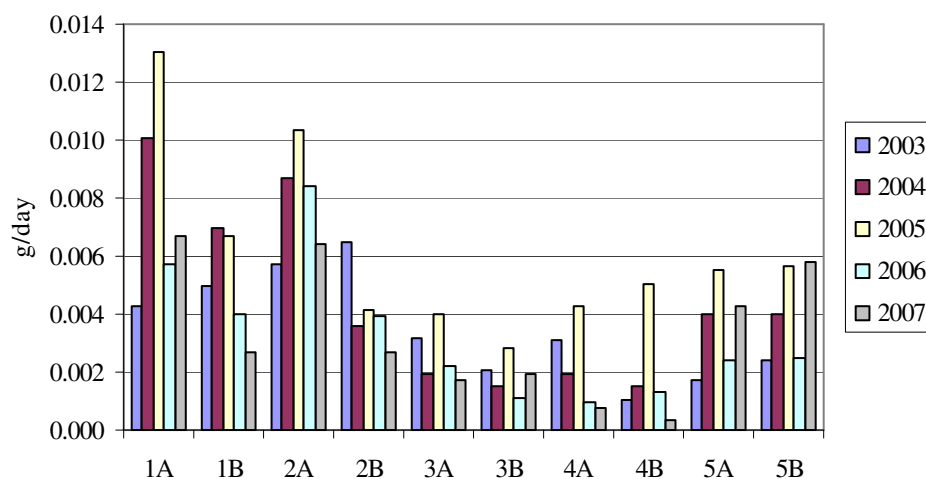


Figure 4.13 The average dust collected per year at each monitoring point A and B at each Monitoring Site 1 to 5.

The fallout dust collected might initially appear to mimic the production figures, but bear in mind that Monitoring Site 4 is the ambient site that would not reflect the mine or road transport influence, only the natural dust. The peaks reflected at the other monitoring sites, reflects the production as a compounded amount on top of the natural dust level.

The difference between monitoring points A and B should be noted, where A had the higher level recorded and was the most prominent at the monitoring sites where there was a clear point or line source. Monitoring Site 1 had a clear point source namely the loading station. Monitoring Sites 2 and 3 had the main road as a line source, where point A is closer to the source, than point B.

From Figure 4.14 it is quite clear that Monitoring Site 1: Station had the heaviest dust fallout. The lowest was at Monitoring Site 3: Dikpens where the mine's transport had no influence, but other transport used the road. Monitoring Site 4: Konnes that measured the ambient dust levels, did not have the lowest fallout. The most obvious reason for this phenomenon was the pan that dried up and created dust naturally (Figure 1.02.).

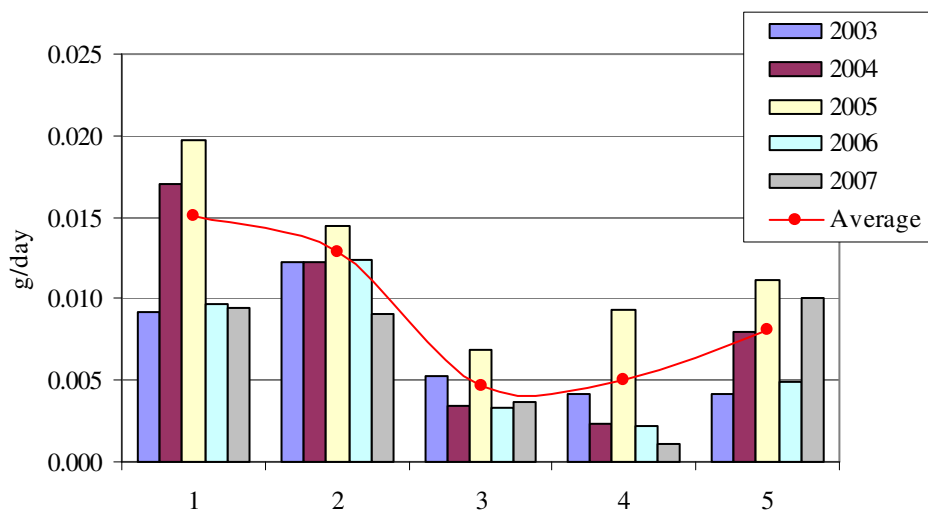


Figure 4.14 The average fallout of the two monitoring points A and B per year per Monitoring Site. The overall average is also indicated.

The two monitoring sites that measure the mine activity directly, Monitoring Sites 1 and 5 are the only sites that indicate an increase over the monitoring period (Table 4.04). Monitoring Site 5: Quarry has an enormous 140% increase in fallout dust. These site's data were in line with the increased production pressure that the mine experienced (Table 4.12).

Table 4.04 Average fallout dust per transect (g/day) and the percentage increase or decrease that was measured over the 5 year monitoring period.

Monitoring Site	1	2	3	4	5
2003	0.0092	0.0123	0.0052	0.0041	0.0042
2004	0.0170	0.0123	0.0034	0.0034	0.0080
2005	0.0197	0.0144	0.0068	0.0093	0.0111
2006	0.0097	0.0123	0.0033	0.0023	0.0049
2007	0.0097	0.0091	0.0033	0.0023	0.0100
Average fallout (g/day)	0.0131	0.0121	0.0044	0.0043	0.0076
% increase or decrease	5.6	-25.6	-37.0	-45.4	139.7

In Table 4.04 the fallout dust percentage increase or decrease site was calculated as the difference over the monitoring period from 2003 to 2007 experience per site.

4.3.3 Vegetation Monitoring

The state of the vegetation varied substantially between the Monitoring Sites. This variation could have been due to the different management practices by different farmers (Blignaut, 2007). The vegetation in the greater region was not generally very well documented and the following is a list of the species identified at the Monitoring Sites (Table 4.05).

The Monitoring Sites were described in terms of a) the percentage cover (Figure 4.15), b) the dominance of individual species (Figure 4.16) and c) the relative frequency at which individual species occur (Table 4.08). The number of species per site was also documented as a measure to ensure that the sensitive species do not unknowingly disappear from the area influenced by the mine dust (Table 4.07).

Table 4.05 List of species identified at the Monitoring Sites. (Blignaut, 2007)

Scientific name	Common name
<i>Aridaria spp.</i>	
<i>Atriplex lindleyi</i>	Blasie brak
<i>Brownanthus spp.</i>	
<i>Drosanthemum spp.</i>	
<i>Eriocephalus decussatus</i>	
<i>Eriocephalus spinescens</i>	Doringkapokbos
<i>Galenia spp.</i>	
<i>Gnidia deserticola</i>	
<i>Lycium spp.</i>	Kriedoring
<i>Pentzia annua</i>	
<i>Psilocaulon spp.</i>	
<i>Psilocaulon utile</i>	
<i>Pteronia paniculata</i>	
<i>Rhigozum trichotum</i>	Driedoring
<i>Ruschia spinosa</i>	
<i>Ruschia spp.</i>	
<i>Salsola tuberculata</i>	Cauliflower ganna
<i>Sarcocaulon salmoniflorum</i>	T'noena-doring
<i>Stipagrostis ciliata</i>	Langbeen Boesmangras
<i>Stipagrostis obtusa</i>	Kortbeen Boesmangras
<i>Zygophyllum lichtensteinianum</i>	
<i>Zygophyllum microcarpum</i>	

The base for the monitoring was the first survey that was done of each Monitoring Site in June 2003. This was done prior to the commencement of the mining activities. The average percentage cover per Monitoring Site was calculated as an average over the 5 year period, while the percentage improvement or decline was calculated by subtracting the results of the last survey done in 2007 from the base survey done in 2003 (Table 4.06).

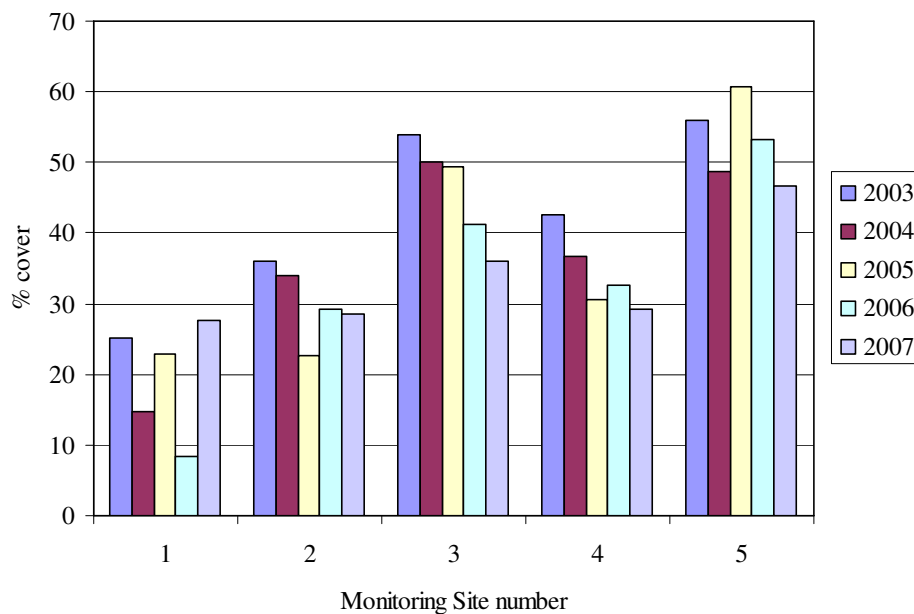


Figure 4.15 Histogram indicating the percentage cover over time.

Table 4.06 Average percentage cover as well as the percentage change experienced by the Monitoring Sites over the 5 year monitoring period.

Monitoring Site	1	2	3	4	5
Jun-03	25.2	36	54	42.66	56
Feb-04	14.8	34	50	36.6	48.6
May-05	22.8	22.6	49.3	30.6	60.6
Mar-06	8.4	29.3	41.3	32.6	53.3
Mar-07	27.6	28.6	36	29.3	46.6
Average % cover	19.76	30.1	46.12	34.352	53.02
% improvement or decline	9.5	-20.6	-33.3	-31.3	-16.8

The variation that occurs within the monitoring of the number of species per Monitoring Site is mostly due to the difficulty in recognising the different species. The 2007 survey was done by a new consultant, hence the drastic change at Monitoring Sites 4 and 5 (Figure 4.16).

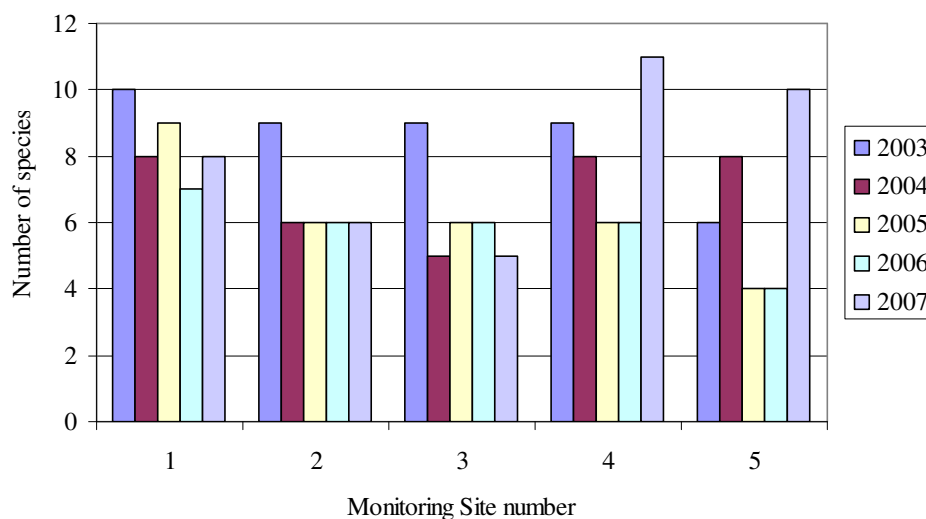


Figure 4.16 Number of species recorded per Monitoring Site.

Table 4.07 Summary of the dominant species change over time at the different Monitoring Sites.

Dominance per Monitor Site number	1	2	3	4	5
Dominance June 2003	<i>Atriplex lindleyi</i> 38.76%	<i>Rhigozum trichototum</i> 31%	<i>Lycium cinereum</i> 37.2%	<i>Brownanthus spp.</i> 4.65%	<i>Stipagrostis obtusa</i> 74.77%
Dominance February 2004	<i>Zygophyllum spp.</i> 30.75%	<i>Lycium cinereum</i> 29.28%	<i>Lycium cinereum</i> 36.3%	<i>Salsola tuberculata</i> 30.92%	<i>Stipagrostis obtusa</i> 48.56%
Dominance May 2005	<i>Zygophyllum spp.</i> 32.74%	<i>Lycium cinereum</i> 67.62%	Unknown 37.2%	<i>Brownanthus spp.</i> 48.33%	Grass 83.88%
Dominance March 2006	<i>Lycium spp.</i> 55.6%	<i>Lycium spp.</i> 46%	<i>Melobium spp.</i> 43.2%	<i>Brownanthus spp.</i> 47%	Grass 84%
Dominance March 2007	<i>Psilocaulon spp.</i> 76.2%	<i>Lycium spp.</i> 54.96%	<i>Melobium spp.</i> 47.82%	<i>Salsola spp.</i> 36.52	<i>Stipagrostis obtusa</i> 42.03%

Table 4.08 Change in the relative frequency of the dominant species over time at the monitoring Sites.

Relative frequency per Monitor site number	1	2	3	4	5
June 2003	<i>Atriplex lindleyi</i> 51.66%	<i>Zygophyllum microcarpum</i> 18.51%	<i>Stipagrostis obtusa</i> 43.2%	<i>Brownanthus spp.</i> 39.61%	<i>Stipagrostis obtusa</i> 81.92%
February 2004	<i>Salsola tuberculata</i> 29.72%	<i>Lycium cinereum</i> 32%	<i>Stipagrostis obtusa</i> 26.76%	<i>Brownanthus spp.1</i> 30.18%	<i>Stipagrostis obtusa</i> 80.28%
May 2005	<i>Gazania spp.</i> 43.1%	<i>Lycium cinereum</i> 52.95%	<i>Grass</i> 36.48%	<i>Brownanthus spp.</i> 41.31%	<i>Grass</i> 95.61%
March 2006	<i>Salsola spp.</i> 20%	<i>Melobium spp.</i> 36.3%	<i>Grass</i> 50%	<i>Brownanthus spp.</i> 58.3%	<i>Grass</i> 90%
March 2007	<i>Psilocaulon spp.</i> 84.05%	<i>Lycium spp.</i> 37.2%	<i>Melobium spp.</i> 37.03%	<i>Brownanthus spp.</i> 41.86%	<i>Stipagrostis obtuse</i> 62.85%

4.4 Discussion of the Findings

The monitoring described in Chapter 4 is ongoing. It forms part of the mine environmental impact management programme. The data and findings are recorded in annual review reports. An important factor that currently does not form part of the survey is the monitoring of the grazing that is taking place within the study area. It could take the form of a count of the sheep per hectare per month. This will give an indication of the grazing stress exerted on the area.

Initial impressions of the findings are that with more production, more dust, less vegetation cover per Monitoring Site. When the data is more closely scrutinised, the picture changes slightly. The climatic information does not vary drastically from the 50 year historical data described in Chapter 3. The wind patterns are slightly different

from that recorded at Pofadder. The annual patterns for the study area remained approximately the same although seasonal changes do occur (Figure 4.17).

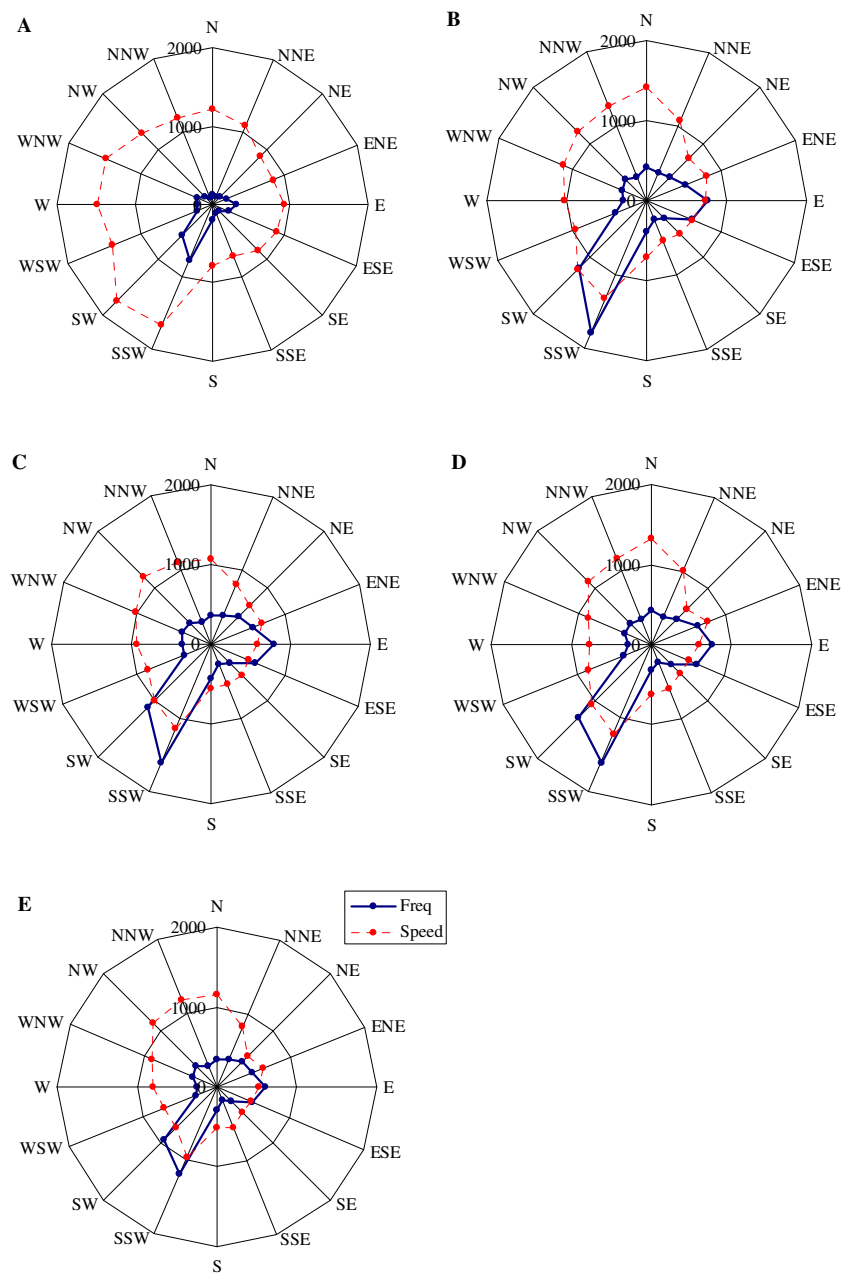


Figure 4.17 The wind pattern over the monitored period from August 2003 to September 2007. Figure A reflects the wind pattern for 2003, B for 2004, C 2005, D 2006 and E 2007.

Note that the wind speed, measured in m/s was multiplied by a factor of 50 in order to be able to represent the values on the same graph as the frequency. The graphs for 2003 and 2007 do not represent full year information. Because the wind patterns

change seasonally, it might have a short term influence on fallout dust settling patterns. Seen over the course of the 5 years, the annual patterns changed very little. Figure 4.18 presents a graph that was devised to monitor changes in the other important climatic indicators. Again the graphs for 2003 and 2007 do not represent full year information.

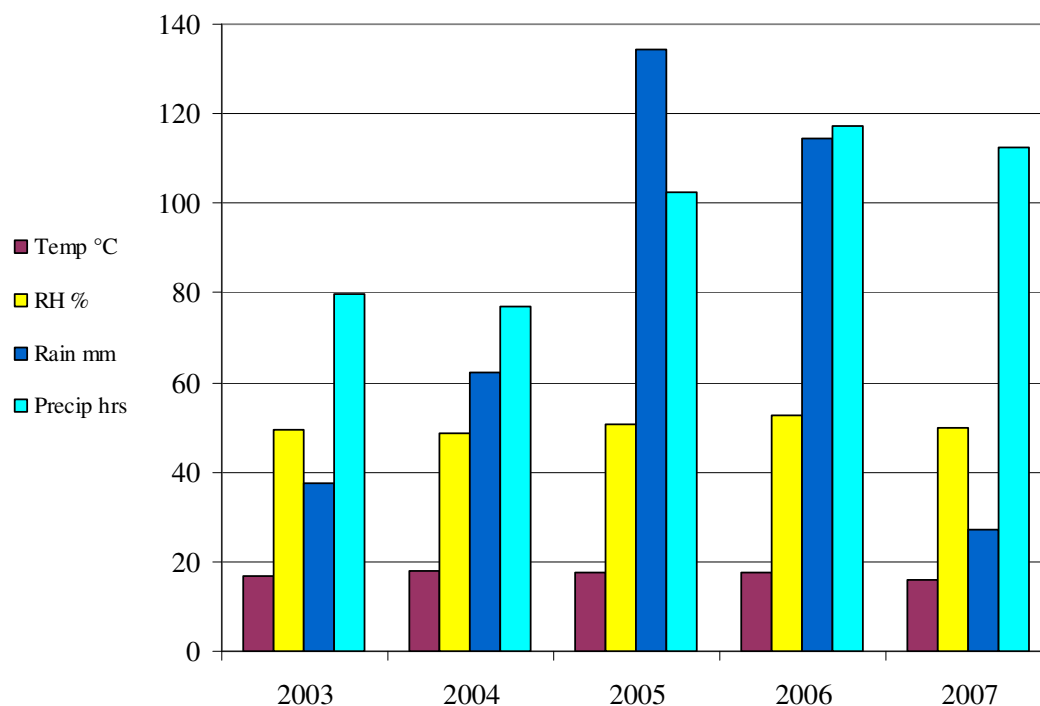


Figure 4.18 A comparative graph of the climatic variation over the monitored period August 2006 and September 2007. Note that the Y-axis scale represents °C for the temperature, % for the relative humidity, mm for the rain and hours for the precipitation.

The graph indicates that the main variation was in rainfall with 2004 being a very dry year. No other major changes were observed over the short monitoring period. Apart from Monitoring Site 1: Station that experienced a dust fallout increase of 5%, but also a percentage cover increase of 9%, all the other Monitoring Sites experienced a decline in the percentage cover. Monitoring Site 3: Dikpens experienced 33.3%

decline in cover since the monitoring commenced, making it the biggest percentage decline in cover. This site is not influenced by mining transport and experienced a decline in dust deposition of 37%. Monitoring Site 4: Konnes, the ambient monitor, experienced the second largest decline at 31%. These Monitoring Sites are heavily grazed. Monitoring Site 5: Quarry, located on the mine, experienced the highest increase in dust deposition of 140%, but only experienced a 16% decline in percentage cover. This site is isolated on the mine site and not grazed. Correlations were drawn between the amount of fallout dust experienced by a Monitoring Site and the change in the percentage cover experienced by the site. It resulted in a negative correlation of -0.48 (Figure 4.19).

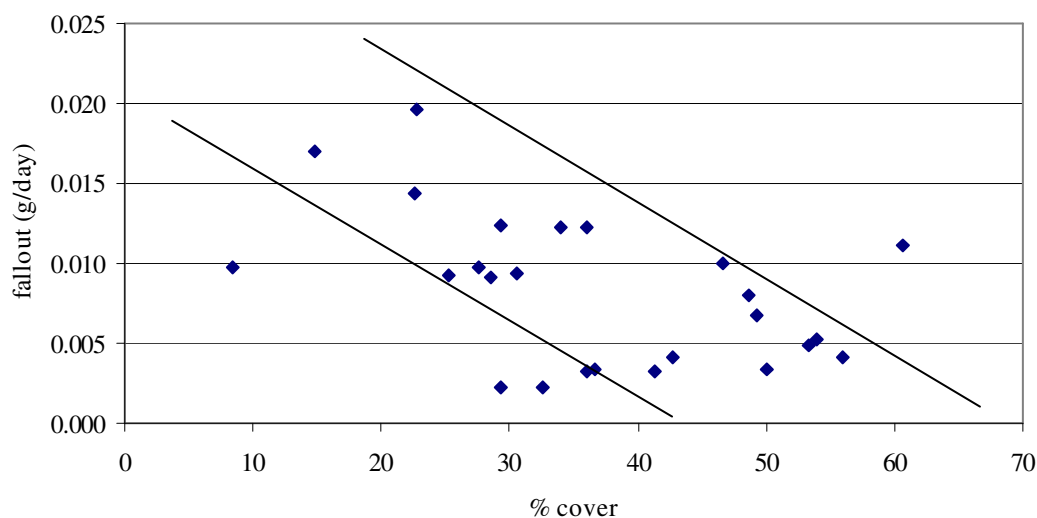


Figure 4.19 Negative correlation between the amount of fallout dust and the percentage cover at the Monitoring Sites for the period 2003 to 2007.

Although the regression statistics are poor, the correlation is negative and a field was identified between a minimum and maximum border (Figure 4.19). A correlation of 0.30 was found between the change in percentage cover and the increase or decrease in the amount of fallout dust over the monitored period. No significant correlation can be drawn between the amount of fallout dust and rainfall, and rainfall and percentage cover per Monitoring Site. It is important to note that longer term monitoring might indicate stronger correlations.

The average of the fallout sedimentation experienced over the monitoring period at the Monitoring Sites 1 to 5 was statistically compared to the dust settling model equation in Figure 3.09 (Clark, 2001). The results are remarkably similar and the assumption is made that the equation of the dust settling model could also be applied to this monitoring system. The result of the application is shown in Figure 4.20.

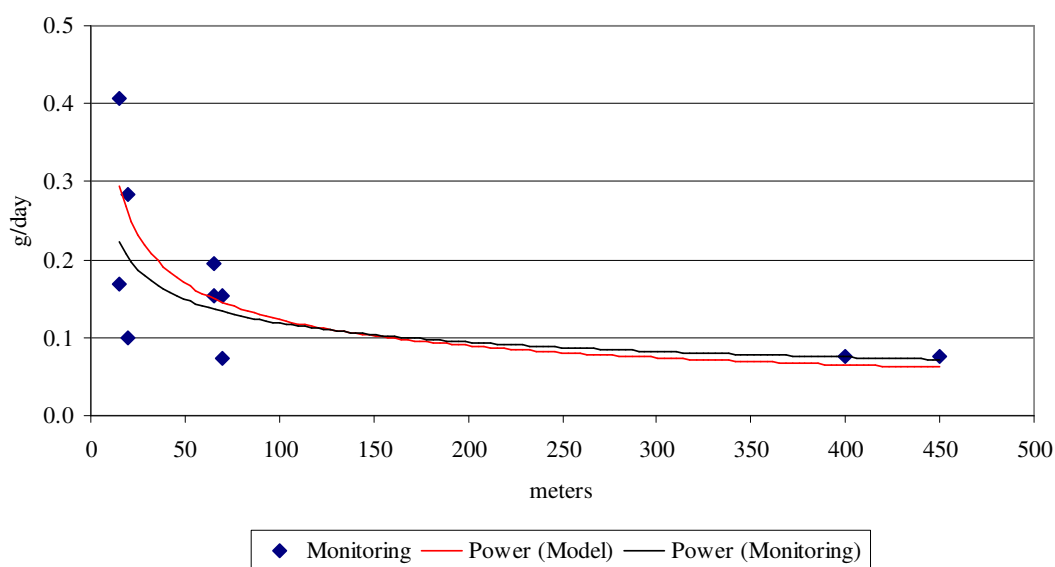


Figure 4.20 A comparison of the settling model with the dust monitoring data.

4.5 Conclusion

During the combined investigation over the past five years, it became evident that the onsite weather information was very valuable. An example of direct monitoring results is the wind speed and direction frequency change that occur seasonally, although the annual patterns appear to repeat. It became quite evident that the wind patterns remain very constant in the long term. An indirect application of the information is calculation of the hours of potential precipitation by applying the climatic information.

Combining the monitoring points proved to be invaluable for the direct correlation of monitoring data, not only between different monitoring aspects at the same monitoring site, but also correlating between the Monitoring Sites. The relative accuracy of a

second application of the dust settling model to a monitoring system increased the confidence that the model can be applied to prediction scenarios.

Finally it became more evident that grazing practices might have a major influence on the vegetation. It could be even more widespread than the settling of wind transported sediment, whether natural or industry generated. A monitoring system is being investigated to monitor and combine the impact of grazing on the vegetation to this continuing study.

5 WINDBLOWN SEDIMENT AND ITS ORIGIN.

5.1 Introduction

Given the information about the dust settling at the various monitoring positions the question arises if the dust could be traced in the soil profile (Figure 5.01). As a first stage investigation, the dust had to be isolated and the physical properties investigated. It became very obvious that the dust fallout accumulates easier in some areas than in others.

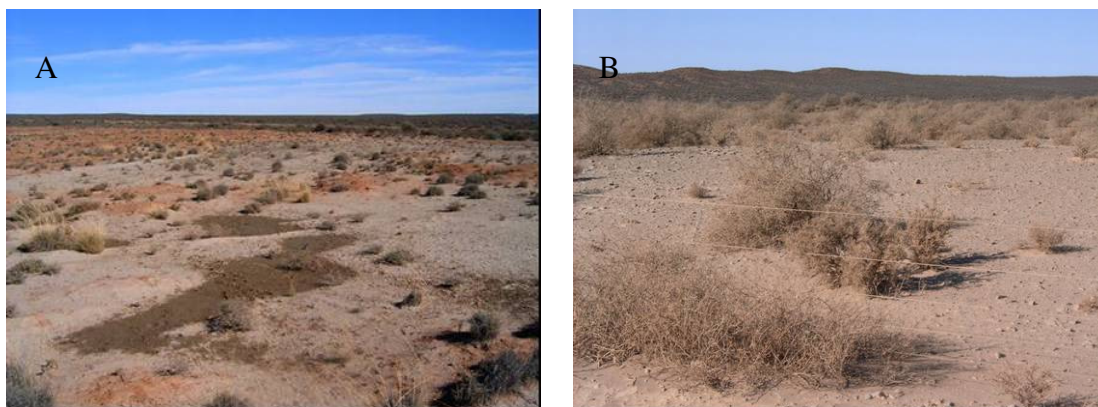


Figure 5.01 Two separate areas where heavier dust fallout is obvious. A. At Monitoring Site 2: Boegoefontein, B. At the intersection of the Loeriesfontein – Brandvlei road and the turnoff to Pofadder at Bitterputs.

Various factors are accountable for this phenomenon i.e., road surface conditions and road construction materials. Topography has a major influence as well as wind speed and direction. Vegetation and surface protection also plays a major role (Khalaf, 1989). In order to understand the origin of the windblown sediment, the geology of the region and the chemistry of the ore body were investigated. In the search to identify an element in the dust to trace and to test the settling model against and to try and predict the influence sphere of the dust generated by the mining operation, the orebody at Waterkuil was investigated in more detail. The area that is influenced by the mining

operation extends over 450 ha. The topography is gently undulating. The top horizon is generally very thin or absent on the slope towards the pan. The soils within the minerals area are red, fine grained aeolian soils classified as the Hutton form. The B horizon is 400 to 600 mm deep, thinning towards the pan edge. The B horizon is underlain by the sub-base horizon which is dominated by the rock-like gypsum deposit, forming an outcrop on the pan slope. Because of the small size of the mine's mineral area, very little soil diversity occurs. The unconsolidated nature of the A and B horizons makes it prone to wind erosion. The shallow to moderately deeper Hutton soils have low dry land production potential. According to the Department of Agriculture, the Granaatboskolk area has a bearing capacity of 12.5 ha per fertile Dorper ewe.

The gypsum outcrop on the pan slope area supports only sparse vegetation of dwarf shrub land type. In the deeper sand area, 300 m to 1 km from the pan edge, open shrub land and well developed grass cover dominate the vegetation.

5.1.1 Gypsum

The chemical formula for gypsum is $\text{CaSO}_4 \cdot 2\text{H}_2\text{O}$. The Molecular Weight is 172.17 gm. The more common impurities encountered in the orebody are sand, shales, silt and salts, namely NaCl and minor MgCl and KCl. Gypsum is chemically stable and is used in some foods, while it is best known as Plaster of Paris. It is used in pottery and as plaster casts for broken limbs. Gypsum is further used for the manufacture of plaster boards, in cement manufacturing and as a group 2 agricultural fertiliser (Brady, 1990).

The gypsum ore body is a whitish to light brown rock-like layer or procrete, covered with aeolian sand and plants in places. The sand cover over the gypsum is fine-grained aeolian sand and covers about 70% of the ore body. The sand is typically from nil to 1.5 m thick and is removed during the mining process before quarrying starts. The sand is commonly referred to as overburden by the mine personnel and is selectively removed. The top 20 cm is removed and stored separately, since this top layer contains the natural vegetation seeds. During the rehabilitation phase of the mining process, the top layer is restored to allow the natural seeds to germinate and restore the vegetation. The gypsum occurs as a horizontal layer varying in thickness from 10 cm

to about 3.5 m. It is generally accepted that gypsum from thicker than 30 cm can be mined profitably.

A) Regional geology: The area is underlain by shale of the Prince Albert Formation of the Eccca Group and shale of the Dwyka Formation with wide spread outcrops of intrusive dolerite dikes. The area is widely overlain by Quaternary and Tertiary age alluvium, sands and calcrete (Cowling et al., 1986; Snyman, 1996).

B) Area geology: The area is underlain by shale of the Prince Albert Formation, overlain by Tertiary age aeolian sands.

C) Deposit geology: The gypsum layer is mostly covered by a layer of reddish aeolian sand with minor shale fractions present in some areas. It varies in thickness from 0 to 8m (Figure 5.02). The gypsum occurs as a solid, massive body with the upper portion mostly light coloured to white. Some shales and sand contamination occur where the gypsum tends to become porous and more crystalline towards the bottom of the layer.

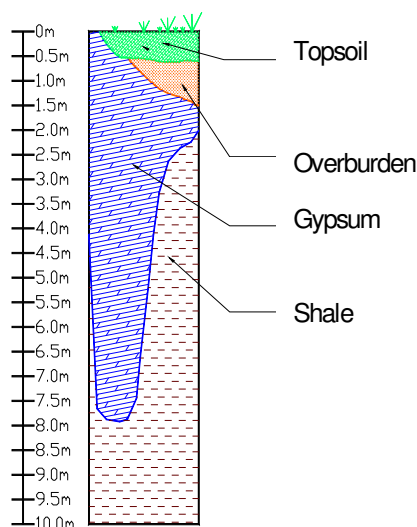


Figure 5.02 A typical ore body profile

The base of the ore body consists of loosely compacted sand or unweathered shale. The bedrock consists of shales of the Eccca Group and Dwyka formation of the Karoo Supergroup (Snyman, 1996). If the dust could be qualified in terms of chemistry, particle size profile, crystal structure or any physical characteristic, it would aid in the tracing thereof in the soil profile.

5.2 Method

The particulate material collected from the monitoring sites was investigated physically and chemically to characterise it and to ensure that the sediment found in the sediment traps was from the mining area and not material originating from the background natural dust fallout of this region. The background or ambient dust was expected to be quite large as described in Chapter 3 and indicated as ambient levels in Figures 3.03 and 3.08. As described in Chapter 4, Monitoring Site 4: Konnes was established to monitor background or ambient conditions (Figures 4.03 and 4.14).

Two transects were isolated where the influence of the mining activities were the most visible. Monitoring point 1: Station is located at the loading facility at the station. The sediment fallout at this monitoring point for the period 2003 to 2007 is 0.0303 g/day. As previously described, each Monitoring Site consisted of two data collection points numbered A and B. Both these data collection points had a container and a polca sampler, 50 m apart. The one collection point was thus 50 m closer to the source of dust than the other (Figure 4.04).

5.3 Results and Discussion

At collection point 1A, the average fallout was 0.0093 g/day or 61% of the collective total dust measured at the two collection points. At collection point 1B, the average fallout was 0.0058 g/day, or 39%. The difference in the physical properties of the dust that was collected by the two types of dust collectors was visible when examined under a microscope (Figure 5.03 and Figure 5.06).

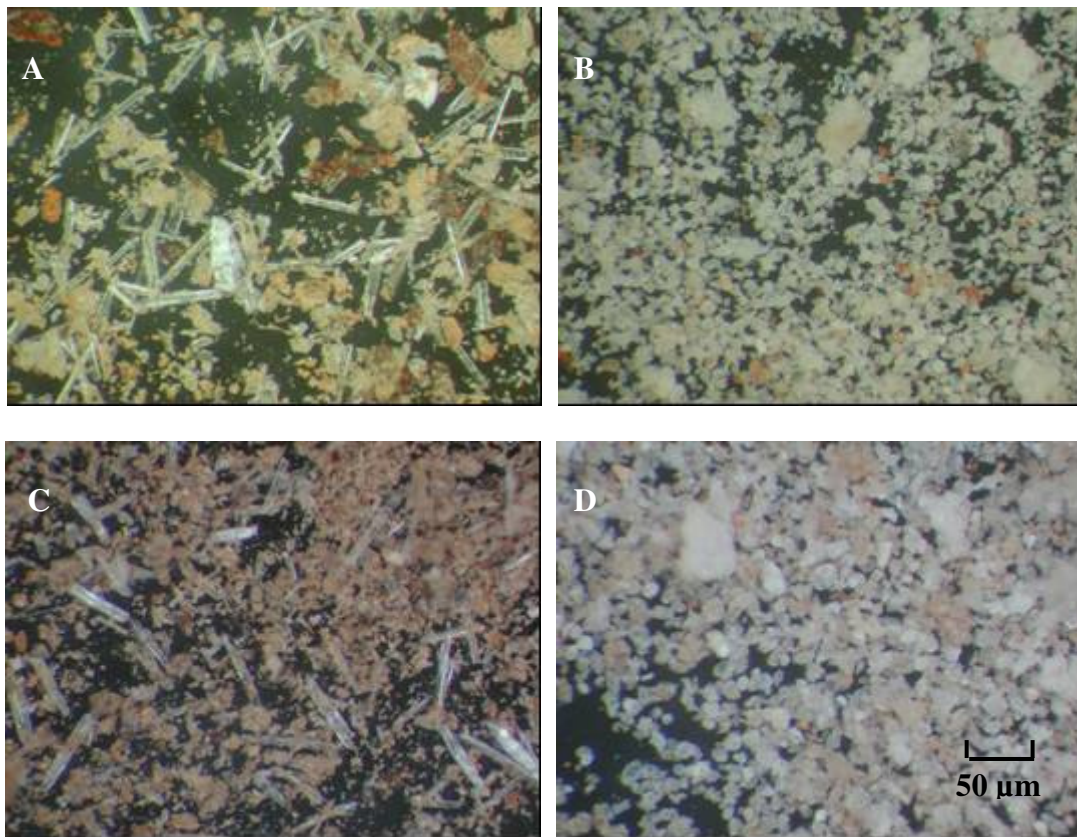


Figure 5.03 Sediment collected at monitoring point 1: Station. A was collected in the container and B in the polca sampler at collection point 1A. C was collected in the container and D in the polca sampler at point 1B, 50 m further away from the dust source. The scale is the same for all the photos.

The sediment (fallout dust) collected by the containers at both collection points, consisted of mainly red and yellow aeolian sand and elongated gypsum crystals. The origin of these crystals was the loading activity of the production at the station. The polca samplers trapped sediments transported by much stronger winds. The sediments were better sorted and rounded and the long gypsum crystals were broken and rounded.

At Monitoring Point 1: Station, the difference in the sediment material collected by the two types of methods, containers and polca samplers are clear to see. The difference in the distance from the source is less obvious from the photos, but rather clearer when the amounts of sediment collected was taken into consideration. The

polca samplers, more effective in high wind conditions, appear to have collected finer, better sorted material, typical of suspension loads. Scaled photos were taken of samples of the sediments collected at Monitoring Sites 1 and 5, using the Scanning Electron Microscope (SEM). All the dust particles within the frame of the photos were measured and counted. At collection point 1A the average particle size collected was $13.79\ \mu\text{m}$. Forty-nine percent of the dust was smaller than PM_{10} (Figure 5.04). This size fraction represented the medium to very fine silt fractions. No particles smaller than $\text{PM}_{2.5}$, or clay size fraction were recorded.

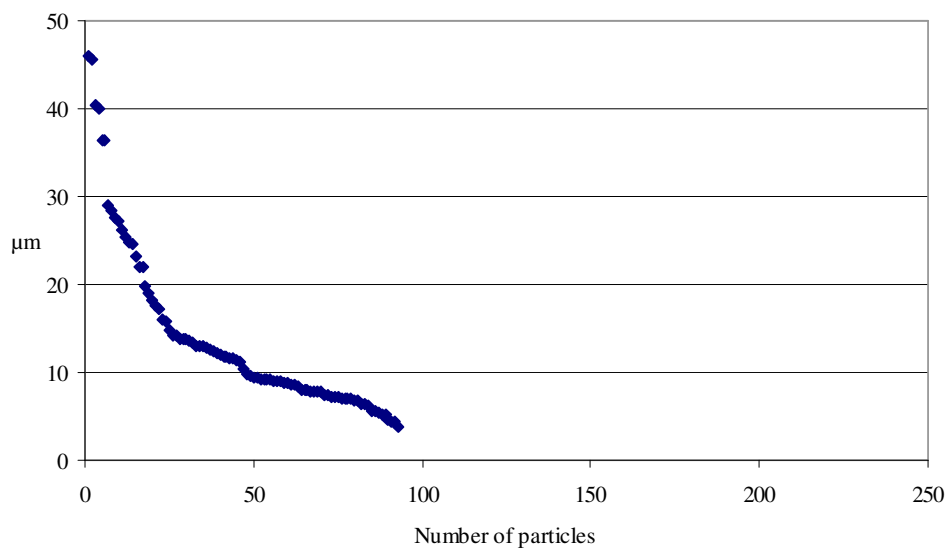


Figure 5.04 Particle size analyses of sediment particles collected at Monitoring point 1A.

The average particle size at monitoring point 1B was $11.7\ \mu\text{m}$. It was smaller than at 1A at. This is expected as this collection point is 50 m further from the point source than collection point 1A. Fifty percent of the collected sediment was smaller than PM_{10} with 1% of the particles smaller than $\text{PM}_{2.5}$ (Figure 5.05). These fractions further indicate that the collected sediment is marginally smaller at collection point 1B than at 1A.

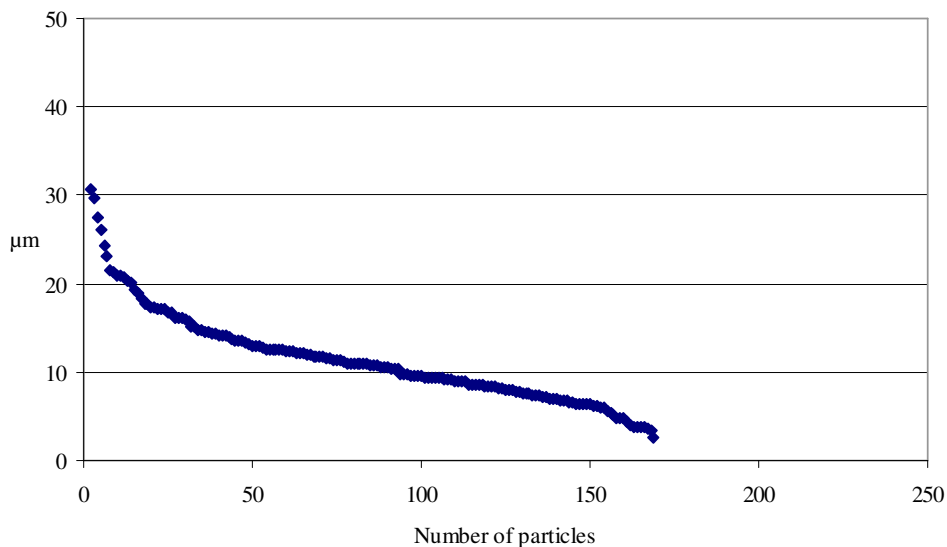


Figure 5.05 Particle size analyses of sediment particles collected at Monitoring point 1B.

The second monitoring point that was isolated to examine the character of sediment associated with the mining operation was at Monitoring Point 5: Quarry. As previously described, it is situated on the mining site, between the mining quarry and the workshop area. It was subjected to total sediment fallout of 0.016 g/day. At collection point 5A the average fallout was 0.0039 g/day, accounting for 48.5% of the total dust measured between the two collection points. At collection point 5B, the average fallout was 0.0041 g/day, or 51.5%. The Monitoring Site layout was slightly more complex than at the other sites. The two monitoring points, 5A and 5B, were placed 50 m apart from a lesser used secondary quarry road, but were equally distant from the mining quarry. The mining quarry seemed to have a much larger influence on the monitoring point than the secondary quarry road. That would explain the marginally higher fallout at collection point 5B. At all the other monitoring points, the A collection point recorded higher fallout. The findings of the microscope investigation also reflected the unique recordings at this monitoring point. At 5A the average particle size collected was 18.64 µm. Sixty-one percent of the dust was smaller than PM₁₀ with 2% of the particles smaller than PM_{2.5} (Figure 5.06). At 5B, the average particle size was 10.5 µm. Fifty-eight percent of the dust was smaller than PM₁₀ with no particles smaller than PM_{2.5} (Figure 5.07).

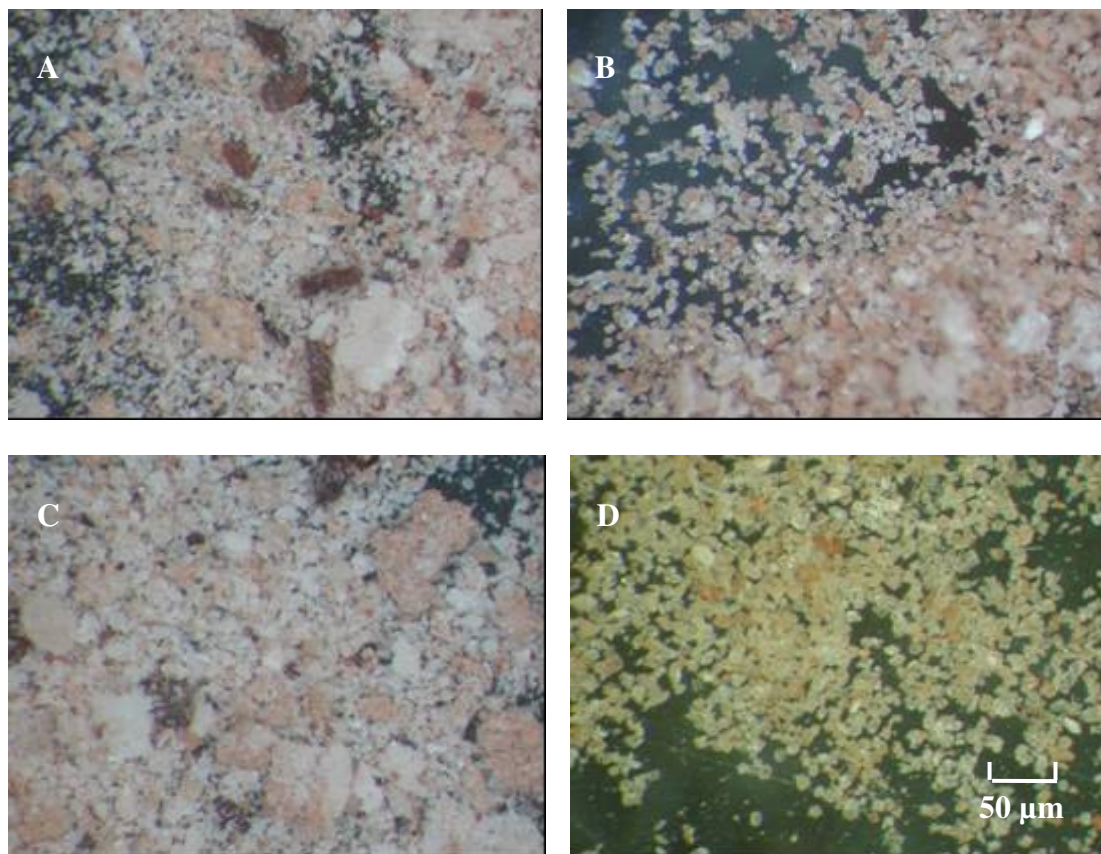


Figure 5.06 Sediment collected at monitoring point 5: Quarry. A was collected in the container and B in the polca sampler at collection point 5A. C was collected in the container and D in the polca sampler at collection point 5B, 50 m further away from the dust source. The scale is the same for all photos.

The microscope investigation yielded the same findings at Monitoring Site 5 as at 1. The polca samplers trapped better sorted and better rounded particles than the containers. The obvious lack of visual gypsum crystals in the sediment is due to the mining cycle during which this sample was collected. As it was collected mostly during a quarry opening phase, more overburden aeolian dust was collected. During a mining and stockpiling phase, the dust is expected to contain more gypsum crystals. As the mining activities move further away from this monitoring point, sediment movement and fallout dust is expected to decline.

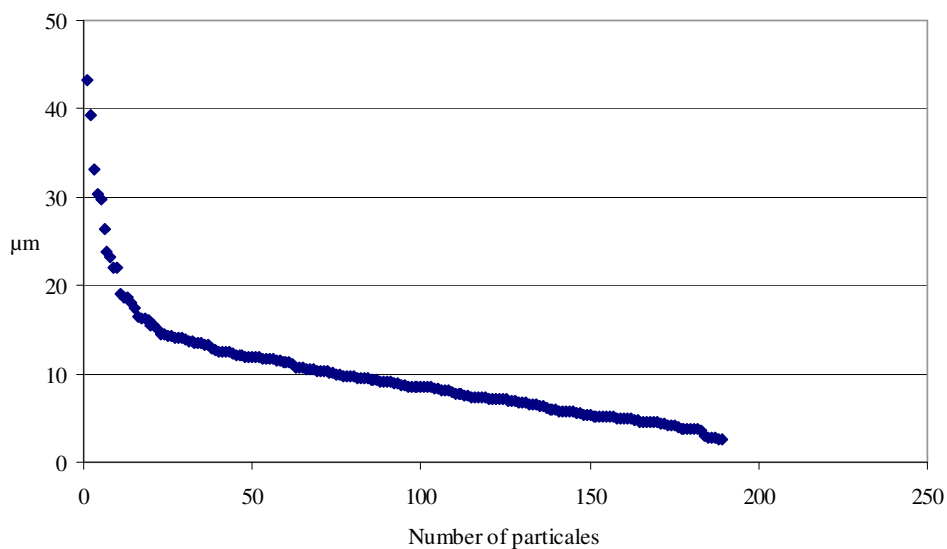


Figure 5.07 Particle size analyses of sediment particles collected at Monitoring point 5A.

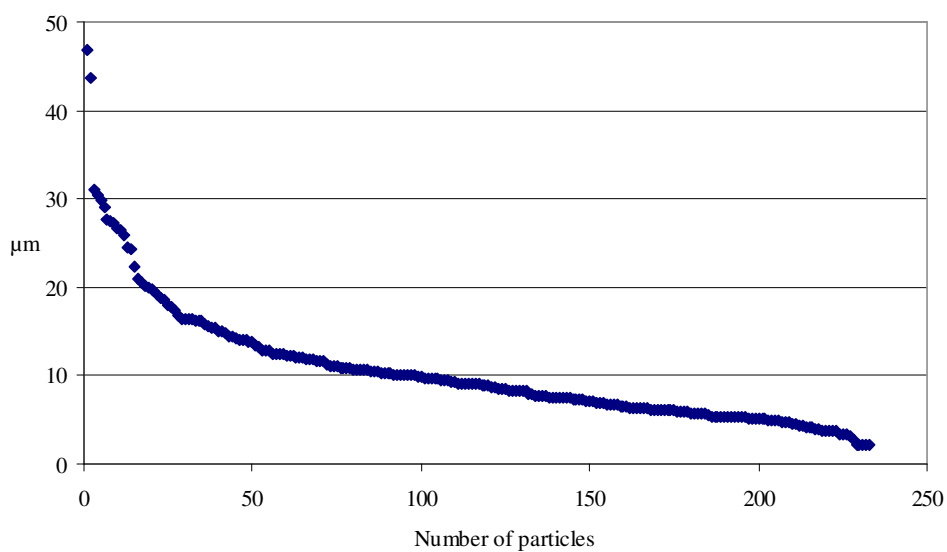


Figure 5.08 Particle size analyses of sediment particles collected at Monitoring point 5B.

The container samples at Monitoring Site 1: Station, collection points A and B, contained clearly identifiable gypsum particles (Figure 5.03). The polca sampler samples at Monitoring Sites 1 and 5, collection points A and B, contained less easily

identifiable particles and were investigated under the SEM (Figure 5.09 and Figure 5.10).

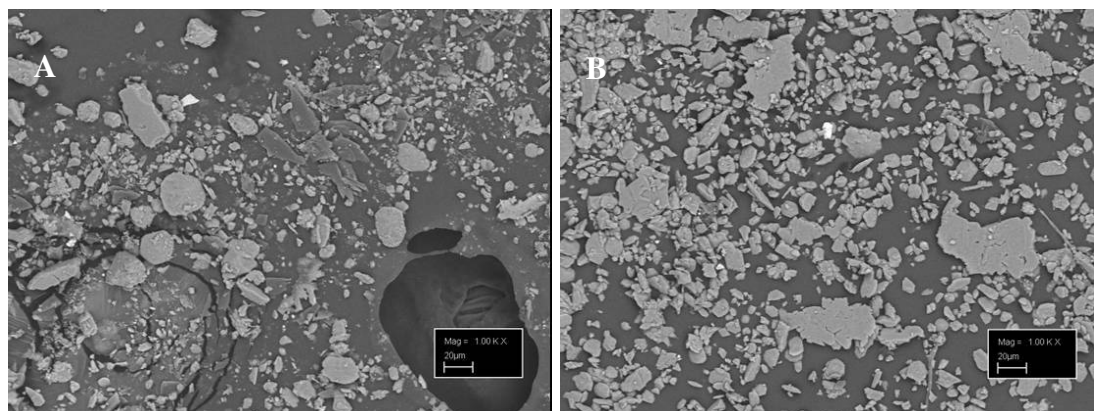


Figure 5.09 SEM images of the polca sampler sediments collected at Monitoring Site 1. A was collected at collection point A (Mag = 100K X, line scale = 20µm). B as collected at collection point B (Mag = 100K X, line scale = 20µm)

Point chemical analyses were done on some of the crystals. The SEM samples were covered in gold dust for the analyses. The chemical analyses were inconclusive (Table 5.01). It became evident that the samples were either coated with fine particles or that the point analysis penetrated through the small particles to produce a combination of more than one mineral in the results. The particles were too small to analyse accurately (Stephens, 2007).

Table 5.01 The SEM point chemical analyses of the polca sampler samples for monitoring point 1, collection point A and B.

Spectrum	% C	% Na	% Mg	% Al	% Si	% S	% K	% Ca	% Fe	% O	%Total	Interpretation
1a	27.165				0.218					72.617	100	Organic
1a						24.567		27.629		47.804	100	Gypsum
1a	13.139				0.928				38.768	47.166	100	Rust / org mix
1b						24.362		27.996		47.642	100	Gypsum
1b	21.397					5.449		5.713		67.441	100	Organic
1b	11.599				0.561			0.907	42.776	44.157	100	Rust / org mix

Point chemical analyses were also done on the polca sampler samples from Monitoring Site 5. The analyses revealed approximately the same results where the analyses were inconclusive (Table 5.02).

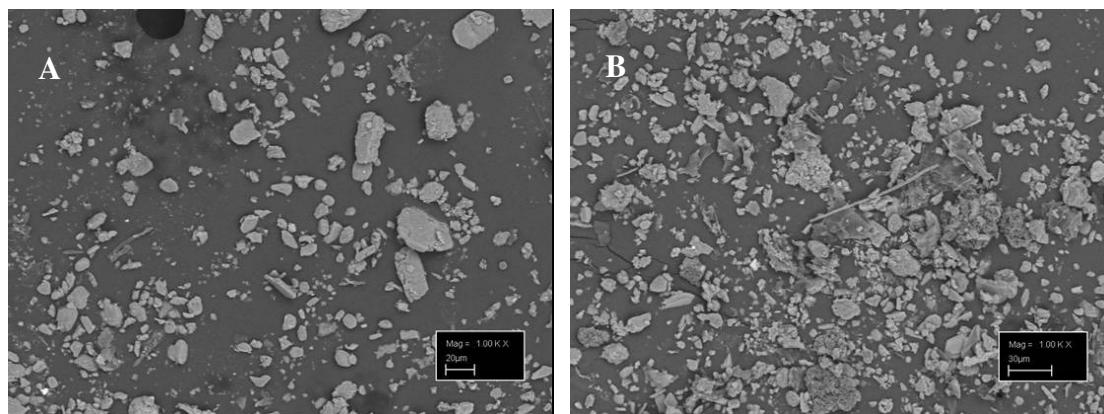


Figure 5.10 SEM images of the polca sampler sediments collected at Monitoring Site 5. A was collected at collection point A (Mag = 100K X, line scale = 20µm). B was collected at collection point B (Mag = 100K X, line scale = 30µm)

Table 5.02 The SEM point chemical analyses of the polca sampler samples for Monitoring Site 5, collection point A and B.

Spectrum	% C	% Na	% Mg	% Al	% Si	% S	% K	% Ca	% Fe	% O	%Total	Interpretation
5a						25.308		26.306		48.385	100	Gypsum
5a				19.345	25.813		6.831			48.012	100	Clay
5a	19.220	0.579	0.626	5.507	6.854		1.203	0.293	0.497	65.029	100	Clay / org mix
5a	16.513			1.040	2.515	7.896		8.888		63.148	100	Organic
5b	25.900			0.211	0.679	0.747		0.917	0.078	71.467	100	Organic
5b	19.986				1.235	5.651		7.044	0.128	65.957	100	Organic
5b	11.704		2.791	4.324	18.391		1.400		2.556	58.834	100	Qz / org mix

During the mining process, the gypsum production is continually sampled and chemically analysed. Apart from the obvious $\text{CaSO}_4 \cdot 2\text{H}_2\text{O}$, the ore is also analysed for

the alkali metal ions sodium (Na^+) and potassium (K^+) and the metal ion magnesium (Mg^{2+}). It is also tested for the chloride anion (Cl^-). The chemical analysis for the gypsum mined at Waterkuil is as follow:

$\text{CaSO}_4 \cdot 2\text{H}_2\text{O}$: 87.26 %, the rest consist of acid insoluble sand, silt and clay and small amounts of salts.

Na	0.0354 % or 353.652 mg/l
K	0.0021 % or 20.7811 mg/l
Mg	0.0130 % or 129.636 mg/l
Cl	0.0235 % or 234.703 mg/l

The results are not conclusive enough to use any of the chemical elements as traces for the mining operations. Natural gypsum deposits that are mined by BPB Gypsum throughout the world have been tested and are being spot checked for heavy metals and mercury content. None have been found that contained significant levels. Metals being checked for are beryllium (Be), vanadium (V), chromium (Cr), manganese (Mn), cobalt (Co), nickel (Ni), copper (Cu), zinc (Zn), arsenic (As), selenium (Se), cadmium (Cd), tin (Sn), thallium (Tl), lead (Pb), and mercury (Hg).

Synthetic gypsum supplies like desulphogypsum and phosphogypsum are routinely checked for heavy metal and rare earth elements. Desulphogypsum is produced during the extraction of sulphur dioxide from flue gasses by treatment with lime and oxidation. Phosphogypsum is obtained from orthophosphoric acid manufacture, which is a wet process involving the breaking down of phosphate ore with sulphuric acid. Practically all the orthophosphoric acid produced is converted into sodium phosphate and superphosphate fertilizers (Bensted, 1979).

In an article on the crystallisation of gypsum in the phosphoric acid production, Rashad et al. (2003) described how the addition of some metal and lanthanide ions into the gypsum crystal lattice imposes a strong impact on the crystallisation parameters. The effect of trivalent metal ions, such as chromium (Cr^{3+}) on the nucleation and growth kinetics is generally more pronounced than the divalent ions. Other trivalent ions that were investigated were the lanthanides, lanthanum (La^{3+}), cerium (Ce^{3+}), europium (Eu^{3+}) and erbium (Er^{3+})(Rashad et al., 2003). Although the

studies were done under simulated conditions of the phosphoric acid production, it was hoped that some of these ions might have had the same effect on the crystal lattice of “naturally” formed gypsum.

Samples were taken of both ore bodies and tested for the lanthanides content in order to try and find trace elements that could be directly related to gypsum dust and sedimentation generated by the mining, transport, stockpiling and loading of the gypsum. Three samples of gypsum were tested at the University of Cape Town for 14 rare earth elements (REE). Two of the samples were taken from the ore body at the closed mine at Waterkuil. These were numbered 2W and 3W (Figure 5.11). A third sample was taken from the current mining operation at a different ore body at Dikpens. It was numbered 1K. (See Figure 4.03 for the mine positions.)

The results of the testing indicated small anomalies in the transition metal element lanthanum and lanthanides cerium and neodymium (Table 5.03). Lanthanum is found with other rare earths in monazite and bastnaesite. Monazite is a rare-earth phosphate and Bastnaesite is a major rare-earth source and occurs in alkaline igneous rocks. Cerium is the most abundant rare-earth metal found in many minerals.

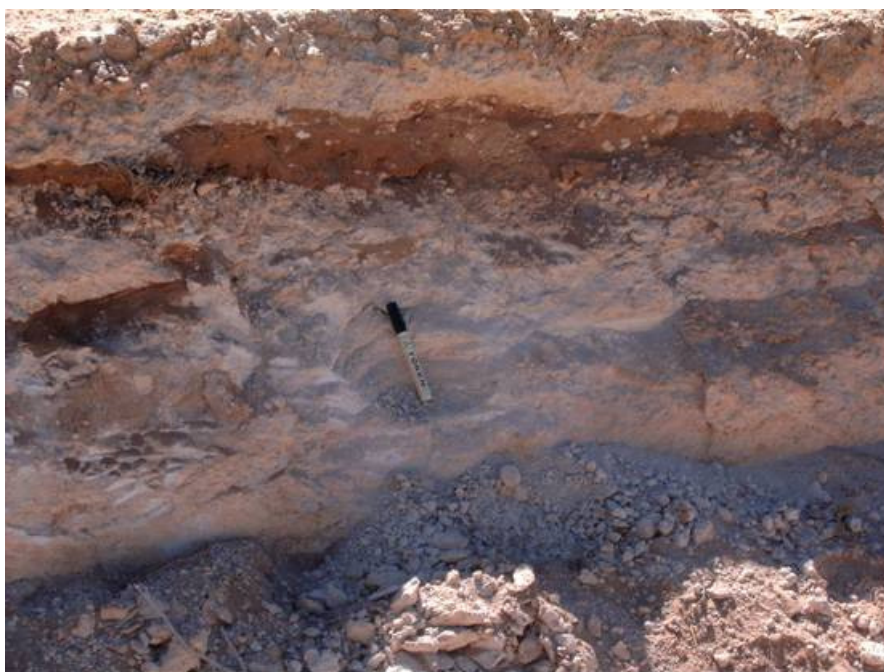


Figure 5.11 Position where sample 2W was taken from the ore body at Waterkuil at a depth of 60 cm below the surface.

Table 5.03 The results of the lanthanides analyses expressed in ppm.

		1K	2W	3W
La	Lanthanum	2.03	0.60	0.88
Ce	Cerium	3.27	1.35	1.54
Pr	Praseodymium	0.46	0.16	0.19
Nd	Neodymium	1.87	0.58	0.81
Pm	Promethium	-	-	-
Sm	Samarium	0.33	0.11	0.15
Eu	Europium	0.094	0.014	0.056
Gd	Gadolinium	0.34	0.087	0.14
Tb	Terbium	0.051	0.011	0.021
Dy	Dysprosium	0.32	0.059	0.16
Ho	Holmium	0.068	0.011	0.031
Er	Erbium	0.19	0.030	0.10
Tm	Thulium	0.030	0.004	0.015
Yb	Ytterbium	0.20	0.018	0.10
Lu	Lutetium	0.029	0.003	0.017

Neodymium is formed from electrolysis of halide salts. Anomalies of europium and erbium would have been quite more significant as a direct correlation with work done on phosphogypsum.

The results of the testing were received with mixed feelings as an anomaly would have provided an easy trace. The upside, however, is that the gypsum that is mined and transported over great distances, poses absolutely no threat of rare-earth pollution to the environment. The anomalies that exist within the gypsum, which are very small, were not further perused. It was quite interesting to find the slightly higher anomalies in the Dikpens sample 1K. This could confirm the suspicion that the two ore bodies, at Waterkuil and Dikpens, are not related. Chemical analyses of gypsum from the Dikpens deposit indicated the following results:

CaSO₄.2H₂O: 90.19 %, the rest consist of acid insoluble sand, silt and clay and small amounts of salts.

Na 0.04866 % or 486.571 mg/l

K 0.0011 % or 11.200 mg/l

Mg 0.0136 % or 135.915 mg/l

Cl 0.0575 % or 574.601 mg/l

This indicates that the Dikpens deposit contains somewhat purer gypsum than at Waterkuil, but also higher levels of the other ions as salts.

5.4 Conclusion

In this study it became evident that only one visual link, the gypsum crystals, could be traced between the sediment trapped in the containers at Monitoring Site 1, but not between the particulate matter trapped by the polca samplers at this site. No exclusive links could be traced for either containers or polca samplers at Monitoring Site 5. The general feeling was that the trapped sediment and the expected origin could not be linked, apart from the one described above. It also became evident from the SEM point analyses that some sediment found in the traps originated from either a natural redistribution of sediment in the region, or background (ambient) noise. No clear physical or chemical traces could be found that would enable the search for the dust in soil profiles or aid with the application of the dust settling model.

6 PROPOSING AND TESTING A SEDIMENT DISTRIBUTION MODEL

6.1 Introduction

Once the settling model was derived and tested against the expanded monitoring system, it was decided to monitor the climatic conditions and relate that to sediment movement and deposition on and around the mining activities. It was also related to vegetation and the changes that occurred. The need was then identified to predict sediment transport and the fate of sediment in the soils surrounding the opencast mining area. In this chapter the focus will be around implementing the crucial weather information, together with the information regarding sediment movement discussed in Chapter 4, in a dynamic approach. In order to test the settling model and investigate the correlation between dust settling patterns along the road and around mining quarries, field sampling was done. Sampling was done on the mine site at Waterkuil. Mining operations at Waterkuil mine ceased one year earlier (Figure 6.01). The area that was sampled was chosen to reflect the influence of the mining operation after closure. Samples were taken in the undisturbed soil around the last quarry that was mined while the mine was operative.

Visual inspection of grab samples around other, older areas of the mine indicated that the mine sedimentation influence almost disappeared altogether. The influence of the mining had to be represented by the sample area. The mine influence in the sampled area was a year old, but also not entirely destroyed by time. The influence was quickly detected using onsite electrical conductivity (EC) testing. The chosen area was isolated from any other influence and sources of mine operation dust, such as quarry roads dust or overburden stockpiles generation dust. It was also not exposed to compounded sedimentation generated by adjoining quarries that are opened and mined at different times during the life of the mine. Mining in the sampling area commenced in February 2002 and ceased in December 2004.

6.2 Methodology

Soil sampling was done on a rough grid pattern of 20m by 20m using a GPS to record the positions of the samples (Figure 6.03). The sampling was done on 11 and 12 March 2005. It was done around an isolated section of the worked-out quarry at the closed mine, Waterkuil (Figure 6.02). 338 Samples were taken by scraping off the top 15 to 20 mm of the soil profile into plastic bags. The average sample weight was 670 g. The aim was to collect the top layer of the surface soil that contained the dust and sediments that were generated during the mining operation. The bags were labeled and sealed for analysis. The sampling area was dormant for a year after mining ceased, prior to the sampling process. Close spaced sampling was done over 12 ha in a square around the quarry, up to 200 m away from the edge of the quarry. Three smaller areas were identified to transect closer spaced sampling to test the variability over short distances. This was done to investigate the influence of the wind shadows behind plants and other obstructions. Each of these transect consisted of 10 samples, taken at 3 m intervals.

Four samples were taken 100 m apart, 400m away from the edge of the quarry towards the south. The aim of these samples was to relate any findings directly to the settling model described in Chapter 3. Finally, another 4 samples were taken 100 m apart at a distance of 600m from the quarry edge, towards the south. These samples were taken to correlate the soil conditions free of any mining activity and also to relate ambient dust conditions to the settling model. The outlier samples added an additional 16 ha to the sampling area. All the soil samples were sieved with a 0.53 mm sieve to remove the large weathered slate fractions. On average the samples contained 12.3% slate. In order to isolate the dust fraction in the soil profile, selected samples were sieved into 4 fractions (Figure 6.08). Samples close to the mining area were selected to maximize the chances of being able to isolate wind transported sediment generated in the mining process (Figure 6.01 and 6.03). Using the following sieve apertures, the Udden-Wentworth grains size scale was applied to the results: 250 μm to isolate the coarse to medium sand fraction, 106 μm to isolate the fine sand fraction, 53 μm to isolate the very fine sand fraction and <53 μm to isolate the silt and clay fraction. The average

fractions per aperture for the samples were: 61% >250 μm , 27% > 106 μm , 10% > 53 μm and 2% < 54 μm (Figure 6.04).

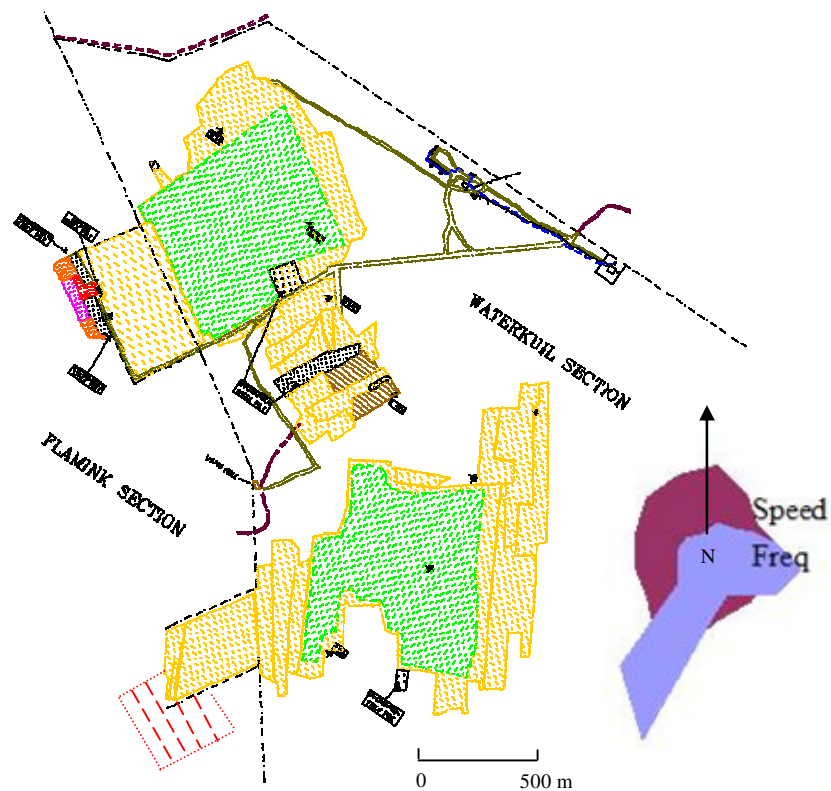


Figure 6.01 Map indicating the sampling area as the red, dash lines. It also shows a wind rose representing the average wind direction frequency and speed recorded by the onsite AWS.



Figure 6.02 A view of the quarry with the sampling area on the right.

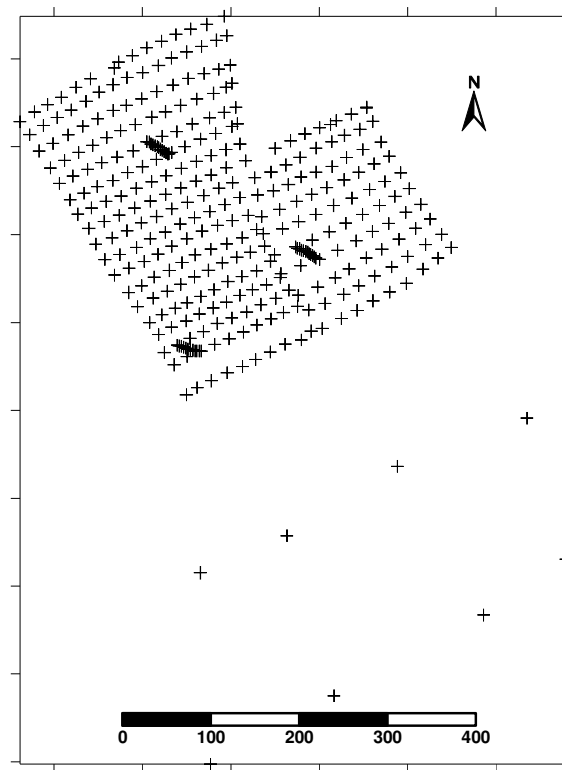


Figure 6.03 Waterkuil mine soil sampling positions.

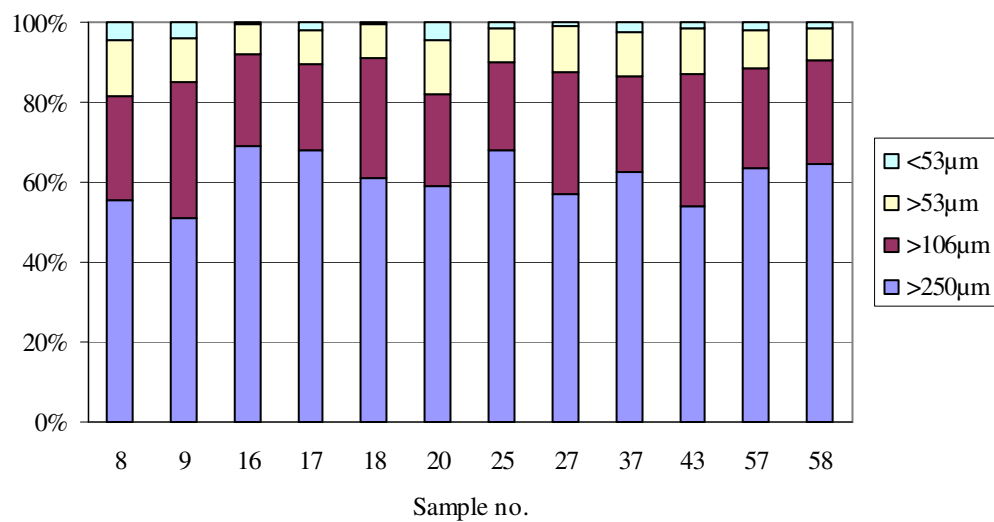


Figure 6.04 Sieved fractions of the selected samples to isolate the silt and clay fractions representing the dust generated by the mining operation.

The sieve analyses yielded surprisingly low quantities of silt and clay fractions. The particle size analyses of wind transported sediments collected by Monitoring Site 5: Quarry, described in Chapter 5.3, indicated that dust generated by the mining operation was silt and clay size particles, $< 54 \mu\text{m}$. Samples 8 and 9 were taken on the quarry border. These samples had the largest silt and clay content of 4 and 5% respectively. The correlation of -0.28 was calculated between distance from the quarry and the silt/clay content of the soil samples. This indicated a problem that had to be addressed in a different way. Sifting of the samples does not reflect the settling model, as can be seen in Figure 6.05.

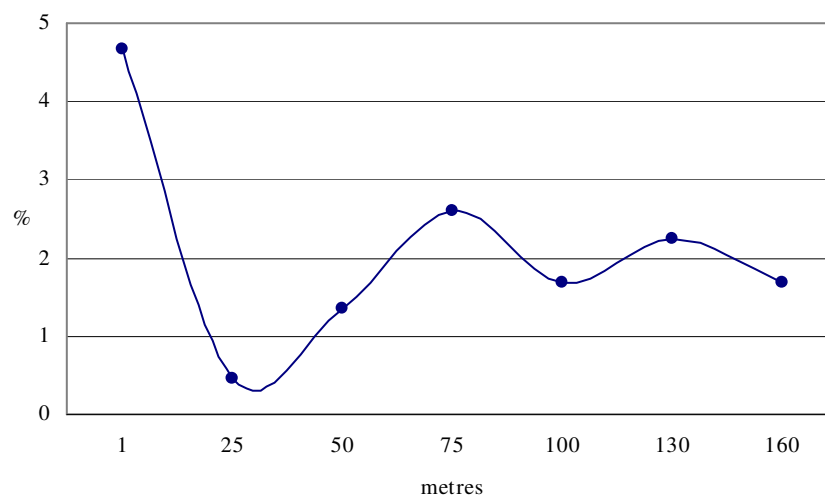


Figure 6.05 Indicating the poor relationship between the percentage particles smaller than $53\mu\text{m}$ and the distance from the quarry edge.

6.2.1 Chemical Investigation

Soil sample no. 17 was identified as a representative sample to be investigated for a possible reason as to why the sieve analyses and the settling model did not tie up. The sample position is indicated on Figure 6.08. The sample was taken at about 30 m from the quarry edge and is well within the settling model's high density fallout range. It was sieved into the same fractions as the previous samples and had 68% in the

fraction $>250\ \mu\text{m}$, 22% in fraction $>106\ \mu\text{m}$, 8% in fraction $>53\ \mu\text{m}$ and 2% $<54\ \mu\text{m}$. See figure 6.04 to correlate the fractions to the rest of the sieving investigation.

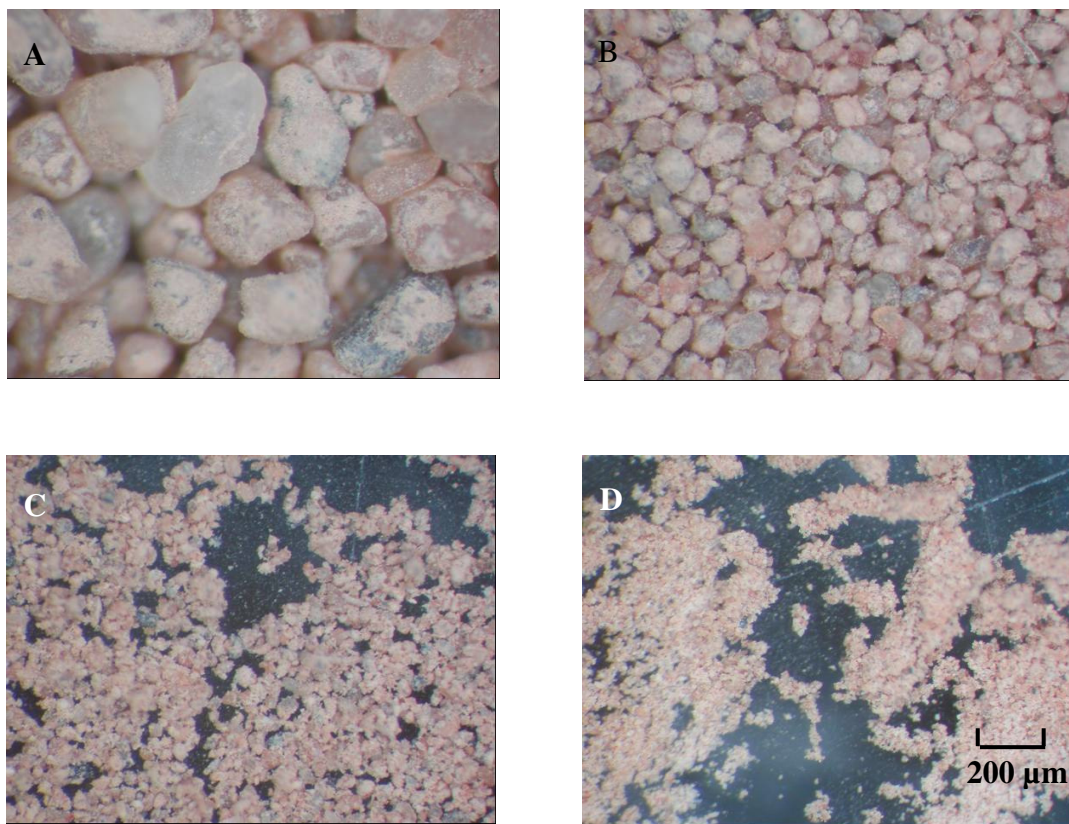


Figure 6.06 Images of sample 17 sieved fractions. A is the $>250\ \mu\text{m}$, B the $>106\ \mu\text{m}$, C the $>53\ \mu\text{m}$ and D the $<53\ \mu\text{m}$ fraction. The scale is the same for all photos.

From Figure 6.06 it was clear that the coarser particles in the range $>53\ \mu\text{m}$ were covered in with a layer of extremely fine material. This layer could not be liberated, even after prolonged periods of sieving. In the silt and clay fraction, $<53\ \mu\text{m}$, the particles stuck together in lumps and almost appear to be wet. It became apparent that the very fine silt fractions are not liberated by sieving and are thus dispersed throughout the fraction ranges. To further investigate the extent of this phenomenon, the sample was examined under a Scanning Electron Microscope (SEM) (Figure 6.07).

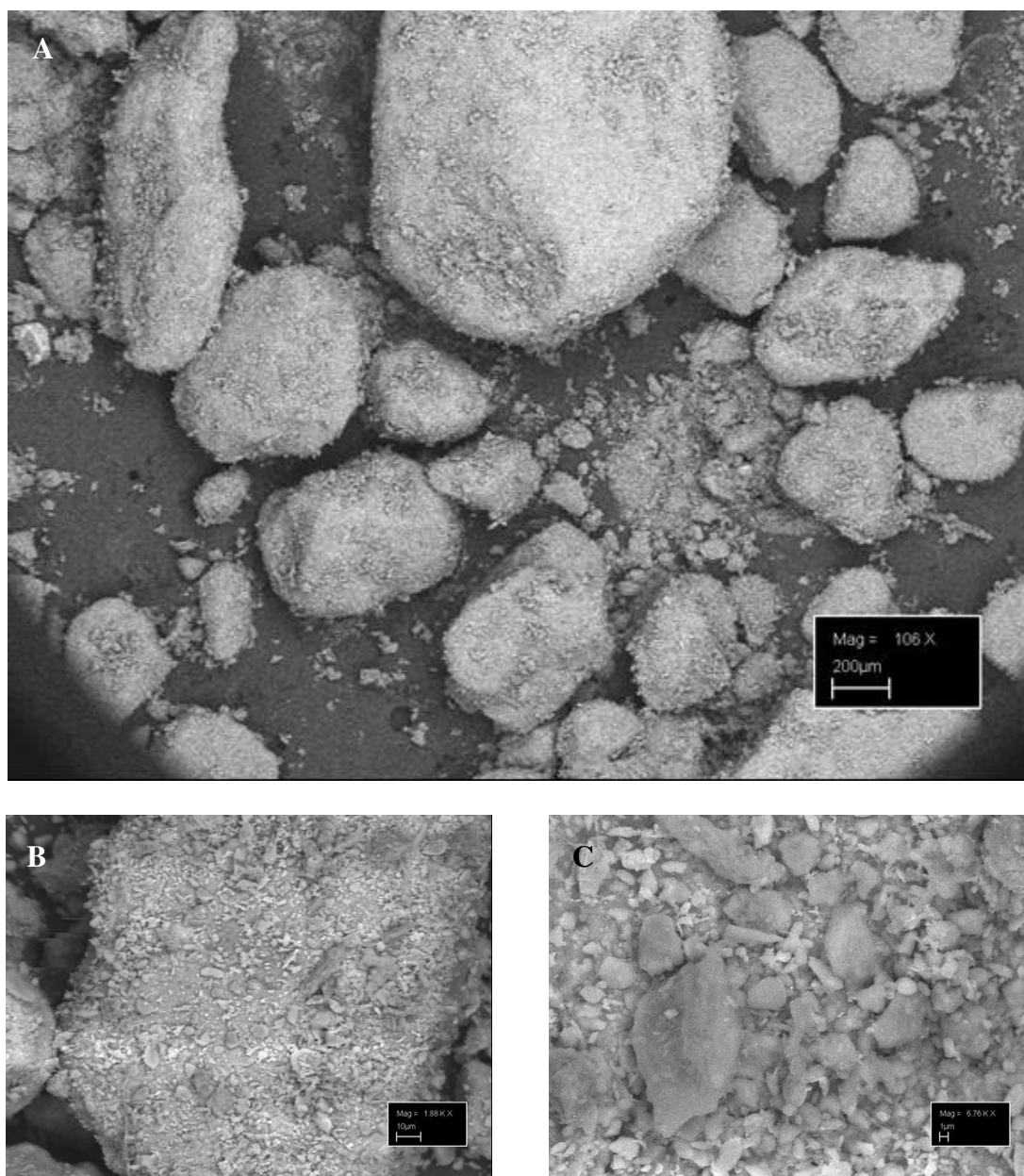


Figure 6.07 Images of sample 17 at A: Mag = 106 X, line scale = 200µm, B: Mag = 1.88K X, line scale = 10 µm and C: Mag = 6.76K X, line scale = 1 µm

The images revealed that the sand grains were indeed coated with a layer of plate like particles. When these images are compared to that of Figure 6.07 image A, it is clear that almost no area on the grains surfaces is clear of the coating for an uncontaminated point chemical analysis. It was almost impossible to tell what the larger grains consisted of. At first it was expected that the small particles forming the “coating” layer might consist of large fractions of mainly gypsum, but point chemical analyses

performed with the SEM indicated that the layer mostly consists of clay particles (Table 6.01).

SEM point chemical analyses indicated that the results might be combination results of more than one particle, as previously described in Chapter 5.3. Even the smaller gypsum particles had clay plates sticking to them, as can be seen in image C of Figure 6.07. Other samples were also examined, but they revealed the same phenomenon.

Table 6.01 Point chemical analyses performed on various soil samples.

Spectrum	% C	% Na	% Mg	% Al	% Si	% S	% K	% Ca	% Fe	% O	%Total	Interpretation
Spec 1	15.454		0.875	4.759	12.07		2.254	1.391	1.903	61.293	100	Clay / org mix
Spec 2	13.054		0.333	1.427	2.738	10.367	0.257	11.524	0.579	59.721	100	Gyp / org mix
Spec 3	13.941		0.415	1.419	3.164	9.444		10.258	0.66	60.699	100	Gyp / org mix
Spec 4			3.462	11.163	27.547		2.143	2.789	6.027	46.869	100	Clay
Spec 5		1.581		9.779	30.982		10.148		0.691	46.819	100	KSP
Spec 6			2.235	9.81	29.186		6.769	1.006	4.476	46.517	100	Clay
Spec 7			2.378	10.658	28.828		5.044	1.62	4.59	46.882	100	Clay
Spec 8	21.51			2.412	4.824				4.903	66.351	100	Organic
Spec 9		1.161	2.839	12.191	27.059		1.593	3.214	4.968	46.975	100	Clay
Spec 10				8.826	11.439			34.335	8.404	36.996	100	Carbo / rust mix
Spec 11				9.961	14.536			21.193	15.881	38.429	100	Carbo / rust mix
Spec 12			0.929	6.495	26.372		24.715			41.489	100	Uncertain result
Spec 13		0.58	0.703	3.248	40.38		2.045		2.385	50.659	100	Qz mix
Spec 14		2.501		9.786	31.142		8.796		0.717	47.058	100	Clay
Spec 15	21.53			2.255	7.877					68.338	100	Organic
Spec 16	21.128			1.623	8.39		0.494	0.696		67.668	100	Organic
Spec 17	13.639			0.544	22.617				0.479	62.722	100	Qz / org mix
Spec 18	18.736		0.717	1.701	5.923		0.295	9.353	0.651	62.625	100	Clay / org mix
Spec 19	4.781	0.253	1.812	6.074	27.947		1.407	0.774	3.962	52.991	100	Clay / org mix
Spec 20				2.463	3.420		0.858		65.069	25.941	100	Rust
Spec 21			2.838	6.819	22.614	5.669	1.443	7.992	5.408	47.217	100	Clay mix
Spec 22			7.525	4.535	24.771		0.615	9.016	9.213	43.873	100	Clay
Spec 23			4.574	9.700	26.750		1.802	4.012	7.057	46.105	100	Clay
Spec 24			3.861	6.348	25.744		1.767	6.717	11.663	43.900	100	Clay
Spec 25			4.514	13.296	26.199		2.737	1.515	4.610	47.130	100	Clay
Spec 26				29.367	33.017					37.616	100	Clay
Spec 27			1.741	12.563	22.451	0.834	7.862	2.676	7.184	44.205	100	Clay mix
Spec 28	9.605	1.157	2.231	6.239	19.943		0.933	0.416	2.637	56.840	100	Clay / org mix
Spec 29	15.241	0.772	1.624	5.451	11.656		0.812	0.768	2.439	61.238	100	Clay / org mix
Spec 30		0.983	1.840	11.811	27.965		3.623	0.961	6.043	46.774	100	Clay
Spec 31			2.821	6.019	16.645		1.036	0.682	35.866	36.932	100	Rust / clay mix
Spec 32	12.211		1.531	5.491	15.027		1.626	1.146	5.158	57.810	100	Clay / org mix
Spec 33			3.306	9.091	28.452		2.431	1.101	9.333	46.286	100	Clay
Spec 34			3.859	9.242	28.134		2.013	3.306	6.922	46.526	100	Clay
Spec 35			4.259	8.698	27.770		2.319	3.450	7.366	46.138	100	Clay
Spec 36			5.040	16.060	28.374		0.968	3.805	6.524	39.229	100	Clay
Spec 37			2.489	12.177	26.381		2.946	1.278	8.622	46.107	100	Clay

Out of 37 point chemical analyses performed on sample 17 and other samples, 51% analyses were inconclusive. The particles that could be identified positively, proved to be mostly clay particles. Not one particle proved positively to be pure gypsum. It was suspected that the clay particles coat and hide not only the larger sand particles, but

also the gypsum particles that should be present in the soil profile surrounding the mining quarry.

It is believed that the coating is not just a result of electrostatic cohesion, but a combination of the latter and climatic conditions (Cooke et al., 1993; Hughes, 1997). From the onsite monitoring that was done with AWS as described in Chapter 4, it is apparent that moisture often precipitates as dew, mist and frost (Agam and Berliner, 2005) (Figures 4.07 and 4.08).

After it became clear that sieving and the SEM point analyses will not yield analytically concise information, the soil samples were prepared for testing of their individual electrical conductivity (EC) and pH (De Clercq and Meirvenne, 2005). The EC is expressed in millisiemens per meter (mS/m) and is a measure of the concentration of salts in solution. The pH was tested for an indication of the degree of acidity/alkalinity of the soil. The method followed was to dissolve 5 grams of sample in 25 ml of distilled water. It was shaken overnight to dissolve the soluble salts.

The pH results indicated that the average pH is 7.3 (neutral), ranging from 6.5 (slightly acidic) to 8.9 (strongly alkaline). The EC results ranged from 5.51 to 301 mS/m, averaging 47.65 mS/m. The results were modelled in Surfer to identify trends that might give an indication of the dust sedimentation generated by the mining operation. The pH-values showed no clear trend around the extremities of the mines quarry. The EC values, however, did show a decreasing trend away from the quarry. The values were Kriged and the results are shown in Figure 6.08 (Clark, 2001; De Clercq and Meirvenne, 2005). The exponential semi-variogram and variogram model, as well as the distribution parameters of the data, are shown in Figure 6.09 and Table 6.02.

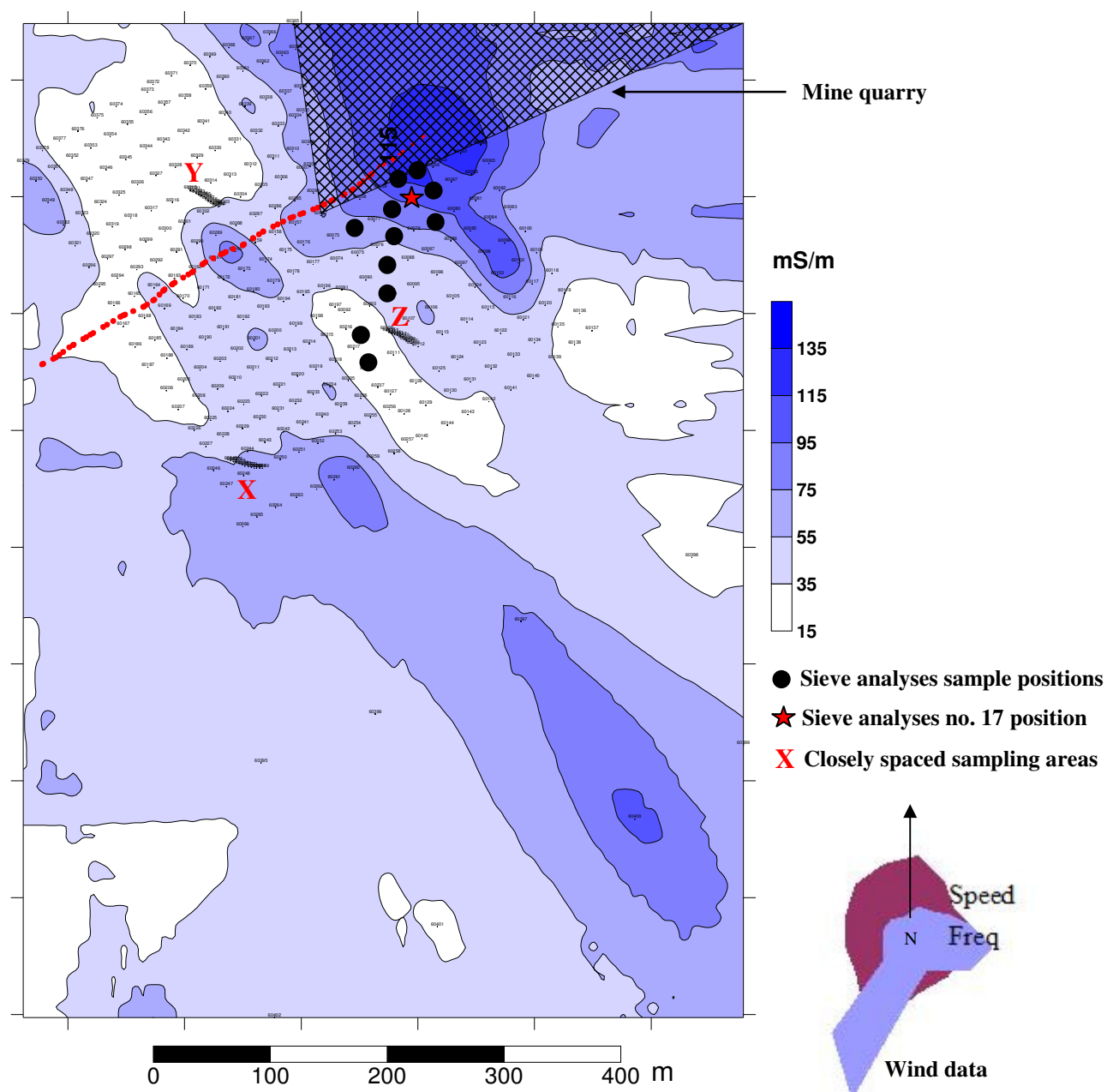


Figure 6.08 Map of the Kriged EC surfer model. The sieve analyses sample positions and the position of sieve sample 17 are also indicated. Note the wind rose in the map legend.

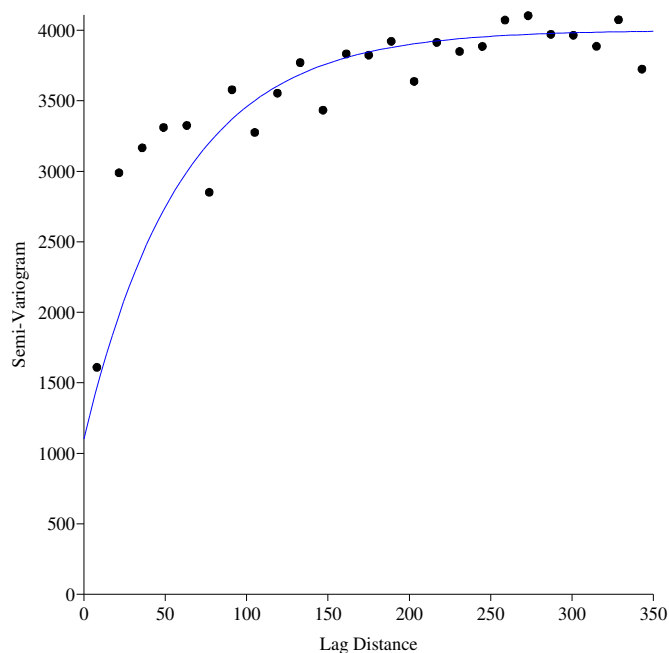


Figure 6.09 Exponential semi-variogram and variogram model of the soil samples from Waterkuil mine.

Table 6.02 The distribution parameters of the EC data (mS/m) from the Waterkuil soil samples.

Minimum:	5.51
25%-tile:	11.46
Median:	19.05
75%-tile:	53.9
Maximum:	301

The normal distribution of the EC from the soil water extracts indicated a negatively skewed database. This is quite typical of EC values from soil samples to be negatively skewed (De Clercq and Meirvenne, 2005).

Chemical analyses were done on 40 selected samples to establish their composition. The samples were tested for the cations calcium (Ca^{2+}), magnesium (Mg^{2+}), sodium (Na^+) and potassium (K^+) with atomic absorption spectrophotometry. They were also

tested for chloride anion (Cl^-), nitrate (NO_3^-), phosphate (PO_4^{3-}) and sulfate (SO_4^{2-}) using ion chromatography.

An investigation was done to establish possible correlations between the EC trend and the chemistry of the samples (De Clercq et al., 2001) (Table 6.03). The correlation between calcium and the EC is 0.995, between sulfate and EC, 0.978 and between calcium and sulfate, 0.990 (Figure 6.10). It is very obvious from this exercise that the EC trend around the mined quarry was caused by the gypsum dust created during the mining process.

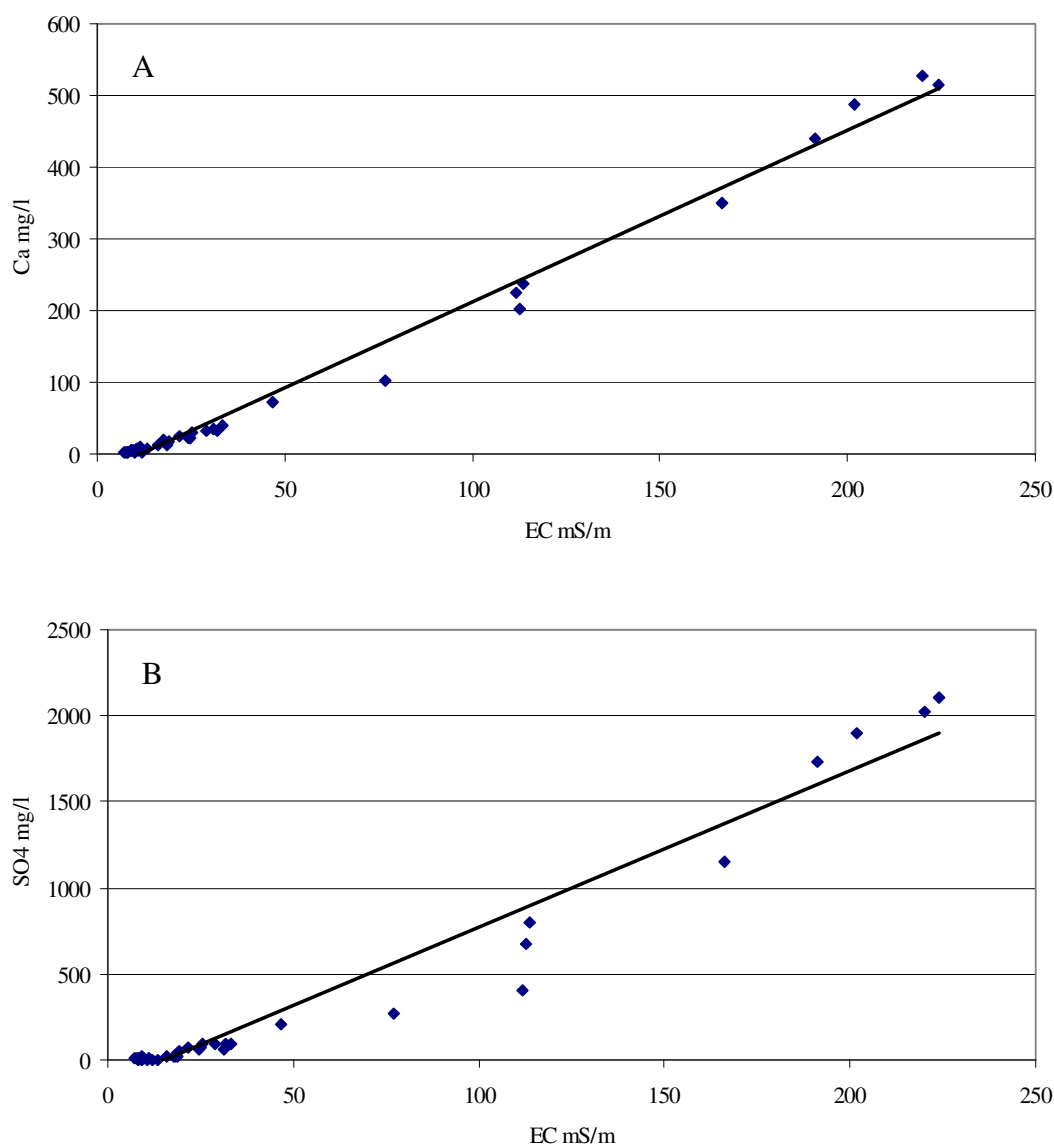


Figure 6.10 Graph A shows the strong correlation between calcium and EC and Graph B shows the equally strong correlation between sulfate and EC.

Table 6.03 The correlation matrix between the EC, pH and the chemistry of the soil samples.

	pH	EC mS/m	Ca mg/l	Mg mg/l	Na mg/l	K mg/l	Cl ⁻ mg/l	NO ₃ mg/l	PO ₄ mg/l	SO ₄ mg/l
pH	1.000									
EC mS/m	-0.273	1.000								
Ca	-0.295	0.995	1.000							
Mg	-0.008	0.552	0.497	1.000						
Na	0.440	0.138	0.091	0.412	1.000					
K	0.271	0.592	0.569	0.518	0.360	1.000				
Cl ⁻	0.325	0.077	0.028	0.384	0.715	0.464	1.000			
NO ₃	0.011	0.010	-0.050	0.467	0.407	0.120	0.545	1.000		
PO ₄	0.047	0.004	-0.047	0.100	0.525	0.091	0.481	0.491	1.000	
SO ₄	-0.303	0.978	0.990	0.434	0.076	0.548	0.018	-0.067	-0.051	1.000

The red aeolian sand that forms the topsoil in the area consists mostly of silica sand and contains between 6 and 15% clay (Cowling et al., 1986). The question again arises as to why the expected gypsum in the dust was not detectable by the SEM and the consequent point analyses if it obviously has quite a strong presence in the soil profile close to the quarry edge. As mentioned previously, the gypsum is covered in a naturally occurring clay layer. The clay particles are wind transported. During the transportation the particles are electrostatically charged (Cooke et al., 1993; Hughes, 1997). They attach themselves to and stick to the neutral sand and gypsum particles, covering them in a thin coating. To further aid the development of the clay layering, the mist, dew and frost precipitation, described in Chapter 4, provides sufficient moisture to assist a hygroscopic bond between the gypsum and clay particles, and the sand grains and clay particles as described by Cooke et al. (1993) and Hughes (1997). Given the mining method, it is expected that the immediate area bordering onto the quarry will have gypsum dust accumulated on the soil profile. Bearing in mind the chemistry of the gypsum deposit at 90% gypsum content, as described in Chapter 4, the clay forming the coating does not originate from mining the deposit. It was introduced as wind transported particles after mining ceased a year prior to the sampling of the area. It is therefore assumed that the clay accumulation represents the natural sediment movement that occurs in that environment. Only by dissolving the samples, are the clay particles removed and the presence of the gypsum dust revealed.

The second strongest correlation of 0.715 exists between sodium and chloride. Because NaCl commonly occurs in large quantities in soil profiles surrounding the salt pans, the pan water and ground water of the region, it was quite surprising to find the poorer correlation of 0.07 and 0.13 with the EC values around the quarry. The ground water in the region is described by the Department of Water Affairs and Forestry as of the Hydro-chemical type with abundant cations sodium (Na^+) and potassium (K^+) and anions chloride (Cl^-) and sulfate (SO_4^{2-}). BPB Gypsum's record of the water sources in the region is included as a point of interest (Figure 6.11 and Table 6.04)

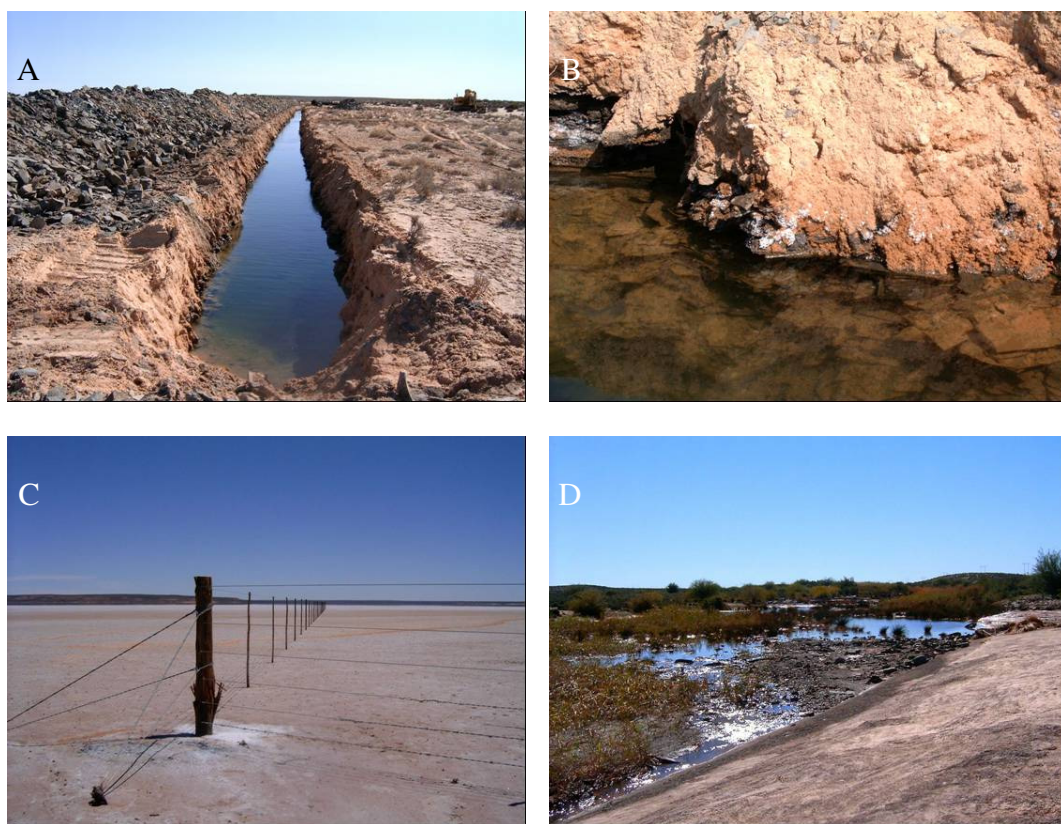


Figure 6.11 Water sources in the region are commonly high in soluble salt content. A: is a water trench on the mine at Dikpens. B: Evaporitic salt deposits are visible on the sides of the trench. C: NaCl is mined on the pan at Dikpens. The salt deposit is visible around the base of the fence pole. D: The Sout (Salt) river drains the region, some 40 km away from the mine.

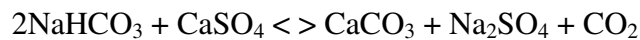
Sodium very often has a high correlation with EC values (Fey and De Clercq, 2004). Given the geographical location of the gypsum orebody, next to a pan, higher sodium correlation values were initially expected. It was even predicted that the sodium might overshadow and mask any other correlations. The presence of sodium was however very low.

Table 6.04 A record of the region's water sources. Note that they are compared to Brakpan tap water and sea water.

	Vaal River 01/11/2004	Sout River 17/05/2005	Dikpens Trench on mine	Dikpens Borehole 14/12/2004 on mine	Brandvlei borehole 28/06/2006	Brandvlei Pan water 28/06/2006	Brakpan Tap Water	Sea Water Average
CaSO ₄ ·2H ₂ O - mg/l	-----	-----	-----	-----	-----	-----	-----	-----
SO ₄ - mg/l	250	24	4086	1390	4424	26265	93	2680
Cl ⁻ - mg/l	68	4798	25865	984	2323	195590	11	19350
Na ₂ O - mg/l	109.2	2393	22850	1267	3269	161419	23	14437
K ₂ O - mg/l	16.3	17	58	6.6	11	122	4	470
MgO - mg/l	57.5	970	1467	207.3	211	10695	14	2172
Suspended Solids - mg/l	12	21	259	12.5	27	649	1	-----
Dissolved Solids - mg/l	516	9692	51000	3717	10302	340732	144	-----
pH	8.01	7.82	7.82	8	7.83	7.55	8.13	-----

A possible reason for the lower than expected correlation between NaCl and the EC, might be provided from an agricultural perspective. Gypsum is regarded as one of the best sources of both calcium and sulphur. The abundance of gypsum dust in the profile might provide the answer. With the addition of very fine gypsum into the soil profile, the structure improves and balances the soil by adding calcium and displacing sodium. With the application of gypsum, the calcium migrate to the clay particles, sticking to them in much the same way as dust will stick to an old vinyl record. Calcium can attach to more than one clay particle at once, causing them to clump together. When calcium moves in to exchange places with sodium, the sulphate captures this sodium and carries it away in the soil water (White, 1987). Often the water originates from the precipitation of dew and mist, as described in Chapter 4.

The use of gypsum on sodic soils is commonly recommended for the purpose of exchanging calcium (Ca^{2+}) for sodium (Na^+) on the micelle and removing bicarbonates from the soil solution.



In another reaction described by Snyman (1996), gypsum can react in an alkaline environment to remove Na^+ in the following reaction:



This reaction is likely to be active in this environment.

6.3 Discussion

After a positive and traceable chemical sediment “footprint” (calcium and sulfate) was established in the soil profile, the next step was to model the fallout pattern around the mining site. As previously described, the EC values were modeled using Surfer 8 and the values Kriged to produce a map of the sedimentation pattern (Figure 6.08.). It should be borne in mind that the strong anomaly that is visible in the far south east of the sampling area, is caused by small gypsum outcrop.

Once the dust settling model, as described in Chapter 3, was applied and tested against the two expanded monitoring systems, it was applied on the settling patterns around the mine quarry. A closely spaced data “slice” was taken through the surfer model. It is very important to note that it was done in the same direction in which the dust settling was derived. Figure 3.03 and Figure 6.12 were compared. The similarity between the distribution pattern in Figure 6.12 and the pattern of the dust settling model in Figure 3.03 was noted. The similarity can be attributed to the fact that the “slice” was taken in the same direction relative to the wind direction as the settling model.

The EC values over distance equation was established to be $y = 671.7x^{-0.506}$. The dust settling model equation was established to be $y = 1.0244x^{-0.4599}$ as described in Chapter 3. Both these equations were applied to the distances of the dust settling

model. The aim was to derive a prediction equation for the settling of mine dust around the quarry, based on the road dust settling model. By comparing the EC distribution around the point of source and sediment distribution as a function of distance from a point source, a prediction trend can be derived. The finding was a linear trend with the equation: $y = 0.0017x + 0.0123$ (Figure 6.13).

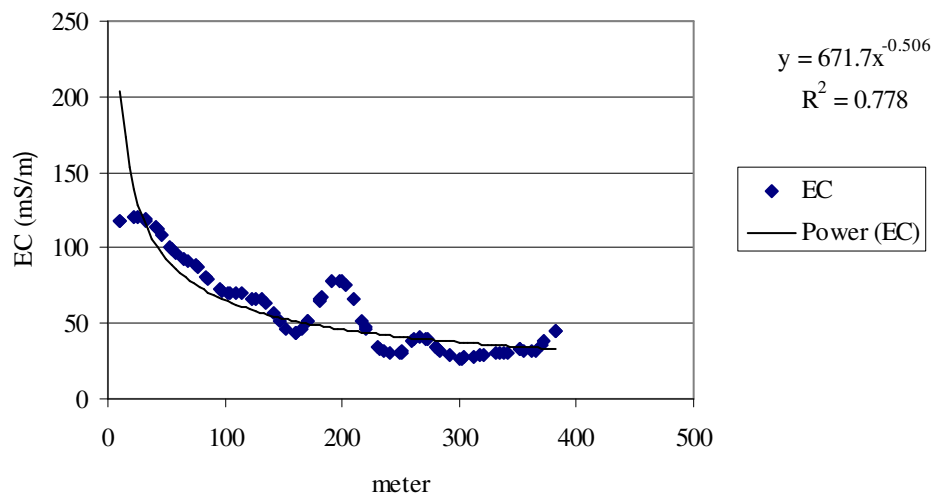


Figure 6.12 The EC values of the “slice” samples and the trend equation.

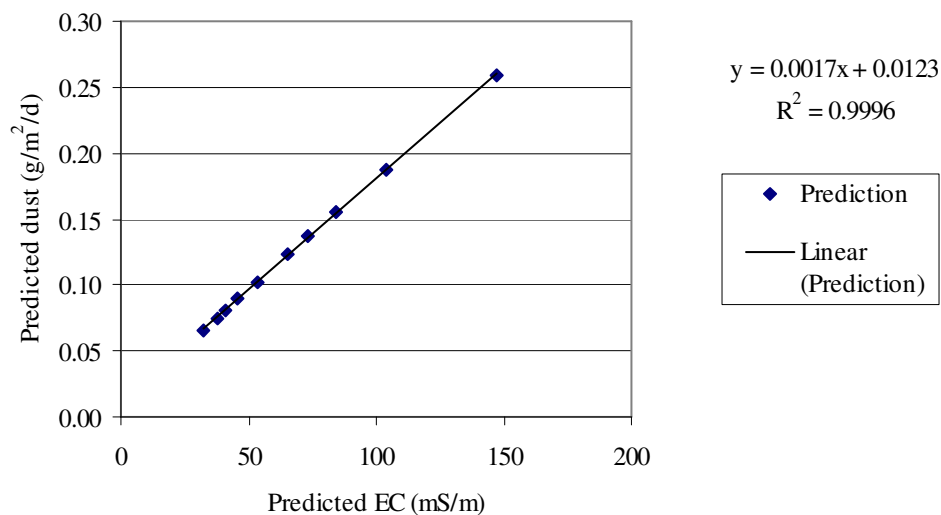


Figure 6.13 The linear prediction trend between dust accumulation and EC values.

This equation makes it possible to predict the amount of dust deposition by testing the electrical conductivity of soil samples that were taken in a controlled manner. In applying this prediction, it is necessary, to consider wind speed and direction information to map the influence sphere of the opencast mine.

6.4 Conclusion

Prior to the soil sampling investigation, many predictions were made that were proven wrong. It was predicted that the fine fraction (silt and clay fraction $< 53\mu\text{m}$), created by the mining and quarry transportation as dust, would be a lot larger than actually encountered, especially close to the quarry border as large amounts of dust are generated during the mining process. When the sieve analyses revealed that it is not the case and that the fine fraction could not be liberated, the samples were microscopically investigated. Prior to the chemical investigation it was predicted that the high levels of soluble salts in the natural profile of the area will mask and disguise any EC anomalies. This prediction was also proven wrong. Kriging of the EC values provided a very typical wind orientated dust settling model of sediment distribution from point sources. Historical sediment accumulation could be predicted using current climatic parameters.

7 CONCLUSIONS

This study evolved over 7 years. It set out to answer mainly two important questions: Can the successful monitoring of climate parameters increase the manageability of dust produced by open cast mines, in particular gypsum mines. The second question is whether the influence sphere of a mine can be predicted from historical weather data and used in the planning phase of mines.

As far as the first question is concerned, the study was successful in deriving a settling model that was tested against two separate monitoring locations. The settling model proved that climatic parameters have an influence on the settling patterns around a dust source.

The second question was also answered positively. Although the wind transported sediments were not directly detectable in the soil profile, the influence sphere of the closed mine was positively predicted. By applying the settling model to the soil samples and with the identification of a traceable chemical footprint, the influence sphere could be predicted. The influence sphere can also be mapped and because it can be mapped, it can be managed.

By further applying the predictions based on climatic parameters, the influence sphere can be modelled. The model is not only applicable to the planning phase of an opencast mine to plan the position of dust sensitive areas like the living quarters, office buildings and workshops, but also to indicate the historical impact that a mining operation had, once a quarry on an active mine is worked out and rehabilitated or a mine is closed, as in the case of Waterkuil. It can also aid in the presentation of the predicted impact on neighbouring communities or activities and avoid later penalties.

During the 7 year research period, many practices were investigated and implemented as standard practice by BPB Gypsum to lower the impact of the windblown sediment. These include speed limits both on and off the mine and private road maintenance of the provincial road. It further included climatic, dust settling and vegetation monitoring to aid with quarry management and planning. The quarry management is

scheduled to coincide with seasonal wind changes and the mine layout planning according to wind direction.

As a direct result of this study, adapted dust monitoring systems were implemented at the Gyproc board manufacturing plant in Parow, Cape Town. The monitoring system forms the basis of a drive towards a reduced dust emitting environment. It has proven to be a powerful tool in monitoring the effectiveness dust reducing initiatives implemented both inside the factory and outside on the factory premises.

The finding of the low REE anomalies in the gypsum was initially perceived as negative. Another chemical trace had to be found, but from an environmental pollution point of view, the finding was very positive. It proved once again that natural gypsum has very little environmental impact.

Another astonishing finding was the ability of natural forces to deal with larger particulate matter, in particular gypsum particles. The SEM photographs indicated the thin clay coating that surrounds these particles. It probably formed as a result of moisture and electrostatic charges on the clay particles, combined with the hygroscopic effect of the larger gypsum particles. The larger particles are almost encrusted.

8 REFERENCES

- Idaho Department of Environmental Quality (2000-2007).
http://www.deq.state.id.us/air/prog_issues/pollutants/dust.cfm
- Agam, N., and P.R. Berliner. 2005. Dew formation and water vapor adsorption in semi-arid environments - A review. *Journal of Arid Environment* 65 (2006):572-590.
- Anda, A. 1986. Effect of cement kiln dust on the radiation balance and yield of plants. *Environmental Pollution* 40:249-256.
- Arslan, M., and M. Boybay. 1990. A study on the characterization of dust fall. *Atmospheric Environment*, 24A:2667-2671.
- Barfield, B.J., and J.F. Gerber. 1979. *Modification of the aerial environment of crops*. American society of Agricultural Engineers. Michigan USA.
- Batanouny, K.H. 1979. Vegetation along the Jeddah-Mecca road; pattern and process as affected by human impact. *Journal of Arid Environments* 2:21-30.
- Bauer, B.O., C.A. Houser, and W.G. Nickling. 2002. Analysis of velocity profiles from wind tunnel experiments with saltation. In: Lee, Feffrey A. and Zobeck, Ted M., 2002, Proceedings of ICAR5/GCTE-SEN Joint Conference, International Center of Arid and Semi-arid Lands Studies. Publication 02-2:10-13.
- Becker, H. 1997. Stopping erosion with gypsum and PAM. *Agricultural Research* 45(9).
- Beckett, K.P., P.H. Freer-Smith, and G. Taylor. 1998. Urban woodlands: their role in reducing the effects of particulate pollution. *Environmental Pollution* 99:347-360.
- Behairy, A.K.A., M.K. El-Sayed, and N.V.N. Durgaprasad Rao. 1985. Eolian dust in the coastal area north of Jeddah, Saudi Arabia. *Journal of Arid Environments* 8:89-98.
- Bensted, J. 1979. Early hydration behavior of Portland cement containing chemical by-product gypsum. *World cement technology*. December 1979: 404-410.
- Blignaut, A. 2007. Vegetation Monitoring results of the BPB Gypsum mine on the farm Konnes. *Anel Blignaut Environmental Consultants, BPB Gypsum Pty. Ltd. Geology Department Internal report*.
- Borka, G. 1980. The effect of cement dust pollution on growth and metabolism of *Helianthus Annuus*. *Environmental Pollution (Series A)* 22:75-79.
- Brady, N.C. 1990. *The Nature and Properties of Soils*, 10th ed Macmillan Publishing Company, New York.
- Brook, R.D., B. Franklin, W. Cascio, Y. Hong, G. Howard, and M. Lipsett. 2004. *Air pollution and cardiovascular disease: a statement for healthcare professionals from the expert panel on population and prevention science of the American Heart Association*. *Circulation* 109:2655-2671.

- Bücher, A. 1993. Saharian dust from ancient times until the present. A note on methods of study. *Journal of Arid Environments* 25:125-130.
- Bueche, F.J. 1988. *Principles of Physics* McGraw-Hill Book Co, Singapore.
- Clark, I. 2001. Practical Geostatistics Geostokos Ltd, Alloa, Scotland.
- Colwill, D.M., J.R. Thompson, and A.J. Rutter. 1982. *An assessment of the conditions for shrubs alongside motorways*. Crowthorne, Berks, Department of the Environment, Department of Transport TRRL Report LR1061 in Thompson, J.R., Mueller, P.W., Flückiger, W. & Rutter, A.J. (1984) 34:171-190.
- Cooke, R., A. Warren, and A. Gaudie. 1993. *Desert Geomorphology* University College London Press, London.
- Cowling, R.M., P.W. Roux, and A.J.H. Pieterse. 1986. The karoo biome: a preliminary synthesis. 124. Foundation for research development. Council for Scientific and Industrial Research. Physical Environment.
- Dämon, M. 2007. Noise, Dust, Vibrations and their impact on quarry planning BPB Gypsum Group Mineral Resources Conference 2007, Gressy, France.
- Dässler, H.G., and S. Börtitz. 1988. *Air pollution and its influence on vegetation* JUNK Publishers, Boston DRW.
- De Clercq, W.P., and V. Meirvenne. 2005. Effect of long-term irrigation application on the variation of soil electrical conductivity in vineyards. *Geoderma* 128:221-233.
- De Clercq, W.P., M.V. Fey, J.H. Moolman, W.P.J. Wessels, B. Eigenhuis, and E. Hoffman. 2001. Establishing the effects of saline irrigation water and managerial options on soil properties and plant performance. WRC Report 695/1/01.
- Dickinson, C.H., and T.F. Preece. 1976. *Microbiology of aerial plant surfaces* Academic Press, London.
- Drinker, S.B., and B.S. Hatch. 1954. *Industrial Dust* McGraw-Hill Book Company, Inc, U.S.A.
- Eller, B.M. 1977. Road dust induced increase of leaf temperature. *Environmental pollution* 13:99-107.
- Eveling, D.W., and A. Bataillé. 1984. The Effect of Deposits of Small Particles on the Resistance of Leaves and Petals to Water Loss. *Environmental Pollution* (Series A) 36:229-238.
- Faith, W.L., and A.A.J. Atkisson. 1972. *Air Pollution* Wiley-interscience, New York.
- Ferguson, J.H., H.W. Downs, and D.L. Pfoest. 1999. Fugitive Dust: Nonpoint Sources. Agricultural publication G1885.
- Fey, M.V., and W.P. De Clercq. 2004. A pilot study investigating the role of dryland salinity in the quality of the water of the Berg River. WRC Report 1342/1/04.
- Flückiger, W., J.J. Oertli, and H. Flückiger. 1979. Relationship between Stomatal Diffusive Resistance and Various Applied particle Sizes on Leaf Surfaces. *Z.Pflanzenphysiol* 91:173-175.

- Gilber, O.L. 1976. An alkaline dust effect on epiphytic lichens. *Lichenologist* 8:173-178.
- Gillies, J.A., V. Etyemezian, H. Khuns, D. Nikolic, and D.A. Gillette. 2004. Effect of Vehicle characteristics on unpaved road dust emissions. *Atmospheric Environment* 39:2341-2347.
- Goossens, D., and Z.Y. Offer. 1995. Comparisons of day-time and night-time dust accumulation in a desert region. *Journal of Arid Environment* 31:253-281.
- Goossens, D., and Z.Y. Offer. 1997. Aeolian dust erosion on different types of hills in a rocky desert: wind tunnel simulations and field measurements. *Journal of Arid Environment* 37:209-229.
- Goossens, D., Z.I. Offer, and G. London. 2000. Wind tunnel and field calibration of five aeolian sand traps. *Geomorphology* 35:233-252.
- Goudie, A. 1978. Dust storms and their geomorphological implications. *Journal of Arid Environment* 1:291-310.
- Green, R., R. Gatehouse, K. Scott, and X.Y. Chen. 2001. Aeolian dust - implications for Australian mineral exploration and environmental management. *Australian Journal of Soil Research* 39:1-6.
- Gupta, A. 1988. *Ecology and development in the third world* Routledge, London.
- Holgate, S.T., J.M. Samet, H.S. Koren, and R.L. Maynard. 1999. *Air Pollution and Health* Academic Press, London.
- Hughes, J.F. 1997. *Electrostatic Particle Charging. Industrial and Health Care Applications* Research Studied Press LTD, Somerset England.
- Jones, D. 1999. A holistic approach to research into dust and dust control on unsealed roads. Seventh international conference on low-volume roads. Washington, DC Transportation Research Board. (TRR 1652).
- Kamra, A.K. 1973. Experimental study of the electrification produced by dispersion of dust into the air. *Journal of Applied Physics* 44:125-131.
- Kawamoto, K., S. Mashino, M. Oda, and M. Tsuyshi. 2004. Moisture structures of laterally expanding fingering flows in sandy soils. *Geoderma* 119:197-217.
- Khalaf, F., and M. Al-Hashash. 1983. Aeolian sedimentation in the north-western part of the Arabian Gulf. *Journal of Arid Environment* 6:319-332.
- Khalaf, F.I. 1989. Desertification and aeolian processes in the Kuwait Desert. *Journal of Arid Environment* 16:125-145.
- Le Roux, A., and E.A.C.L.E. Schelpe. 1981. *Namakwaland en Clanwilliam. Veldblomgids van Suid-Afrika*. Botaniese Vereniging van Suid-Afrika, Claremont.
- Le Roux, A., and T. Schelpe. 1997. *Namaqualand. South African Wildflower Guide 1* Botanical Society of South Africa, Claremont.
- Loppi, S., and S.A. Pirintsos. 2000. Effect of dust on epiphytic lichen vegetation in the Mediterranean area (Italy and Greece). *Israel Journal of Plant Sciences* 48:91-95.

- Low, A.B., and A.G. Rebelo. 1998. Vegetation of South Africa, Lesotho and Swaziland Department of Environmental Affairs and Tourism, Pretoria.
- Magihid, M.M., and S.M. El-Darier. 1995. Effect of cement dust on three halophytic species of the Mediterranean salt marshes in Egypt. *Journal of Arid Environment* 30:361-366.
- Manning, W.J., and W. Feder. 1980. *Biomonitoring Air Pollutants with plants* Applied Science Publishers LTD, Essex England.
- McTainsh, G.H., R. Burgess, and J.R. Pitblado. 1989. Aridity, drought and dust storms in Australia (1960-84). *Journal of Arid Environment* 16:11-22.
- Middleton, N.J. 1986. Dust storms in the Middle East. *Journal of Arid Environment* 10:83-96.
- Milton, S., and R. Dean. 1987. Padreserves dalk ons veld se uitkoms. *Landbouweekblad*: 20-21.
- Mishra, M.P., and V.S. Sai. 1988. Penalization of the biotic environment due to particulate matter and gaseous substances by cement dust plant at Kymore. *Asian Environment* 10:63-67.
- Modaihsh, A.S. 1997. Characteristics and composition of the falling dust sediments on Riyadh city, Saudi Arabia. *Journal of Arid Environment* 36:211-223.
- Monteith, J.L. 1975. *Vegetation and the atmosphere* Academic Press, London.
- Mudd, J.B., and T.T. Kozlowski. 1975. *Responses of plants to Air Pollution* Academic Press, New York.
- Neinhuis, C., and W. Barthlott. 1988. Seasonal changes of leaf surface contamination in beach, oak, and ginkgo in relation to leaf micromorphology and wettability. *New Phytologist* 138:91-98.
- Nickling, W.G. 1989. The insulation of particles movement by wind. *Sedimentology* 5:499-511.
- Offer, Z.I., D. Goossens. 1990. Airborne dust in the Northern Negev Desert (January-December 1987): general occurrence and dust concentration measurements. *Journal of Arid Environment* 18:1-19.
- Paige-Green, P., and D. Jones. 2000. The use of gypsum and brine in roads in the Northern Cape - Restricted Report **CR - 2000/60**. CSIR Transportek, Pretoria.
- Péwé, T.L. 1981. *Desert dust: origin, characteristics and effect on man*. Academic Press, London.
- Prospero, J.M. 1999. Assessing the Impact of Advected African Dust on Air Quality and Health in the Eastern United States. *Human and Ecological Risk Assessment* 5: 471-479.
- Pye, K. 1987. *Aeolian dust and dust deposits*. Academic Press, London.
- Ramsperger, B., N. Peinemann, and K. Stahr. 1998. Deposition rates and characteristics of Aeolian dust in the semi-arid and sub-humid regions of the Argentinean Pampa. *Journal of Arid Environments* 39:467-476.

- Rashad, M.M., H.M. Baioumy, and E.A. Abdel-Aal. 2003. Structural and spectral studies on gypsum crystals under simulated conditions of phosphoric acid production with and without organic and anorganic additives. *Crystal Research Technology* 38:433-439.
- Reheis, M. 1997. Dust studies in Southern Nevada and California. *US Geological Survey*. <http://wrgis.wr.usgs.gov/mojaveEco/dustweb/dusttraps.html>
- Reheis, M.C., and R. Kihl. 1995. Dust Deposition in Southern Nevada and California, 1984-1989: Relations to Climate, Source Area, and Lithology. *Journal of Geophysical Research* 5:8893-8918.
- Reynolds, R., N. Mazza, P. Lamothe, M. Rehers, J. Belnap, and S. Phillips. 2000. *Earth Surface Processes. Eolian dust on the Colorado Plateau - How much is from the Mojave Desert?* <http://climchange.cr.usgs.gov/info/sw/bsc/index.html>.
- Ricks, G.R., and R.J.H. Williams. 1974. Effects of atmospheric pollution on deciduous woodlands part 2: effects of particulate matter upon stomatal diffusion resistance in leaves of *Quercus Petraea*. *Environmental Pollution* 6:87-106.
- Sai, V.S., M.P. Mishra, and G.P. Mishra. 1987. Effect of cement dust pollution on trees and agricultural crops. *Asian Environment* 9:11-14.
- Samet, J.M., F. Dominici, F.C. Curriero, I. Coursac, and S. Zeger. 2000. Fine particulate air pollution and mortality in 20 US cities, 1987-1994. *N Engl J Med* 343:1742-1749.
- Schmidt, A. 2000. Report on a Study to Establish the Influence of Gypsum and Road Dust on Natural Vegetation. *BPB Gypsum Pty. Ltd. Geology Department Internal report*.
- Schmidt, A. 2002. Strip-mine rehabilitation in Namaqualand., pp114. *University of Stellenbosch. M.Sc thesis. December 2002*.
- Schmidt, A. 2003. Strip-mine rehabilitation in Namaqualand - Guidelines., pp. 42. *BPB Gypsum Pty. Ltd. Geology Department Internal report*.
- Sharifi, M.R., A.C. Gibson, and P.W. Rundel. 1997. Surface Dust impacts on gas exchange in Mojave Desert shrubs. *Journal of Applied Ecology*: 837-846.
- Shearing, D. 1994. Karoo. *Veldblomgids van Suid-Afrika* 6. Botaniese Vereeniging van Suid-Afrika, Claremont.
- Sittig, M. 1977. *Particulates and fine dust removal. Processes and equipment* Noyes Data Corporation, New Jersey, U.S.A.
- Smith, R.L. 1974. *Ecology and Field Biology* Harper & Row, New York.
- Snyman, C.P. 1996. *Geologie vir Suid Afrika, Volume 2*. Departement Geologie, Universiteit van Pretoria.
- Spencer, H.J., N.E. Scott, G.R. Port, and A.W. Davidson. 1988. Effects of roadside conditions on plants and insects. I. Atmospheric conditions. *Journal of Applied Ecology* 25:699-707.

- Spencer, S., and R. Tinnin. 1997. Effects of coal dust on plant growth and species composition in an arid environment. *Journal of Arid Environments* 37:475-485.
- Stephens, G. 2007. Peronal communication regarding SEM chemical analyses, 15 October 2007.
- Tanaka, T., and H. Howard. 2007. Global dust budget. [Online] http://www.eoearth.org/article/Global_dust_budget (posted April 30, 2007; verified July 31, 2007).
- Thompson, J.R., P.W. Mueller, W. Flückiger, and A.J. Rutter. 1984. *Environmental Pollution*. Series A 34:171-190.
- Treshow, M. 1970. *Environment and plant response* McGraw-Hill Book company, New York.
- Tyson, P.D., F.J. Kruger, and C.N. Louw. 1988. *Atmospheric pollution and its implications in the Eastern Transvaal Highveld* 150. South African National Scientific Programmes.
- Van Jaarsveld, F. 2002. Dust Monitoring Report - Trial Period April 2000 to December 2001. *BPB Gypsum Pty. Ltd. Geology Department Internal report*.
- Van Jaarsveld, F. 2003. Initial Dust Monitoring Report - June 2003. *BPB Gypsum Pty. Ltd. Geology Department Internal report*.
- Van Jaarsveld, F. 2004. Dust Monitoring Report - October 2004. *BPB Gypsum Pty. Ltd. Geology Department Internal report*.
- Van Jaarsveld, F. 2007. Dust Monitoring Report - March 2007. *BPB Gypsum Pty. Ltd. Geology Department Internal report*.
- Weinan, C., D.W. Fryrear, and D.A. Gillette. 1998. Sedimentary characteristics of drifting sediments above an eroding loessal sandy loam soil as affected by mechanical disturbance. *Journal of Arid Environments* 39:421-440.
- Whalley, W.B., and B.J. Smith. 1981. Mineral content of harmattan dust from northern Nigeria examined by scanning electron microscopy. *Journal of Arid Environment* 4:21-29.
- White, R.E. 1987. *Introduction to the Principles and Practice of Soil Science*. 2 ed. Blackwell Scientific Publications, Oxford.
- Yaalon, D.H., and E. Ganor. 1973. The influence of dust on soils during the quaternary. *Soil Science* 115:146-155.
- Young, J.A., and R.A. Evans. 1986. Erosion and deposition of fine sediments from *playas*. *Journal of Arid Environment* 10:103-115.
- Zaady, E., Z.Y. Offer, and M. Shachak. 2001. The content and contributions of deposited aeolian organic matter in a dry land ecosystem of the Negev Desert, Israel. *Atmospheric Environment* 35:769-776.
- Zangvil, A. 1996. Six years of dew observations in the Negev Desert, Israel. *Journal of Arid Environment* 32:361-371.

ADDENDUM

ID	Coordinate		Elevation	pH	EC	Ca	Mg	Na	K	Cl	NO3	PO4	SO4
No	East	South	m		mS/m	mg/l	mg/l	mg/l	mg/l	mg/l	mg/l	mg/l	mg/l
3	249553.730	-3343455.781	871.266										
5	249512.986	-3343474.693	870.675	7.24	202	487.92	1.68	12.71	10.61	4.19	3.68	0.4	1894
4	249416.767	-3343516.166	869.954	8.48	29.8								
6	249450.163	-3343501.978	868.415	7.25	216								
7	249467.611	-3343493.474	869.747	7.59	70.5								
8	249483.837	-3343485.458	870.292	6.74	224	515.02	1.07	13.07	10.51	9.62	2.6	2.6	2105
9	249500.456	-3343478.548	870.343	6.53	203								
10	249519.350	-3343470.360	870.004	6.85	138.6								
11	249536.594	-3343462.956	869.709	6.82	231								
12	249553.755	-3343454.983	869.597	6.79	220	526.99	2.12	13.31	10.99	11.39	2.98	0	2022
13	249560.826	-3343471.428	870.285	6.87	46.4								
14	249546.082	-3343480.392	869.251	6.80	226								
15	249528.620	-3343487.127	870.681	7.05	25.2								
16	249514.206	-3343494.365	869.202	6.87	221								
17	249496.519	-3343501.633	868.053	7.29	43.0								
18	249478.397	-3343512.237	868.902	6.93	123.4								
19	249462.407	-3343520.997	868.907	7.63	15.26								
20	249445.446	-3343528.863	869.089	6.96	131.5								
21	249427.198	-3343535.286	868.356	7.21	64.7								
22	249430.338	-3343555.116	868.950	6.85	16.14								
23	249448.270	-3343550.064	868.705	7.03	17.12								
24	249465.002	-3343543.095	868.699	7.00	10.74								
25	249479.569	-3343534.355	869.332	7.27	13.89								
26	249496.516	-3343528.967	868.695	7.29	109.3								
27	249514.706	-3343522.501	868.489	7.21	58.5								
28	249530.909	-3343512.374	868.723	7.43	17.63								
29	249549.561	-3343503.278	866.712	7.26	39.5								
30	249569.925	-3343494.775	869.644	7.38	12.55								
31	249579.248	-3343510.919	866.716	7.49	18.81	14.99	0.95	17.85	5.30	7.8	5.35	4.91	20.62
32	249562.107	-3343519.575	866.539	7.60	13.59								
33	249544.806	-3343529.207	866.633	6.89	215								
34	249528.145	-3343537.656	866.938	7.30	12.44								
35	249508.598	-3343546.601	867.210	7.02	46.6	71.62	0.96	11.19	4.44	7.93	3.84	1.86	209.2
36	249491.555	-3343554.236	867.156	7.32	10.53								
37	249474.557	-3343562.239	866.934	7.21	17.57								
38	249455.288	-3343571.288	868.299	7.34	9.03	5.71	1.13	10.46	3.33	6.38	3.5	0	3.85
39	249434.888	-3343579.636	866.922	7.21	10.50								
40	249436.870	-3343598.994	869.955	7.04	27.9								
41	249458.609	-3343593.480	866.905	7.01	34.3								
42	249476.658	-3343585.254	867.661	7.33	14.96								
43	249496.173	-3343577.149	866.815	7.07	104.9								
44	249516.366	-3343566.891	867.543	7.35	9.48								
45	249537.061	-3343558.564	866.684	7.16	16.54								
46	249557.025	-3343548.948	867.112	7.19	20.1								
47	249574.214	-3343539.730	867.171	7.25	301								
48	249592.238	-3343529.598	867.869	7.85	16.36								

ID	Coordinate		Elevation	pH	EC	Ca	Mg	Na	K	Cl	NO3	PO4	SO4
No	East	South	m		mS/m	mg/l	mg/l	mg/l	mg/l	mg/l	mg/l	mg/l	mg/l
49	249601.897	-3343547.761	867.499	7.60	11.01								
50	249585.783	-3343556.578	867.480	6.77	233								
51	249568.083	-3343567.186	867.152	6.82	287								
52	249548.950	-3343577.390	867.449	7.49	26.3								
53	249530.123	-3343587.100	868.012	7.33	17.26								
54	249511.443	-3343597.071	867.506	6.78	115.6								
55	249492.218	-3343606.272	866.907	6.95	119.4								
56	249473.316	-3343614.045	870.637	7.24	15.95								
57	249449.636	-3343623.032	868.706	6.88	50.0								
58	249456.909	-3343644.459	869.432	7.80	16.79								
59	249479.064	-3343635.433	869.451	7.68	13.34								
60	249500.365	-3343628.330	869.793	7.45	11.54								
61	249521.015	-3343617.784	869.259	6.95	60.2								
62	249541.987	-3343607.223	869.350	7.02	23.7								
63	249560.189	-3343596.515	869.423	7.54	16.31								
64	249578.698	-3343587.468	869.697	7.85	58.0								
65	249598.074	-3343574.719	869.500	7.36	8.03								
66	249615.041	-3343565.596	869.476	7.28	48.2								
67	249625.670	-3343582.294	869.761	6.86	9.26	5.22	1.01	8.57	5.66	5.82	4.61	0	16.69
68	249609.107	-3343592.981	868.639	8.51	18.04								
69	249590.355	-3343605.275	870.666	8.57	15.72								
70	249570.964	-3343616.786	871.005	7.94	86.5								
71	249553.191	-3343626.701	869.215	8.80	13.39	8.50	1.19	16.97	7.83	6.74	2.03	0	3.03
72	249533.822	-3343639.124	869.313	7.48	27.3								
73	249518.113	-3343649.191	869.403	6.79	171.8								
74	249498.287	-3343659.700	871.972	7.05	21.8	23.79	0.57	10.11	6.14	6.67	4.13	2.69	67.57
75	249476.485	-3343668.949	871.466	7.17	9.54								
76	249488.124	-3343685.815	870.336	7.24	10.40								
77	249506.684	-3343678.513	869.586	7.11	7.41								
78	249527.751	-3343667.947	869.551	7.74	20.9								
79	249544.792	-3343658.454	869.322	7.33	8.58								
80	249562.736	-3343647.150	869.102	7.44	52.2								
81	249582.081	-3343636.935	868.974	7.77	21.4								
82	249599.881	-3343624.852	868.885	7.38	49.1								
83	249620.174	-3343611.462	869.190	7.09	7.12								
84	249638.625	-3343599.837	869.183	6.87	8.13								
85	249649.333	-3343614.685	869.573	6.65	11.03	5.91	0.91	10.34	5.06	4.02	1.4	0	12.51
86	249634.351	-3343626.765	871.979	6.94	6.13								
87	249617.328	-3343639.480	869.168	6.99	7.40								
88	249598.849	-3343655.423	872.325	7.89	122.2								
89	249579.692	-3343665.465	872.412	8.13	31.1	34.29	1.40	18.68	12.25	30.73	5.79	1.75	65.83
90	249560.937	-3343675.376	872.299	8.17	17.38								
91	249542.883	-3343686.415	872.499	7.95	11.37								
92	249525.304	-3343695.549	872.366	6.98	7.45								
93	249503.437	-3343706.984	871.904	7.53	10.72	6.50	1.07	11.25	6.35	7.18	4.33	0	4.66
97	249394.884	-3343523.955	868.425	6.91	214								
98	249377.701	-3343532.250	869.045	7.72	11.38								
99	249360.662	-3343539.229	869.237										
100	249343.487	-3343546.909	869.501	7.25	219								
101	249326.296	-3343554.306	869.734	7.06	213								

ID	Coordinate		Elevation	pH	EC	Ca	Mg	Na	K	Cl	NO3	PO4	SO4
No	East	South	m		mS/m	mg/l	mg/l	mg/l	mg/l	mg/l	mg/l	mg/l	mg/l
102	249308.995	-3343561.865	869.947	7.38	14.92								
103	249291.261	-3343569.772	870.810	6.91	12.06								
104	249273.772	-3343577.960	869.390	7.13	174.1								
105	249256.788	-3343585.116	870.302	8.93	25.3								
106	249239.322	-3343593.052	869.676	8.48	25.0								
107	249247.415	-3343610.929	870.121	7.58	24.5	21.83	0.94	18.13	7.79	15.92	4.79	2.29	57.72
108	249265.644	-3343603.839	870.132	7.42	11.09								
109	249282.784	-3343595.637	869.963	7.37	11.42								
110	249298.749	-3343586.822	869.556	7.46	10.59								
111	249316.039	-3343579.578	869.809	7.64	24.3								
112	249333.395	-3343570.727	870.129	7.19	11.27	8.80	0.96	10.03	4.20	3.49	0	0	9.62
113	249351.011	-3343563.336	869.266	6.76	50.4								
114	249369.509	-3343555.615	870.090	7.29	11.69								
115	249386.564	-3343547.334	871.451	7.86	22.5								
116	249401.970	-3343541.141	869.562	7.24	152.2								
117	249410.172	-3343557.924	870.190	7.47	13.72								
118	249393.241	-3343566.025	869.415	7.24	36.2								
119	249376.345	-3343573.779	870.122	6.79	217								
120	249358.989	-3343580.934	869.682	7.76	13.69								
121	249342.829	-3343588.075	870.124	7.22	8.23								
122	249325.877	-3343597.276	869.749	7.83	51.9								
123	249308.885	-3343604.869	870.339	7.2	30.8								
124	249293.284	-3343614.786	869.734	7.01	93.1								
125	249274.522	-3343622.769	870.051	6.89	28.5								
126	249257.582	-3343628.550	871.028	7.62	20.2								
127	249268.480	-3343645.944	871.528	7.24	7.30								
128	249284.764	-3343638.188	870.581	7.52	12.72								
129	249301.929	-3343630.698	869.399	7.22	14.75								
130	249317.683	-3343622.281	870.220	6.90	23.2								
131	249333.133	-3343613.303	871.028	7.09	10.46								
132	249350.277	-3343604.858	870.964	7.26	30.7								
133	249367.441	-3343596.017	870.724	6.97	8.85								
134	249384.873	-3343589.542	870.579	6.86	7.80								
135	249401.780	-3343583.925	871.953	7.13	8.23								
136	249419.607	-3343578.261	870.385	7.18	35.2								
137	249429.080	-3343594.421	870.932	6.89	10.62								
138	249413.076	-3343603.700	870.985	6.78	11.39								
139	249395.359	-3343610.479	870.767	6.92	14.86								
140	249377.520	-3343616.645	871.132	7.00	125.7								
141	249359.535	-3343622.994	870.921	6.74	190.5								
142	249344.820	-3343631.853	871.209	6.80	19.04	17.80	0.90	10.82	4.64	6.88	7.76	3.81	54.91
143	249330.429	-3343640.793	870.426	6.96	24.7								
144	249313.351	-3343648.393	872.453	6.62	115.5								
145	249299.215	-3343658.307	870.842	7.69	14.72								
146	249284.470	-3343666.013	871.781	6.89	7.85	3.69	0.96	9.24	4.29	6.18	4.13	0	6.34
147	249294.537	-3343682.086	871.355	6.93	6.86								
148	249312.157	-3343672.325	871.075	6.81	45.9								
149	249328.234	-3343664.447	872.486	6.85	103.9								
150	249343.233	-3343656.756	870.825	7.33	37.7								
151	249358.775	-3343648.146	872.286	6.81	111.9								

ID	Coordinate		Elevation	pH	EC	Ca	Mg	Na	K	Cl	NO3	PO4	SO4
No	East	South	m		mS/m	mg/l	mg/l	mg/l	mg/l	mg/l	mg/l	mg/l	mg/l
152	249374.747	-3343640.689	871.417	7.01	9.95								
153	249390.408	-3343632.376	871.382	6.75	9.06								
154	249406.842	-3343625.776	871.134	6.69	33.1								
155	249422.114	-3343620.040	871.254	6.67	69.0								
156	249438.334	-3343613.322	872.003	6.81	26.4								
157	249444.940	-3343630.254	872.128	7.19	15.30								
158	249429.345	-3343641.281	871.789	7.54	6.68								
159	249412.579	-3343647.637	870.875	7.05	38.4								
160	249396.843	-3343653.530	871.395	7.31	7.61								
161	249381.281	-3343662.718	872.027	7.09	30.7								
162	249366.037	-3343670.382	871.124	7.25	8.84								
163	249350.666	-3343677.637	872.181	7.10	10.88								
164	249337.138	-3343683.682	871.280	6.96	14.81								
165	249322.152	-3343691.339	871.484	6.84	30.6								
166	249308.217	-3343699.997	872.459	6.91	34.6								
167	249318.290	-3343713.818	871.649	6.90	25.4	29.83	0.76	13.10	2.95	6.35	5.56	2.26	97.36
168	249332.975	-3343705.395	871.064	6.93	17.06								
169	249349.612	-3343698.380	872.119	7.27	6.29								
170	249364.483	-3343690.341	872.194	7.13	8.29								
171	249380.182	-3343683.386	871.844	7.11	9.35	5.34	0.87	10.37	3.32	5.62	4.4	0	11.5
172	249395.047	-3343676.916	871.789	7.08	7.06								
173	249410.267	-3343669.190	872.117	6.66	68.0								
174	249424.525	-3343662.751	871.310	6.57	193.6								
175	249440.315	-3343657.277	871.736	6.92	9.42								
176	249456.036	-3343648.912	871.698	6.90	16.81								
177	249465.705	-3343663.198	872.048	6.94	62.3								
178	249451.047	-3343672.577	872.459	7.15	11.27								
179	249434.103	-3343679.606	871.515	6.93	59.5								
180	249417.932	-3343688.293	871.474	6.97	26.9								
181	249401.167	-3343694.941	871.216	7.07	9.43								
182	249384.695	-3343701.161	872.232	6.52	176.6								
183	249368.889	-3343710.241	872.576	7.13	19.05								
184	249353.950	-3343718.061	872.067	7.11	12.24								
185	249339.536	-3343725.965	871.701	6.91	58.5								
186	249324.834	-3343734.323	873.282	6.81	174.0								
187	249335.857	-3343748.087	870.911	7.07	39.5								
188	249350.586	-3343738.786	873.216	7.19	27.8								
189	249366.671	-3343732.477	872.601	6.91	79.7								
190	249381.995	-3343724.898	871.970	6.83	66.1								
191	249398.224	-3343718.696	870.752	7.03	13.97								
192	249414.288	-3343711.078	871.790	6.84	32.2								
193	249429.502	-3343702.930	872.219	7.14	17.52								
194	249445.591	-3343696.147	872.516	7.02	32.6								
195	249459.397	-3343688.806	871.274	6.86	81.0								
196	249475.569	-3343681.909	872.543	7.54	9.46								
197	249490.941	-3343709.901	873.909	6.76	19.2								
198	249479.642	-3343719.874	873.452	7.23	11.86								
199	249461.501	-3343724.736	872.977	7.29	10.36								
200	249444.655	-3343733.656	873.021	6.78	207								
201	249428.189	-3343742.317	873.476	6.54	227								

ID	Coordinate		Elevation	pH	EC	Ca	Mg	Na	K	Cl	NO3	PO4	SO4
No	East	South	m		mS/m	mg/l	mg/l	mg/l	mg/l	mg/l	mg/l	mg/l	mg/l
202	249413.212	-3343750.348	873.229	7.29	8.24	2.54	1.13	10.69	3.94	6.15	3.46	0	10.9
203	249395.969	-3343757.326	872.874	7.04	21.4								
204	249378.004	-3343766.127	872.363	7.24	13.69								
205	249361.972	-3343774.159	873.255	7.13	46.9								
206	249349.879	-3343782.442	874.115	6.98	113.6	238.66	0.86	11.31	2.92	4.37	2.95	0	801.6
208	249364.358	-3343732.230	871.013	6.91	46.7								
209	249361.654	-3343732.328	871.907	6.98	213								
210	249359.600	-3343732.456	871.187	6.85	192.7								
211	249357.174	-3343731.366	871.308	7.07	57.4								
212	249354.338	-3343730.822	871.512	6.90	85.2								
213	249351.649	-3343730.585	871.219	6.88	64.4								
214	249349.188	-3343729.228	872.716	7.13	34.8								
215	249346.733	-3343728.045	870.474	7.09	84.1								
216	249344.253	-3343726.965	871.321	6.88	22.4								
217	249341.712	-3343726.736	871.650	7.69	11.29								
221	249410.296	-3343496.879	871.704	7.59	17.73	19.60	0.74	11.04	6.77	4.09	1.57	0	23.33
222	249394.513	-3343503.396	870.732	7.40	8.56								
223	249377.622	-3343510.054	870.253	7.24	20.7								
224	249361.054	-3343516.778	871.127	7.89	14.84								
225	249344.022	-3343524.604	870.100	7.24	14.29								
226	249326.736	-3343533.033	869.976	7.07	191.2	440.62	2.74	12.31	10.68	5.36	2.83	0	1728
227	249310.599	-3343539.823	870.367	6.96	5.51								
228	249292.986	-3343547.419	869.702	7.40	11.74								
229	249275.763	-3343556.330	869.760	8.16	14.04								
230	249258.972	-3343562.445	870.156	7.99	11.05								
231	249242.414	-3343569.642	870.535	6.92	9.50								
232	249226.938	-3343576.904	871.455	6.68	9.69	5.05	0.97	10.46	5.01	6.34	13.28	0	7.65
233	249218.098	-3343560.509	871.164	7.15	90.1								
234	249233.937	-3343553.040	870.419	7.45	8.41								
235	249248.944	-3343545.269	870.155	7.37	25.4								
236	249266.758	-3343538.550	869.419	7.14	10.34								
237	249283.231	-3343529.391	870.844	7.28	50.2								
238	249300.038	-3343522.884	870.852	7.21	8.05								
239	249315.862	-3343514.427	870.872	7.17	10.29								
240	249333.066	-3343506.590	871.172	6.85	118.5								
241	249347.931	-3343500.143	870.188										
242	249365.557	-3343491.412	869.494	7.65	10.09								
243	249382.876	-3343485.166	869.189	7.73	12.11								
244	249401.427	-3343477.072	869.915	7.34	7.92								
245	249407.637	-3343473.962	870.319	7.32	9.92								
246	249405.753	-3343455.333	870.182	7.18	64.2								
247	249392.613	-3343461.184	869.855	7.08	149.2								
248	249375.931	-3343467.268	870.006	7.62	8.75								
249	249356.509	-3343474.184	868.406	7.44	18.16								
250	249338.966	-3343482.863	869.081	7.80	20.6								
251	249322.304	-3343488.172	868.030	8.15	14.81								
252	249304.858	-3343494.404	869.083	7.65	26.5								
253	249289.635	-3343504.853	869.263	8.21	18.98								
254	249271.421	-3343511.879	867.282	8.07	15.21								
255	249253.847	-3343518.304	870.171	8.23	17.21								

ID	Coordinate		Elevation	pH	EC	Ca	Mg	Na	K	Cl	NO3	PO4	SO4
No	East	South	m		mS/m	mg/l	mg/l	mg/l	mg/l	mg/l	mg/l	mg/l	mg/l
256	249238.119	-3343525.759	871.097	7.86	14.43								
257	249221.411	-3343533.415	869.153	7.69	14.28								
258	249206.056	-3343541.881	867.916	7.81	9.89								
259	249195.986	-3343524.193	867.835	7.04	111.7	225.16	2.16	9.02	9.09	2.92	1.51	0.72	407.1
260	249211.942	-3343515.615	868.725	7.89	11.09								
261	249227.921	-3343506.773	869.434	8.09	16.13								
262	249243.736	-3343498.595	868.412	7.69	10.45								
263	249259.638	-3343489.610	868.115	7.78	11.31								
264	249275.444	-3343481.858	867.755	7.09	14.67								
265	249292.169	-3343474.834	867.336	7.76	28.9	32.56	0.97	16.15	5.62	7.77	4.07	1.11	92.21
266	249310.633	-3343466.556	866.862	7.64	44.4								
267	249326.186	-3343460.355	867.564	7.87	16.28								
268	249343.148	-3343453.106	868.185	7.25	33.2								
269	249361.603	-3343445.691	867.537	7.36	19.54								
270	249380.356	-3343439.377	869.062	7.75	35.1								
271	249394.793	-3343432.384	868.445	7.67	37.9								
272	249401.443	-3343428.022	869.104	7.54	33.3	39.20	1.60	29.05	6.45	17.58	14.41	3.08	89.91
273	249399.348	-3343407.183	867.513	7.46	17.77								
274	249386.468	-3343411.900	868.104	7.55	53.9								
275	249369.737	-3343416.880	867.420	7.58	17.09								
276	249351.779	-3343422.513	868.388	7.44	202								
277	249334.518	-3343429.862	868.370	7.65	11.46								
278	249316.172	-3343437.436	867.916	7.45	13.89								
279	249299.190	-3343445.547	867.721	7.48	29.8								
280	249281.988	-3343453.029	866.485	7.63	17.44								
281	249267.027	-3343458.752	868.856	7.67	61.4								
282	249249.443	-3343468.250	868.271	7.56	11.03								
283	249232.678	-3343476.903	868.502	7.09	12.18								
284	249216.075	-3343486.605	869.513	7.62	14.87								
285	249198.872	-3343496.399	869.227	7.68	74.0								
286	249183.104	-3343504.984	868.899	8.3	83.0								
287	249172.539	-3343486.412	869.419	7.45	188.6								
288	249188.265	-3343476.181	868.867	8.12	17.25								
289	249203.600	-3343466.843	869.022	7.96	14.41								
290	249219.521	-3343458.257	867.960	7.63	19.98								
291	249236.212	-3343448.500	868.331	7.59	9.7								
292	249250.884	-3343437.955	869.541	8.29	17.11								
293	249266.796	-3343429.547	868.376	7.61	12.68								
294	249282.689	-3343421.270	869.072	7.56	9.54								
295	249300.310	-3343415.686	868.304	7.74	15.81								
296	249317.997	-3343407.726	868.461	7.44	8.57								
297	249332.840	-3343399.094	867.535	7.72	20.2								
298	249349.994	-3343392.235	868.391	7.69	20.0								
299	249366.981	-3343385.758	868.973	7.69	26.6								
300	249383.702	-3343378.966	869.016	7.17	150.8								
301	249395.350	-3343373.828	868.106	7.37	96.7								
302	249392.605	-3343351.656	869.199	7.64	31.9	31.80	1.59	16.04	7.58	11.22	6.47	4.1	90.9
303	249372.824	-3343360.908	867.808	7.70	45.6								
304	249354.495	-3343366.066	868.329	7.30	189.1								
305	249337.955	-3343372.409	868.856	8.06	74.3								

ID	Coordinate		Elevation	pH	EC	Ca	Mg	Na	K	Cl	NO3	PO4	SO4
No	East	South	m		mS/m	mg/l	mg/l	mg/l	mg/l	mg/l	mg/l	mg/l	mg/l
306	249321.583	-3343380.099	868.707	7.41	16.46								
307	249304.773	-3343387.412	868.560	7.50	8.85								
308	249288.712	-3343396.528	868.131	7.88	15.49								
309	249272.944	-3343403.882	868.836	7.49	79.7								
310	249268.194	-3343410.412	869.519	7.68	28.3								
311	249241.382	-3343422.769	868.534	7.71	18.53	12.08	1.15	11.39	10.22	5.08	2.25	0	16.39
312	249225.034	-3343432.425	868.688	7.25	88.2								
313	249208.510	-3343443.831	867.433	7.65	10.84								
314	249192.725	-3343452.167	867.827	8.22	16.29								
315	249178.101	-3343460.407	868.231	8.19	21.1								
316	249161.578	-3343471.559	867.719	7.77	15.99	13.27	0.57	10.59	5.35	4.47	2.16	0	15.71
318	249307.967	-3343494.821	868.464	7.80	13.91								
319	249309.688	-3343496.938	868.087	7.95	16.91								
320	249311.992	-3343497.957	868.317	7.84	11.59								
321	249314.554	-3343499.057	868.928	7.77	13.65								
322	249316.864	-3343499.968	868.041	7.99	16.78								
323	249318.226	-3343501.147	869.366	7.75	9.41								
324	249320.299	-3343503.115	869.383	7.18	13.09								
325	249322.572	-3343504.198	868.253	7.63	19.89								
326	249324.722	-3343505.708	869.131	7.99	25.8								
327	249326.800	-3343507.278	868.413	8.03	16.24								
328	249328.853	-3343508.528	868.693	7.86	15.30								
329	249329.932	-3343508.065	868.520	7.67	10.89								
333	249365.533	-3343984.695	874.364	7.19	25.0	22.87	1.07	12.72	4.72	8.06	10.19	1.38	73.57
334	249463.394	-3343942.807	874.166	6.97	7.95	2.05	1.20	10.29	3.80	5.81	4.13	0	3.82
335	249588.326	-3343863.580	874.596	7.37	112.8	203.18	3.06	12.30	7.80	5.64	2.27	0	672.7
336	249734.901	-3343808.804	874.210	7.28	7.21	2.05	1.28	9.88	3.60	6.37	4.04	0	5.7
337	249779.017	-3343969.533	874.425	7.43	77.0	101.83	4.05	18.83	9.70	22.85	51.09	4.45	272.7
338	249685.959	-3344032.827	875.069	7.13	166.3	350.67	5.33	21.02	10.35	14.88	8.77	0.75	1149
339	249516.694	-3344124.802	875.084	7.26	9.80	1.58	0.81	12.15	4.52	7.56	7.43	0	8.73
340	249377.062	-3344202.557	877.200	7.52	11.94	2.54	1.15	12.72	11.86	8.56	1.8	0	2.33
345	249496.182	-3343626.923	869.450	7.94	25.4								
346	249494.429	-3343625.375	871.044	7.68	10.94								
347	249492.585	-3343623.943	871.072	7.65	25.7								
348	249490.253	-3343622.896	869.840	7.34	68.4								
349	249488.663	-3343621.875	869.590	7.33	87.5								
350	249487.090	-3343620.055	869.947	7.25	94.6								
351	249484.836	-3343619.230	869.380	7.23	32.3								
352	249482.106	-3343618.555	868.761	7.50	28.9								
353	249480.057	-3343617.772	869.011	7.30	7.24								
354	249477.967	-3343616.284	870.006	7.59	11.33								
355	249475.325	-3343615.820	868.681	7.26	53.9								